ROLE OF NITRIC OXIDE IN MODULATING RETINAL, CHOROIDAL, AND ANTERIOR UVEAL BLOOD FLOWS IN THE DOMESTIC PIGLET

1993

JACOT

UNIFORMED SERVICES UNIVERSITY OF THE HEALTH SCIENCES
F. EDWARD HÉBERT SCHOOL OF MEDICINE
4301 JONES BRIDGE ROAD
BETHESDA, MARYLAND 20814-4799

APPROVAL SHEET

GRADUATE EDUCATION

TEACHING HOSPITALS
WALTER REED ARMY MEDICAL CENTER
NAVAL HOSPITAL, BETHESDA
MALCOLM GROW AIR FORCE MEDICAL CENTER
WILFORD HALL AIR FORCE MEDICAL CENTER

Title of Dissertation: "Role of Nitric Oxide in Modulating Retinal, Choroidal, and Anterior Uveal Blood Flows in the Domestic Piglet"

Name of Candidate: Jorge L. Jacot
Doctor of Philosophy Degree
November 17, 1993

Dissertation and Abstract Approved:

Committee Chairperson	11/17/93 Date
Committee Member	11/17/93 Date
Committee Member	11/17/93 Date
Committee Member	11/17/93 Date
Committee Member	11/23/93 Date

The author hereby certifies that the use of any copyrighted material in the dissertation manuscript entitled:

" The Role of Nitric Oxide in Modulating Retinal, Choroidal, and Anterior Uveal Blood Flow in the Domestic Piglet"

beyond brief excerpts is with the permission of the copyright owner, and will save and hold harmless the Uniformed Services University of the Health Sciences from any damage which may arise from such copyright violations.

Jorge L. Jacot

Department of Physiology

Uniformed Services University

ABSTRACT

Title of Dissertation: The Role of Nitric Oxide in Modulating Retinal, Choroidal, and Anterior Uveal Blood Flow in the Domestic Piglet

Jorge L. Jacot, Doctor of Philosophy, 1993

Dissertation Directed by: Jack E. McKenzie, Ph.D., Associate Professor; Department of Physiology

The role of nitric oxide in modulating the autoregulatory capacity of the retinal circulation and in maintaining the basal vascular tone of the uveal circulation was investigated. Volumetric blood flow (ml/min/100 gm dry weight) to ocular tissues was determined in 23 anesthetized piglets (3-4 kg) using six radiolabelled microspheres. Temporal control studies (n=6) were performed to determine optimal post-surgical time for subsequent blood flow measurements. Additional experiments were conducted utilizing the inactive enantiomer D-NAME as vehicle control (n=6) and L-NAME as an inhibitor of nitric oxide synthase (n=6). Ocular perfusion pressure was defined as mean arterial pressure minus intraocular pressure. Intraocular pressure was manipulated hydrostatically by needle cannulation of the anterior chamber of the eye. Ocular perfusion pressure was decreased during intravenous infusion (30mg/kg/hr) of either D-NAME or L-NAME. Blood flows were determined at baseline and ocular perfusion pressures of: 60, 50, 40, 30, and 20 mmHg. Compared to D-NAME treated animals mean baseline choroidal and anterior uveal blood flows with L-NAME showed a 47% and 43% reduction ($p<.001$) respectively, while mean baseline retinal blood flow did not differ. Retinal blood flow with L-NAME was reduced at all other ocular perfusion pressures when compared to D-NAME (repeated measures ANOVA:protected T-tests $p<.05$). Both groups revealed partial retinal blood flow autoregulation as determined by closed loop gain formula. Retinal autoregulation was significantly compromised with L-NAME. Choroidal and anterior uveal blood flows were linearly

correlated with ocular perfusion pressure in both groups (Choroid r=0.80 D-NAME , r=0.75 L-NAME ; anterior uvea r=0.74 D-NAME , r=0.86 L-NAME). Five animals were utilized to evaluate the blockade of nitric oxide synthase with intra-atrial bolus administration of L-arginine (180 mg/kg). Following L-arginine administration we obtained mean choroidal and anterior uveal blood flow values above the 95% confidence limits for mean blood flow values in the L-NAME treated animals. These data support the hypothesis that nitric oxide plays a significant role in maintaining the autoregulatory capacity of the retinal vasculature and is a mediator in maintaining the vascular tone of the choroidal and anterior uveal circulation in-vivo.

THE ROLE OF NITRIC OXIDE IN MODULATING RETINAL, CHOROIDAL, AND ANTERIOR UVEAL BLOOD FLOW IN THE DOMESTIC PIGLET

by

Jorge L. Jacot

Dissertation submitted to the Faculty of the Department of Physiology

Graduate Program of the Uniformed Services University

of the Health Sciences in partial fulfillment of the

requirements of the degree of

Doctor of Philosophy 1993

ACKNOWLEDGEMENTS

My sincere appreciation and graditude to my "adoptive" mentor and friend Dr. Jack E. McKenzie for having had the courage and willingness to take on the responsibility of my training. Dr. Mckenzie is an inspiration to those who wish to run their lives with integrity and honor. I have not only learned from him valuable scientific principles but humanistic qualities that are seldom found and frequently sought.

It has been stated that there are different levels of an educator, those that merely teach by lecturing and those that inspire by their teachings. Dr. McKenzie is one of those truly inspirational educators which has inspired me to maintain my scholarly interest in science. His dedication, enthusiasm and generous assistance will always be remembered.

A special thanks to: Dr. William Freas, Dr. Chu-Shek Lo, Dr. Frederick Pearce, and Dr. James Terris, members of my graduate advisory committee for their friendship and valuable scientific guidance in the development of this dissertation.

I thank my friends Mrs. Debbie M. Scandling and Ms. Shanda D. West, two outstanding individuals which are very talented in their profession. They were always "ready" to assist when needed. Their contribution and effort should not be undermined, and shall not be forgotten.

I am particularly appreciative of my friend Dr. Terry Tamaroglio for her loving support, understanding, and companionship throughout this difficult journey.

DEDICATION

To my parents for their love and unwavering support. I hope to one day have the opportunity to share with my own children the same love and dedication my parents have so unselfishly shown me.

TABLE OF CONTENTS

BACKGROUND AND SIGNIFICANCE

Anatomy of Ocular Circulation 1

Control of Ocular Blood Flow 3

Myogenic Hypothesis 5

Metabolic Hypothesis 7

Nitric Oxide

Properties 8

Synthesis 12

Nitric Oxide Synthases 13

Mode of Action of Nitric Oxide 16

Blockers of Nitric Oxide Synthases 18

Role of Nitric Oxide in the Vasculature 18

Nitric Oxide in the Central Nervous System 19

Role of Nitric Oxide in the Ocular Circulation 21

MATERIALS AND METHODS

Selection of Animal Model 25

Surgical Preparation 26

Temporal Control Studies 33

Studies with Vehicle Control D-NAME and NOS Inhibitor L-NAME 34

Hemodynamic Parameters 35

MAP and IOP Matched Animals 40

Reversal of NOS blockade with Exogenous L-Arginine 40

Microspheres

Historical Development 43

Current Manufacturing Specifications 44

Counting Equipment 47
Simultaneous Equation Method 51
Principles and Assumptions 55
Determination of Blood Flow and Cardiac Output 56
Determination of Vascular Resistance 58
Quantitation of Autoregulation 58
Determination of Compensatory Power in Blood Flow Regulation 60
Statistical Analysis 61
RESULTS
Temporal Control Studies 62
D-NAME and L-NAME Treated Animals 62
Choroidal Blood Flow 69
Anterior Uveal Blood Flow 69
Retinal Blood Flow 74
Retinal Autoregulation 74
Contralateral Eye Blood Flow 77
Blood Gas Analysis for D-NAME, L-NAME, and Contralateral Eye 82
MAP and IOP Matched Animals 82
Vascular Resistances 89
Reversal with L-Arginine 89
Kidney Blood Flows 94
DISCUSSION 97
BIBLIOGRAPHY 109
APPENDIX
Composition of Mock Aqueous Humor 120
Diagram of Ocular Circulation 121

LIST OF FIGURES

		PAGE
BACKGROUND		
Figure 1	The endothelium as a metabolically active mediator of vascular smooth muscle tone.	11
Figure 2.	The L-arginine/Nitric Oxide pathway mechanism for the stimulation of the soluble guanylate cyclase	15
MATERIALS AND METHODS		
Figure 3.	Apparatus for monitoring and manipulating intraocular pressure.	29
Figure 4.	Intraocular pressure tracings	32
Figure 5.	Systemic blood pressure effects of D-NAME and L-NAME infusions.	39
Figure 6.	Systemic blood pressure effects of L-NAME infusion and L-arginine administration	42
RESULTS		
Figure 7.	Temporal control studies of ocular blood flow for the retina, choroid, and anterior uvea.	66
Figure 8.	Blood flow at six ocular perfusion pressures in the presence of D-NAME and L-NAME.	73
Figure 9.	Retinal blood flow and ocular perfusion pressure data normalized to control flow-pressure values and autoregulatory gain (G_c) of the retinal circulation.	76

Figure 10.	Blood flow for the contralateral eye at six time points in the presence of D-NAME and L-NAME.	81
Figure 11.	Mean arterial pressure and ocular perfusion pressure in the contralateral eye over time for D-NAME and L-NAME treated groups.	84
Figure 12.	Retinal, choroidal, and anterior uvea blood flows matched by mean arterial pressure and ocular perfusion pressure in the presence of D-NAME and L-NAME.	88
Figure 13.	Retinal, choroidal, and anterior uvea vascular resistances.	91
Figure 14.	Reversal of nitric oxide synthase blockade with exogenous L-arginine administration.	93

LIST OF TABLES

Table I.	Hemodynamic parameters.	37
Table II.	Physical characteristics of the isotopes.	46
Table III.	Gamma counts for each isotope in the region of interest (ROI) windows.	50
Table IV.	Cross-over factor source matrix for the isotopes.	53
Table V.	Ocular blood flow measurements for the retina, choroid, and anterior uvea at various time points post-completion of surgical protocol.	64
Table VI.	Arterial blood data for the temporal control studies.	68
Table VII.	Retinal, choroidal, and anterior uvea blood flow measurements at six perfusion pressures in the presence of D-NAME and L-NAME.	71
Table VIII.	Contralateral eye blood flows at six time points in the presence of D-NAME and L-NAME.	79
Table IX.	Arterial blood data for the D-NAME and L-NAME treated groups at each ocular perfusion pressure tested.	86
Table X.	Arterial blood data prior to and after L-arginine administration.	96

Ach	Acetylcholine
ANOVA	Analysis of variance
ATP	Adenosine triphosphate
ATPase	Adenosine triphosphatase
AVMA	American Veterinary Medical Association
ARVO	Association for Research in Vision and Ophthalmology
BBB	Blood brain barrier
BF	Blood flow
BRB	Blood retinal barrier
BP	Blood pressure
Ca^{2+}	Calcium ion
cAMP	Cyclic adenosine monophosphate
ceNOS	Endothelial nitric oxide synthase
cGMP	Cyclic guanosine monophosphate
CO_2	Carbon dioxide
C.O.	Cardiac output
cm	Centimeters
CNS	Central nervous system
$(C.O._t)$	Total cardiac output
(C_t)	Total counts
df_{D+L}	Degrees of freedom for D-NAME and L-NAME treated groups
df_i	Degrees of freedom for individual group
D-NAME	N^G-Nitro-D-arginine methyl ester
EDRF	Endothelium derived relaxing factor
ERG	Electro retinogram
ESS_D	Error sum of squares for D-NAME treated group

ESS_L	Error sum of squares for L-NAME treated group
ESS_{L+D}	Error sum of squares for L-NAME and D-NAME treated groups
(F)	Cross-over fraction
FAD	Flavin adenine dinucleotide
Fe^{2+}	Ferrous ion
FMN	Flavin mononucleotide
GABA	Gamma-aminobutyric acid
GC	Guanylate cyclase
G_c	Closed loop autoregulatory gain
^{153}Gd	Gadolinium
GTP	Guanosine triphosphate
H_1	Histamine receptor (Type 1)
H_2	Histamine receptor (Type 2)
HB^+	Reduced hemoglobin
Hct	Hematocrit
H_2O_2	Hydrogen peroxide
HO^-	Hydroxyl ion
HO^*	Hydroxyl radical
H_4BPT	Tetrahydrobiopterin
hr	Hour
HR	Heart rate
i	Isotope
^{121}I	Iodine
^{114m}IN	Indium
iNOS	Inducible nitric oxide synthase

IOP	Intraocular pressure
IV	Intravenous
K^+	Potassium
kDa	Kilodalton
KeV	Kilo electron volts
KCL	Potassium chloride
Kg	Kilogram
L	Liter
L-ARG	L-arginine
L-NLA	Nitro L-arginine
L-NIO	N-imino ethyl-L-ornithine
L-NAME	N^G-Nitro-L-arginine methyl ester
L-NNA	N^G-Nitro-L-arginine
L-NMMA	N^G-monomethyl-L-arginine
MAP	Mean arterial blood pressure
mCi	MilliCurie
mEq	Milliequivalents
min	Minute
mg	Milligram
ml	Milliliters
µm	Micrometer
mOsm	Milliosmole
MLCK	Myosin light chain kinase
mmHg	Millimeters of mercury
NADPH	Nicotinamide adenine dinucleotide phosphate, reduced form

NaI	Sodium iodide
NaCl	Sodium chloride
NANC	Non-adrenergic Non-cholinergic
^{95}Nb	Niobium
NEN	New England Nuclear Co.
N^G	Guanidino nitrogen
NH_3	Ammonia
NMDA	N-methyl-D-aspartate
NO	Nitric oxide
NOS	Nitric oxide synthase
nNOS	Neuronal nitric oxide synthase
NO_2^-	Nitrite
NO_3^-	Nitrate
O_2	Oxygen
O_2^-	Superoxide anion
O_2Hb	Oxyhemoglobin
OPP	Ocular perfusion pressure
OPP_c	Control ocular perfusion pressure
OPP/OPP_c	Ocular perfusion pressure normalized to control ocular perfusion pressure
OPPs	Ocular perfusion pressures
pH	$-\log[H^+]$
PKA	Protein kinase A
PKC	Protein kinase C
PCO_2	Partial pressure of carbon dioxide (mmHg)
PO_2	Partial pressure of oxygen (mmHg)

Q	Flow
Q_c	Control flow
$(\Delta Q/Q/\Delta P/P)$	Slope of normalized perfusion pressure flow curve at specified points
(Q_r/C_r)	Ratio of flow in reference withdrawal to countss in reference withdrawal sample
ROI	Region of interest window
^{46}Sc	Scandium
SEM	Standard error of the mean
sGC	Soluble guanylate cyclase
SOD	Superoxide dismutase
^{113}Sn	Tin
^{85}Sr	Strontium
Tween 80	Polyoxyethylene 80 sorbitan monooleate
USUHS	Uniformed Services University of the Health Sciences
(y^+)	Brain transport system for cationic amino acid

BACKGROUND AND SIGNIFICANCE

Anatomy of the Ocular Circulation:

The ocular circulation is comprised of two distinct vascular systems; the retinal and uveal circulations (see Appendix). The uveal circulation includes the vascular beds of the iris, the ciliary body, and the choroid (Bill, 1983). In humans the ocular blood vessels are derived from the ophthalmic artery, which is a branch of the internal carotid artery. The ophthalmic artery branches to form the central retinal artery which courses through the center of the distal portion of the optic nerve to reach the eye. Near the optic nerve head the central retinal artery branches into four major quadrant branches which nourish the INNER layers of the retina (Bill, 1983). In pigs, the ocular circulation is supplied from an ophthalmic artery arising from the internal maxillary artery which is a branch of the external carotid artery (Prince et al, 1960). Anatomical orientation of the various posterior eye structures are customarily described in reference to the direction of incident light from the pupil (Wolff, 1976). By conventional orientation, the retinal vasculature is the "inner" vascular bed relative to the choroidal vasculature. The inner two-thirds of the retina are vascularized by the retinal vessels. The outer layers of the retina (approximately 130μ thick in humans) are "avascular" (Moses & Hart, 1987). One of the main functions of the choroidal vasculature is to supply nutrients to the OUTER avascular retinal layers.

The complexity of the circulation of the eye stems from the unique characteristic of a need to supply the intraocular tissues with nutrients without interfere with vision (Novack & Stefansson, 1990). The retinal circulation which emanates from the optic nerve head supplies oxygen and nutrients to the inner retina. The retinal venous blood is drained by the central retinal vein that leaves the eye via the optic nerve and eventually drains into the cavernous sinus (Leber, 1983). Direct occlusion of retinal arteries in pigs has demonstrated that they are end arteries without anastomoses (Moses & Hart, 1987). The retinal capillaries in humans are approximately 4-6μm in diameter, slightly smaller than cerebral capillaries. (Bill, 1983). It is proposed that the outer

avascular retinal layers obtain their nutrition by diffusion from the choriocapillaris, the inner most layer of the choroid. It has been estimated by oxygen microelectrode studies that only twenty to forty percent of the oxygen consumed by the retina is delivered by the retinal blood vessels; the rest (80 to 60%) is supplied by the choroid (Ernest, 1989a,b).

The choriocapillaris is a dense, single-layer network of fenestrated capillaries with a lobular arrangement and few anastomoses (Hayreh, 1975). It is separated from the avascular outer retinal layers by Bruch's membrane (2-4μm thick) and the retinal pigment epithelium (10μm thick). The choriocapillaris is supplied by three to four posterior ciliary arteries that branch from the ophthalmic artery and traverse the white fibrous scleral tunic at the posterior pole of the orbit. The choroid is drained by four vortex veins in each quadrant of the posterior pole of the eye. The uveal capillaries are of larger diameter than those of the retina. The capillaries of the choroid are of smaller diameter at the posterior uveal circulation than in the anterior uveal circulation (Stjernschantz et al, 1976).

Direct choroidal venous blood sampling in pigs and other species has shown an arterio-venous oxygen content difference of approximately 3% (Tornquist and Alm, 1979). The high oxygen tension found in choroidal venous blood suggests that the choroid functions to enhance the diffusion of oxygen to the outer retinal layers. Some investigators have ascribed additional functions to the choroid besides fulfilling nutritional requirements to the outer avascular retina. It may play a role in the stabilization of temperature for the outer retinal layers and retinal pigment epithelium (RPE), possibly protecting the eye from thermal damage (Parver et al 1980; Auker et al, 1982). Because the capillaries of the choroid are fenestrated and have a relatively high protein permeability the exchange of the retinol complex, which is required by photoreceptors, is facilitated (Bill, 1983; Bok, 1990). The choroidal vasculature lacks a blood-brain barrier and a blood-retinal barrier (Tornquist et al, 1990).

Control of Ocular Blood Flow:

The retina is able to maintain a constant level of metabolism during changes in perfusion pressure by altering vascular resistance to maintain a constancy of blood flow. This phenomenon is known as autoregulation of blood flow (Bayliss, 1902). The phenomenon of blood flow autoregulation appears to involve the interaction of intrinsic myogenic vessel tone and the opposing effects of endogenous vasodilator agents. Both myogenic and metabolic mechanisms seem to contribute to the adjustment of retinal vascular resistance (Ernest, 1989a).

The mechanisms operative in the modulation of blood flow to the retina and choroid are very different. The retina, which is embryologically an extension of the central nervous system, demonstrates a similar autoregulatory capacity to that of other brain structures by maintaining a constant blood flow over a broad range of perfusion pressures (Ernest, 1989b; Alm & Bill, 1972a). The retina develops from the walls of the optic cup, which is an outgrowth of the forebrain (Moore, 1988). There are several comparisons which can be drawn between the retinal circulation and the cerebral circulation. The capillaries of the retina, like those of the brain, have tight junctions in the endothelial cells which provide a blood-retinal barrier (Cunha-Vaz et al, 1966). Studies with microperoxidase and horseradish peroxidase have shown that the tight junctions of the retinal capillaries are a comparable counterpart to the blood-brain barrier in terms of permeability to particular substances (Bill, 1975). Both the retina and brain have transvascular transport mechanisms for glucose, amino acids, and lactate. In pigs net glucose extraction determined from retinal venous blood is approximately 12%, which is comparable to extraction by the brain (Bill, 1983). The response of the eye vasculature to CO_2 is similar to that of the cerebral vessels; both the retina and uvea circulations respond to elevations in CO_2 by vasodilation (Alm & Bill, 1972b). Retinal blood flow appears to be controlled similar to other tissues which are highly dependent on oxidative metabolism. Oxygen extraction from the retina and brain vasculature is high (30-50%) (Tornquist and Alm, 1979). Despite these similarities there are some remarkable contrasts between the ocular and cerebral circulations. The nutritional interrelationship between the retina and

choroidal vascular beds is unique to the eye and has no counterpart in the cerebral circulation (Bill, 1983).

Investigations into the autoregulatory capacity of the choroidal circulation have led to controversial findings. Alm & Bill (1973b) reported a lack of autoregulatory capacity by the choroidal circulation and have described it as a pressure passive vasculature. Others (Chemtob et al, 1991; Kiel & Shepherd, 1992) have reported that the choroid demonstrates autoregulation. The mechanism(s) responsible for autoregulation have not yet been clearly elucidated. It has been reported that metabolic mechanisms predominate. Chemtob et al, (1991) utilizing radioactive microspheres to measure blood flow in piglets have claimed that prostaglandins play a major role in establishing the autoregulatory capacity of the choroidal circulation. Kiel & Shepherd (1992) have shown that choroidal autoregulation is strongly dependent on a myogenic mechanism. The choroid receives more blood flow per gram of tissue than any other tissue in the body (Bill & Sperber, 1990). This high flow rate is not due to metabolic demands of the tissue and it is unknown what mechanism(s) regulate the very low vascular tone of the choroidal circulation.

Blood flow regulation in the choroid is believed to be similar to blood flow regulation in peripheral tissues (Ernest, 1989b). The role of vasoactive nerves in modulating the uveal circulation has been documented by histologic and physiologic experiments (Bill, 1983). Parasympathetic innervation is via the oculomotor (ciliary ganglion), facial, and ophthalmic division of the trigeminal nerve. Sympathetic nerves from the superior cervical ganglion innervate the uvea (Alm & Bill, 1973a). Sympathetic stimulation causes pronounced vasoconstriction and reductions of uveal blood flow, while minimally affecting retinal blood flow (Bill & Sperber, 1990; Moses & Hart, 1987; Bill, 1983). It has been reported that there are no vasomotor nerves in the retina (Bill, 1983). Others (Toda et al, 1993) have demonstrated that the pterygopalatine ganglion can be a source of vasodilator nitroxidergic nerves in the canine retinal circulation. The uveal circulation has abundant sympathetic innervation which is believed to provide vasoconstriction and protection from overperfusion (Bill, 1983). During high perfusion pressures extravasation of plasma from the

microcirculation in the retina, optic nerve, iris, and ciliary process occurs, promoting the breakdown of the blood-aqueous and blood-retinal barriers (Bill & Sperber, 1990; Moses & Hart, 1987; Bill, 1983). A similar phenomenon occurs in the cerebral circulation with regional overperfusion. Although the control mechanisms in the uveal circulation appear to be very different from the retinal circulation, the retina is dependent, to a significant degree, on the choroidal blood flow for its metabolic supply.

Myogenic Hypothesis:

The myogenic hypothesis of blood flow regulation states that the vascular smooth muscle contracts in response to an increase in vessel wall tension and relaxes with a reduction in tension. Stimuli for the myogenic mechanism of autoregulation are variations in wall tension, not blood flow or oxygen delivery (Folkow, 1964). Raising ocular perfusion pressure increases the transmural pressure of the vessel and by passive stretch increases the radius, resulting in an increased wall tension as expressed by the Laplace equation ($T = \Delta P \times r$). The law of LaPlace states that vascular wall tension (T) is a function of the transmural pressure gradient (ΔP) and the vessel radius (r) (Kiel & Shepherd, 1992). The myogenic hypothesis states that myogenic vasoconstriction occurs when the transmural pressure gradient across the vascular wall is increased by increasing arterial pressure (Johnson, 1964). Constriction of the vessel in response to the increased tension results in a reduction of its diameter so that the product of pressure (increased) and radius (decreased) is restored to the control level (Johnson, 1964). Therefore, the initial increase in flow produced by an increase in ocular perfusion pressure which distends the blood vessel is followed by a return of blood flow to the initial level by contraction of the vascular smooth muscle.

When the transmural pressure gradient is decreased by lowering arterial pressure, the myogenic hypothesis predicts vasodilation and a decrease in vascular resistance (Johnson, 1964; Kiel & Shepherd, 1992). If the perfusion pressure gradient is decreased by raising venous pressure the transmural pressure gradient is increased and myogenic vasoconstriction occurs. Therefore,

elevations in venous pressure will produce constriction according to the myogenic hypothesis, but vasodilation according to the metabolic hypothesis.

It has been reported (Bill, 1963) that pressure in the vortex veins, which drain the uveal circulation, is approximately equal to the intraocular pressure. In the eye, it has been shown by direct measurements, that the venous pressure equals the intraocular pressure at normal and high intraocular pressures (Bill & Sperber, 1990). Therefore, ocular perfusion pressure is considered to be mean arterial pressure minus intraocular pressure (MAP-IOP). Ocular perfusion pressure can be varied by controlling mean arterial pressure, venous pressure, or intraocular pressure.

Lemmingson (1968) investigated the myogenic mechanism in the regulation of ocular blood flow in cats. He found more frequent spontaneous arteriolar contractions in young cats than in the adult animals. These findings suggest that there may be an age-dependent contribution of the myogenic response in the regulation of ocular circulation.

The skepticism surrounding the myogenic hypothesis is that for flow to remain constant following an increase in perfusion pressure, it is necessary for the caliber of the resistance vessels to be less than it was prior to the elevation of pressure. Therefore, the negative feedback stimulus for the contractile response would be eliminated (Folkow, 1964).

Resistance vessels in a variety of tissues have shown intermittent contraction and relaxation. It has been proposed that an increase in the frequency of contractility occurs with elevations of perfusion pressure (Lemmingson, 1968). This mechanism suggests that the resistance vessels spend more time in the contracted state than in the relaxed state during elevations in perfusion pressure. The mechanism of intermittent contractility to explain autoregulation of blood flow, as opposed to a sustained contractile state of the vascular smooth muscle, is appealing. This mechanism does not require that the caliber of the resistance vessel be less than it was prior to the initial perturbation, thereby maintaining the feedback stimulus for the contractile response.

Metabolic Hypothesis:

The metabolic hypothesis of blood flow regulation states that blood flow is governed by the metabolic activity of the tissue. An inadequate O_2 supply to meet tissue metabolic demands gives rise to the formation and accumulation of vasodilator metabolites, which act locally to cause relaxation of the vascular smooth muscle (Gaskell, 1877).

It has been shown that retinal arteries and veins constrict when the arterial blood oxygen tension (PO_2) is increased and dilate when it is decreased (Ernest, 1989a). However, direct measurements at resistance vessels in a number of vascular beds indicate that over a broad range of PO_2 there is little correlation between oxygen tension and arteriolar diameter (Duling, 1974). Although tissue PO_2 is one of the most commonly attributed controlling factors in the metabolic hypothesis it is clearly not the only regulatory factor (Johnson, 1964). The phenomenon of reactive hyperemia refutes a direct role of PO_2 in regulating vascular smooth muscle tension. There is a strong positive correlation between the duration of arterial occlusion and the duration of the hyperemia following the occlusion. However, it has been shown that venous blood is well oxygenated within seconds following a short or prolonged arterial occlusion. The arterial vascular smooth muscle must be exposed to a high PO_2 in such instances (Duling, 1974). These observations are more consistent with the release of a vasoactive metabolite from the tissues rather than a direct effect of PO_2 on the vascular smooth muscle.

A surplus of oxygen can be delivered to the tissues when either a decreased metabolic activity or increased perfusion pressure exists. During an increased O_2 supply/demand ratio the tissue concentration of the vasodilator metabolite falls. A decrease in metabolism or an increase in the washout (or inactivation) of the metabolite elicits an increase in vascular resistance. The metabolic hypothesis is attractive because it closely couples blood flow to tissue metabolic activity (Berne, 1964).

Many substances have been proposed as mediators of metabolic vasodilation. Several vasoactive metabolites can be involved in any particular vascular bed and different metabolites

predominate in the various tissues. Some commonly cited mediators of metabolic vasodilation have been: lactic acid, CO_2, hydrogen ions, potassium ions, inorganic phosphate, interstitial fluid osmolarity, catecholamines, histamine, acetylcholine, serotonin, angiotensin, adenosine, prostaglandins and endothelium derived relaxing factor (EDRF) (Berne, 1964; Furchgott & Zawadzki, 1980). Some of these vasodilator agents produce only transient increases in blood flow and the decrease in vascular resistance induced by pharmacological concentrations of these dilator agents fails to induce the degree of dilation observed under physiological conditions (Berne, 1964).

NITRIC OXIDE (NO)

Properties of Nitric Oxide :

The simple nitrogen derivative molecule nitric oxide (NO) has recently emerged among the leading vasoactive substances regulating vascular smooth muscle tone. The endothelium has been shown to be a metabolically active mediator of vascular smooth muscle tone (Vanhoutte, 1988). The endothelium posses the necessary metabolic pathways for the formation of NO, which is a potent relaxant of vascular smooth muscle. The findings that the endothelium is a modulator of arterial tone was first demonstrated in 1980 by Robert F. Furchgott and J.V. Zawadski using isolated blood vessel preparations. They demonstrated that the presence of the endothelium was required for relaxation of the vascular smooth muscle by vasoactive agents (**Figure 1**). Furchgott determined that the vasodilator mechanism was triggered by the endothelial cells and coined the term "endothelium-derived relaxing factor" (EDRF). In 1986, Furchgott and Ignarro independently characterized EDRF as nitric oxide (Palmer et al, 1987). Numerous studies have substantiated their findings (Ignarro et al, 1981 & 1988a,b; Palmer et al, 1987; Shikano et al, 1988). However, more recent findings suggest the likelihood of more than one relaxing factor (Munakata et al, 1990; Rosenblum, 1992).

Nitric oxide is small and electrically neutral and diffuses freely through biological membranes (Lancaster, 1992). An inorganic gas, nitric oxide has an ephemeral half-life of about ten to thirty

seconds (in oxygenated medium at physiological pH) before it is converted by oxygen and water to either of two unreactive anions, nitrates (NO_3^-) and nitrites (NO_2^-). These reactions ($2NO + O_2$ --> $2NO_2$ and $2NO_2 + H_2O$ --> $NO_2^- + NO_3^- + 2H^+$) appears to be the principal metabolic pathway for inactivation of nitric oxide by cells (Lancaster, 1992). Because of the strong predilection of NO to react with molecular oxygen (O_2), cells do not require an enzymatic mechanism for the removal of NO. It is possible that reversible reactions with thiols to form S-Nitroso compounds contribute to the removal of NO (Knowles & Moncada, 1992). Nitric oxide is a paramagnetic molecule (free-radical structure with 15 electrons) that is highly labile. The unpaired electron of nitric oxide makes it extremely reactive with other paramagnetic molecules, such as superoxide (O_2^-) and various metal-bearing proteins. The reactions with molecular oxygen and metalloproteins dominate the molecular mechanism of action of nitric oxide (Lancaster, 1992).

Figure 1: Schematic diagram of the endothelium as a metabolically active mediator of vascular smooth muscle tone. NO mediates the vasoactive actions of acetylcholine (Ach) and bradykinin in vascular smooth muscle. The binding of Ach and Bradykinin to cell surface receptors promotes an influx of Ca^{2+} into the endothelium which activates NOS and promotes the conversion of L-arginine (L-ARG) to NO. NO diffuses freely to activate the soluble guanylate cyclase (sGC) and promote the conversion of GTP to cGMP which leads to relaxation of the vascular smooth muscle cell. Physical stimuli such as shear stress, and pulsatile stretching of the vessel wall stimulates NO release, possibly mediated with an increase in Ca^{2+} influx or a flow-sensitive K^{+} channel. The role of O_2 tension in influencing NOS activity is less clear. Hypoxia may inhibit NOS activity through depletion of oxygen (a necessary substrate) or hypoxia may stimulate NOS activity due to an increase in cellular Ca^{2+} at a low PO_2.

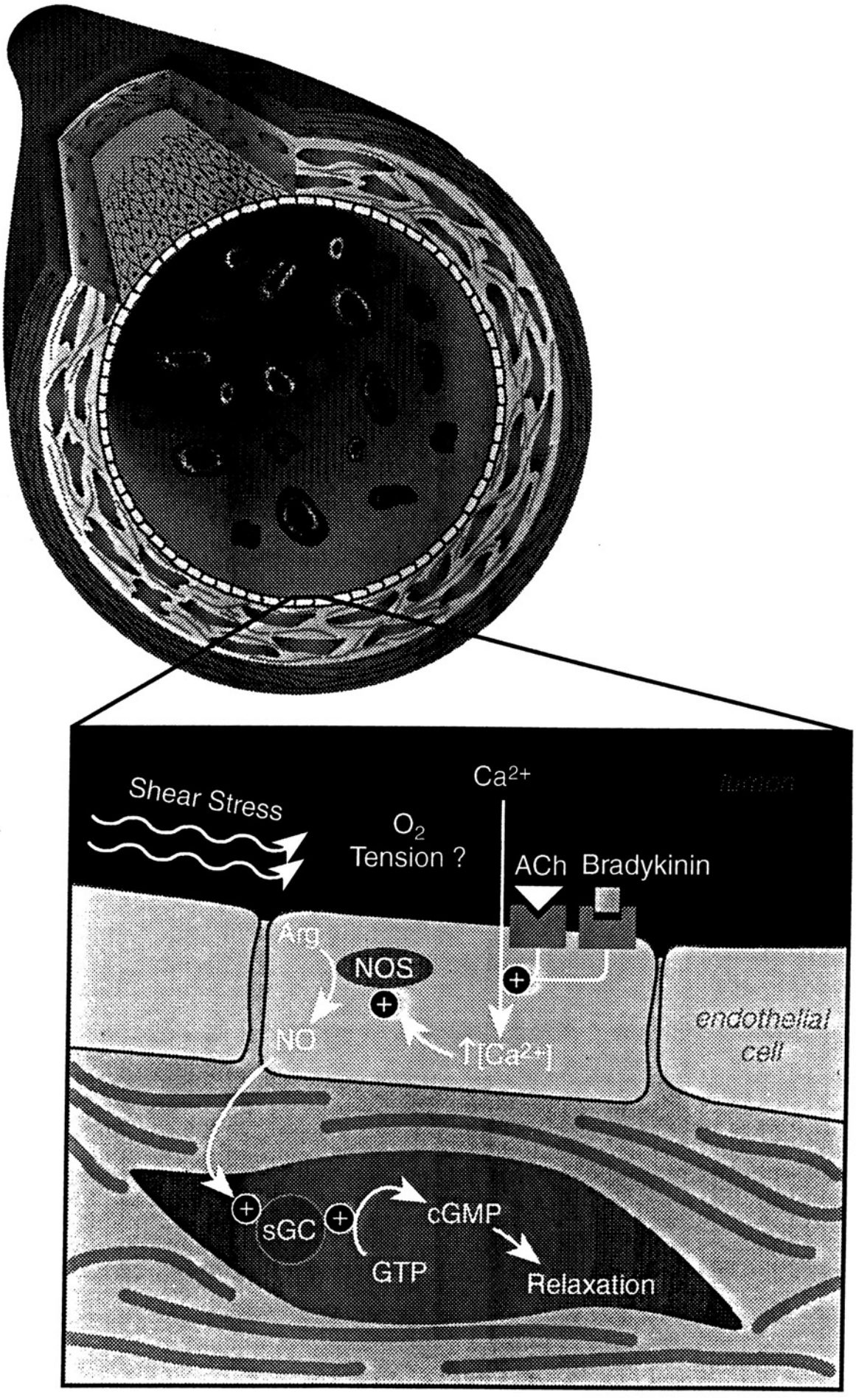
Shear Stress
O_2 Tension ?
Ca^{2+}
lumen
ACh
Bradykinin
Arg
NOS
NO
↑[Ca^{2+}]
endothelial cell
sGC
cGMP
GTP
Relaxation

Nitric oxide vigorous reactions with oxyhemoglobin, deoxyhemoglobin, and superoxide (O_2^-) rapidly convert NO to nitrate (NO_3^-) (Knowles & Moncada, 1992):

$$NO + O_2Hb \rightarrow NO_3^- + Hb^+$$

$$NO + Hb \rightarrow NOHb$$

$$NO + O_2^- \rightarrow ONOO^- \rightarrow NO_3^-$$

Once NO diffuses into the lumen of the blood vessel it is quickly inactivated by the above reactions due to the high concentration of hemoglobin (heme) which binds directly to NO. Nitric Oxide is stabilized by the free radical scavenger superoxide dismutase (SOD), suggesting that oxygen free radicals contribute to the inactivation of nitric oxide (Fantone and Ward, 1985). Superoxide dismutase is present in eukaryotic and prokaryotic cells and is capable of dismutating two molecules of O_2^- to form hydrogen peroxide and oxygen. The effects of NO are blocked by methylene blue an inhibitor of guanylate cyclase (Fantone and Ward, 1985). Others have reported that the mechanism by which methylene blue blocks endothelium dependent vasodilation is by the generation of superoxide (oxygen radical). Hydrogen peroxide is subsequently produced by spontaneous dismutation of superoxide. The superoxide in combination with hydrogen peroxide produce a hydroxyl radical by the iron-catalyzed Haber-Weiss reaction: $O_2^- + H_2O_2 \rightarrow O_2 + HO^- + HO^*$. The hydroxyl radical inhibits vasodilation by oxidation of nitric oxide (Marshall et al, 1988).

Synthesis of Nitric Oxide:

Nitric oxide is synthesized from the amino acid L-arginine by the cytosolic enzyme nitric oxide synthase (NOS). The reaction requires one of two terminal guanidino nitrogens from L-arginine and the oxygen from molecular oxygen to synthesize nitric oxide (Rees et al, 1990). The reaction also requires the electron donor nicotinamide adenine dinucleotide phosphate (NADPH) and the cofactor tetrahydrobiopterin (H_4BPT). All NOS contain FMN, FAD, non-heme Fe^{2+}, as prosthetic groups in each subunit (Forstermann et al, 1991; Mayer et al, 1991). These prosthetic groups are believed to be involved with the oxidation of L-arginine. The removal of nitrogen from

L-arginine during the reaction forms the amino acid co-product L-citrulline (**Figure 2**) (Lancaster, 1992). The correlation between NO and L-citrulline formation in terms of their time course, substrate requirements, and inhibitor sensitivity demonstrate that they are coproducts of the same reaction (Knowles et al, 1989). The mechanism of the reaction by which L-arginine is oxidized to citrulline and nitric oxide has not been clearly elucidated. The formation of N^G-hydroxy-arginine is an intermediate in the reaction (Leone et al, 1991; Stuehr et al, 1991). Several mechanisms have been proposed depending on cell type. For the macrophage lineage it has been suggested that L-arginine undergoes a deamination reaction followed by oxidation of NH_3 to nitric oxide (Knowles et al, 1989). The proposed mechanism for the vascular endothelial cells is a monooxygenation reaction followed by the formation of NO and L-citrulline by hydrolysis (Knowles et al, 1989).

Nitric Oxide Synthases:

Findings suggest that at least three distinct isoenzymes of nitric oxide synthase exist. Each synthase consists of two 125-160kDa subunits which form a homodimer (Forstermann et al, 1991). NOS is an oxidative enzyme which utilizes molecular oxygen to hydroxylate substrates and to facilitate the five-electron transfer during catalysis (Bredt et al, 1992; Knowles & Moncada, 1992). The immune system has an inducible form of nitric oxide synthase (iNOS) which functions independently of calcium concentration. In the immune system NO has both tumoricidal and bactericidal properties (Bredt et al, 1992). The two forms of nitric oxide synthase; inducible (the cells make the enzyme only when it receives a specific molecular signal) and constitutive (the enzyme is present at all times) are differentially inhibited by analogues of L-arginine.

Nitric oxide synthases found in the central nervous system (nNOS) and in the vascular endothelium (ceNOS) are constitutive enzymes. Endothelium-dependent NOS is smaller than nNOS and is usually associated with the cytosolic surface of the endothelial cell membrane. The catalytic activity of NOS is regulated at several sites. Both enzymes are activated by the binding of calmodulin which in turn is activated by an influx of Ca^{2+} into the cell (Knowles et al, 1989 & 1992).

Figure 2: Diagram of the L-arginine (L-ARG)/Nitric Oxide (NO) pathway showing the mechanism for the stimulation of the soluble guanylate cyclase (sGC). NO is synthesized from L-ARG by the enzyme NOS. The reaction requires nitrogen from L-ARG, O_2, NADPH and H_4BPT. All NOS contain FMN, FAD, non-heme Fe^{2+}, as prosthetic groups in each 125-160 kDa subunit for oxidizing L-ARG. Nitrogen from L-ARG forms the co-product L-citrulline. L-NAME is an enantiomerically specific inhibitor of NOS. Three isoenzymes of NOS exist (ceNOS, nNOS, iNOS). NOS is activated by binding to calmodulin as a result of Ca^{2+} influx into the cell. nNOS is phosphorylated at serine sites by cAMP dependent PKA, PKC. NO reactions with O_2^- converts NO to inactive NO_2^- and NO_3^-. Synthesis of c-GMP from GTP is catalyzed by GC receptors. These receptors can exist as a heterodimer linked by intermolecular S-S bonds and a heme prosthetic group. NO acts by binding to the iron in the heme moiety of the GC, inducing a conformational change which activates the GC and promotes synthesis of cGMP. It is speculated that protein phosphorylation of myosin light chain kinase (MLCK) leads to vascular smooth muscle relaxation.

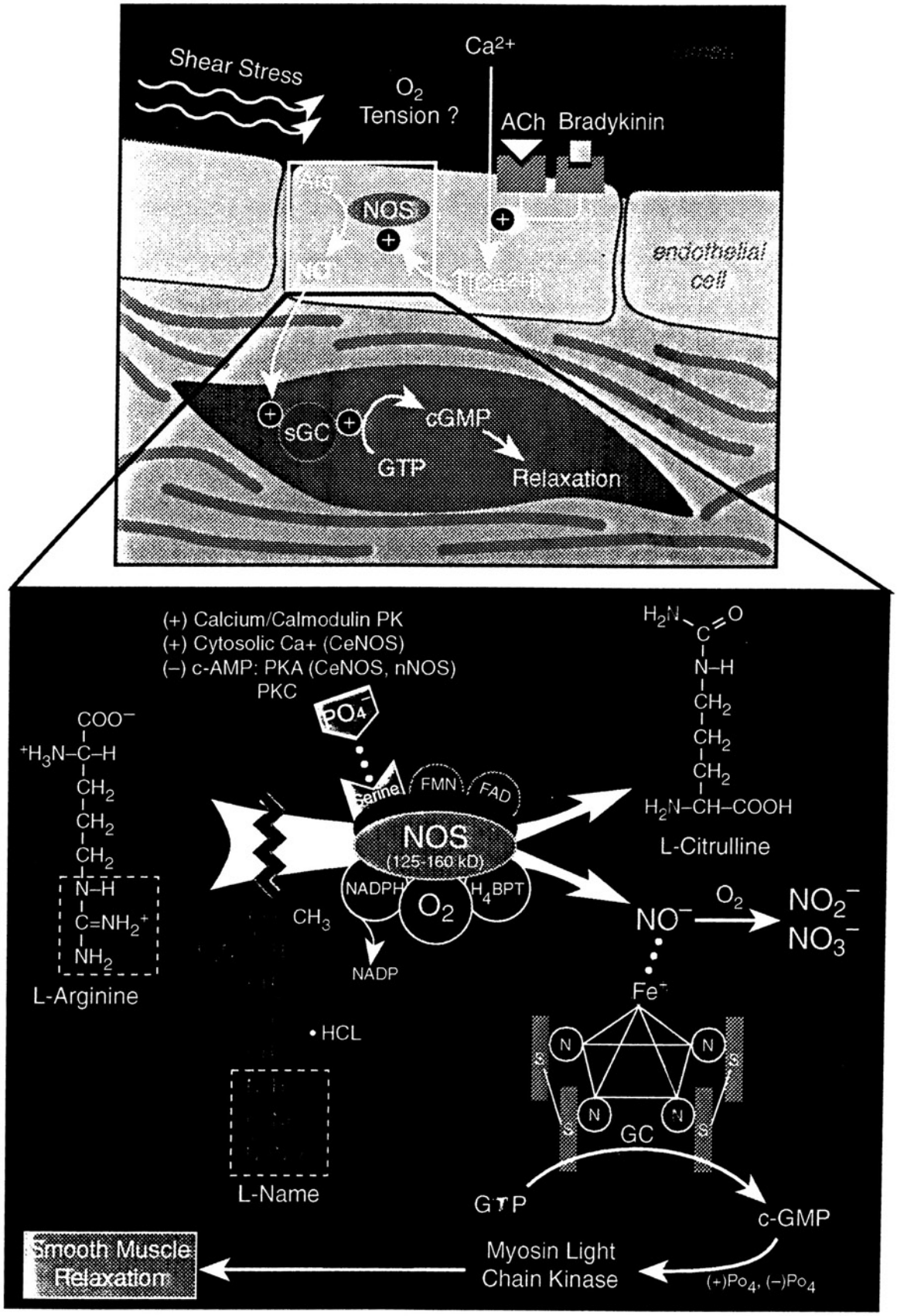
Shear Stress
Ca^{2+}
O_2 Tension ?
ACh
Bradykinin
Arg
NOS
NO
endothelial cell
sGC
cGMP
GTP
Relaxation
(+) Calcium/Calmodulin PK
(+) Cytosolic Ca+ (CeNOS)
(–) c-AMP: PKA (CeNOS, nNOS)
PKC
PO_4^-
Serine
FMN
FAD
NOS
(125-160 kD)
NADPH
H_4BPT
O_2
CH_3
NADP
L-Arginine
L-Citrulline
NO^-
O_2
NO_2^-
NO_3^-
Fe^+
• HCL
L-Name
N
S
GC
GTP
c-GMP
Myosin Light Chain Kinase
$(+)Po_4$, $(-)Po_4$
Smooth Muscle Relaxation

Cytosolic calcium concentrations regulate the activity of ceNOS. A five-fold increase in intracellular calcium concentration will increase the rate of ceNOS synthesis nearly one-hundred fold (Knowles & Moncada, 1992). Purified brain nitric oxide synthase is phosphorylated at selective serine sites by a cAMP dependent protein kinase (PKA), Protein kinase C, and calcium/calmodulin-dependent protein kinase enzyme (Bredt et al, 1992). Both ceNOS and nNOS have a c-AMP-dependent protein kinase phosphorylation site. Phosphorylation of nNOS by PKA has not been shown to affect catalytic activity. The effect of phosphorylation of ceNOS by PKA is not clear but it may decrease the catalytic activity of the enzyme (Bredt et al, 1992).

Mode of Action of Nitric Oxide:

It has been suggested that the L-arginine/nitric oxide pathway in the central nervous system, endothelial cells, and phagocytic cells functions as a widespread transduction mechanism for the stimulation of the soluble guanylate cyclase (Knowles et al, 1989). The synthesis of cyclic guanosine monophosphate (cGMP) from GTP is catalyzed by a group of cell surface and cytoplasmic receptors known as guanylyl cyclases (GC). A major group of guanylate cyclases exists as a heterodimer with two distinct subunits linked by intermolecular disulfide bonds and a heme prosthetic group. Nitric oxide diffuses into target cells and acts by binding to iron in the heme moiety of the enzyme guanylate cyclase (GC). The binding of NO to the iron containing heme group of the GC enzyme induces a conformational change which activates the enzyme and promotes the synthesizes of cyclic guanosine monophosphate (cGMP) (Wong & Garbes, 1992).

The mechanism by which increased cGMP levels in vascular smooth muscle cells leads to relaxation is not clearly elucidated. It has been observed that protein phosphorylation patterns in vascular smooth muscle are similar to those seen with nitroprusside treatment and after acetylcholine mediated relaxation (Ignarro et al, 1981). It has been proposed that altered protein phosphorylation of the myosin light chain kinase or myosin light chain, leads to relaxation of the vascular smooth muscle (Rapoport et al, 1983; Vanhoutte, 1988).

The common mechanism leading to vascular smooth muscle contraction is a transient rise in intracellular Ca^{2+} (Berk & Alexander, 1989). A rise in intracellular Ca^{2+} results in formation of Ca^{2+}-Calmodulin complexes which bind and activate myosin light chain kinase (MLCK). The activated MLCK phosphorylates myosin light chains which catalyze actomyosin ATPase activity resulting in actin-myosin interactions leading to cross-bridge formation and subsequent contraction (Adelstein & Conti, 1975; Berk & Alexander, 1989). Dephosphorylation is assumed to be unregulated.

Other possible regulatory mechanisms have been implicated. The phosphorylation theory has extensive experimental support, but it is clearly insufficient to explain the mechanism of the contractile process and the means by which NO exerts its physiological effects. Phosphorylation of CaM-Kinase II may play a role in desensitization of the vascular smooth muscle contractile system and may be a mechanism by which NO exerts its effects (Hartshorne & Kawamura, 1992). It is also possible that a receptor-linked mechanism influences the kinase-phosphatase balance. Alterations in the phosphorylation balance could then be responsible in modulating Ca^{2+} sensitivity (Hartshorne & Kawamura, 1992). Thin-filament-linked regulatory proteins such as caldesmon and calponin maybe involved in some aspect of regulation (Hartshorne & Kawamura, 1992). These proteins inhibit the actin-activated ATPase activity of phosphorylated myosin. When these proteins are phosphorylated they fail to bind and cannot exert their inhibitory effects (Winder & Walsh, 1990).

The full mechanism by which the cyclic nucleotides, such as cGMP, produce smooth muscle relaxation is not clearly elucidated. It has been proposed that intracellular accumulation of cGMP leads to a reduction in intracellular Ca^{2+} causing myosin dephosphorylation leading to vascular smooth muscle relaxation (Lincoln et al, 1990). Nitric oxide could induce vascular relaxation by other cyclic nucleotide-independent mechanisms, including hyperpolarization and activation of K^+ channels (Said, 1992).

Blockers of Nitric Oxide Synthases:

Analogues of L-arginine that are substituted at the quanidino nitrogens are competitive inhibitors of nitric oxide synthase in a dose-dependent and enantiomerically specific manner (Rees et al, 1990). Arginine analogues prevent the formation of new NO, and temporarily block any process dependent on nitric oxide production. N^G-Nitro-L-arginine methyl ester (L-NAME), N^G-monomethyl-L-arginine (L-NMMA), and N-imino ethyl-L-ornithine (L-NIO) have been shown to cause concentration dependent inhibition of the Ca^{2+} dependent nitric oxide synthase (Rees et al, 1990). In isolated rat aortic rings the L-arginine analogues inhibited Acetylcholine and bradykinin induced relaxation in vitro, and hypotension in vivo. The L-enantiomers of the inhibitors caused a dose dependent increase in mean arterial blood pressure. L-NAME caused the least increase in mean blood pressure, approximately 13% less, when compared to the same dose range of the other two blockers (Rees et al, 1990). The competitive blockade of NOS by L-arginine analogues is sensitive to reversibility with L-arginine but not its inert enantiomer D-arginine.

Role of Nitric Oxide in the Vasculature:

Endothelial denudation of cerebral and renal arteries have shown that the endothelium plays a role in autoregulation possibly by abolishing the constrictor response elicited by increasing pressure (Ueeda et al, 1992). Others (Griffith & Edwards, 1990) have shown that myogenic autoregulation of flow may be inversely related to endothelium-derived relaxing factor activity in the isolated rabbit ear.

Studies in guinea pigs using an electromagnetic flow probe and a Langendorff heart preparation have shown that the coronary endothelium modulates autoregulation by the production of NO. The administration of (N^G-nitro-L-arginine (L-NNA) enhanced autoregulatory capacity at the high end of the autoregulatory plateau in response to changes in perfusion pressure (Ueeda et al, 1992).

The role of NO in autoregulation of the renal vasculature has been examined in dogs (Majid

& Navar, 1992). An Electromagnetic flow probe was placed around the renal artery and blood flow monitored during intrarenal infusion of nitro L-arginine (NLA). It was concluded from this study that NO contributes to the basal tone of the renal vasculature but did not significantly influence the autoregulatory response to changes in arterial pressure.

Role of Nitric Oxide in the Central Nervous System:

The involvement of NO in the central nervous system has been implicated in at least four radically different roles. The binding of the excitatory amino acid neurotransmitter glutamate to the post synaptic N-methyl-D-aspartate (NMDA) receptor triggers an influx of Ca^{2+} which activates calmodulin-dependent NOS enzyme leading to increases in NO and cGMP levels in target cells (Bredt & Snyder, 1989; Garthwaite, 1991). It has also been shown that L-NMMA prevents NO mediated neurotoxicity by NMDA activation of excitatory amino acids in primary cortical cultures (Faraci & Breese, 1993; Dawson et al, 1991). Nitric oxide is involved in refinement of axonal projections in the nervous system (synaptic plasticity) including long-term depression in the cerebellum (Purkinje cells) and long-term potentiation in the hippocampus (Shibuki & Okada, 1991). Nitric oxide has also been shown to be released in neurotransmission of autonomic non-adrenergic, non-cholinergic (NANC) nerves in the peripheral nervous system (Martin & Gillespi, 1990; Bush et al, 1993). NADPH-diaphorase staining neurons have been shown to be nitric oxide synthase containing neurons which are resistant to hypoxia and anoxic damage (Hope et al, 1991). These subpopulations of cells have been found to exist in the inner nuclear layer of the retina with a specific and consistent distribution in a wide variety of mammals (Sandell, 1985). The functional significance of these cell types in the retina has yet to be specified.

Nitric oxide has also been implicated in control of regional cerebral blood flow. Faraci and Heistad (1991) investigated endothelium-dependent mechanism(s) on cerebrovascular smooth muscle relaxation in-vivo. The response of the cerebral microcirculation to various vasoactive agents has been documented in-vivo by the use of a cranial window (Marshall et al, 1988). Using

this technique in cats it has been shown (Marshall et al, 1988) that topical administration of methylene blue inhibited Ach-induced cerebral arteriolar dilation, suggesting that the vasodilation of cerebral arterioles to Ach is dependent on the formation of NO.

Another in-vivo study in rats (Faraci, 1990) using a cranial window was the first to report that topical application of N^G-monomethyl-L-arginine (L-NMMA) constricted the basilar artery. Furthermore, L-NMMA abolished the dilatory response of the basilar artery to Ach. Taken together these findings suggest that the formation of NO plays a role in the resting tone of the basilar artery, which is a resistance vessel of the cerebral circulation, and that the response of this vessel to Ach is mediated via an NO pathway (Faraci & Heistad, 1991).

Increases in CO_2 are known to cause marked increases in cerebral, retinal and uveal blood flow (Deutsch et al, 1983). It has recently been shown that the cerebrovasodilation elicited by hypercapnia (PCO_2 = 55-61 mmHg) is mediated by NO (Iadecola, 1992). Studies in rats, using both laser-Doppler probes and ^{14}C iodoantipyrine to measure blood flow thru a cranial window, have shown that topical superfusion of N^G-nitro-L-arginine (L-NA) to the sensory cortex decreases hypercapnic cerebrovasodilation by 93±6% and 87±6%, respectively (Iadecola, 1992). Studies using radiolabelled microspheres in rats have shown that an infusion of L-NAME attenuated the hyperemic response to cerebral hypercapnia (PCO_2 = 70-80 mmHg) by greater than 60% (Pelligrino et al, 1992). Administration of L-NAME alone resulted in a 30-50% reduction in regional cerebral blood flow. It appears that the cerebrovasodilatory effects of NO are independent of local metabolic activity. Utilizing 2-deoxyglucose it was determined that NOS-inhibition does not alter cerebral glucose utilization (Pelligrino et al, 1992).

Role of Nitric Oxide in the Ocular Circulation:

Previous studies investigating the role of NO in the ocular circulation have mostly been in-vitro studies in large ophthalmic vessels. To date few in-vivo studies have been conducted. No studies have investigated the role of NO in the ocular microcirculation using radiolabelled microspheres with simultaneous measurement of blood flow to the retina, choroid and anterior uvea. The current literature reveals little regarding the role of NO in the ocular circulation. The contribution of NO to the autoregulatory capacity of the retinal vasculature in-vivo and the role of nitric oxide in maintaining the low basal tone of the uveal circulation has not been fully investigated.

Horio & Murad (1991) solubilized, isolated and characterized guanylate cyclase (GC) in bovine rod outer segments. Immunoreactivity of monoclonal antibodies against the soluble GC failed to recognize the retinal GC. This suggests that retinal GC is a particular isoform, possibly an axoneme associated protein, of the soluble GC which is activated by NO. They were able to activate retinal GC with NO, suggesting the presence of a heme-prosthetic group similar to the soluble isoform of GC.

Yao et al (1991) investigated the role of the endothelium in the regulation of vascular tone using isolated porcine ophthalmic arterial rings suspended in a myograph system to measure the isometric-tension changes. In arterial rings with intact endothelium the inhibitor of nitric oxide N^G-monomethyl-L-arginine (L-NMMA) evoked concentration dependent contractions (52% of the increase in tension induced with 20mM KCL) which were reversible with L-arginine but not D-arginine. Contractions were abolished by removal of the endothelium with saponin (200 μM/ml). Furthermore, L-NMMA treatment inhibited acetylcholine and bradykinin induced relaxations. These in-vitro findings demonstrate that the endothelium affects the vascular tone of the porcine ophthalmic arteries under basal conditions, and after stimulation with acetylcholine and bradykinin. It is proposed that acetylcholine and bradykinin receptors in the endothelium stimulate the production of NO by promoting calcium entry into the endothelial cell which in turn stimulates

ceNOS (Knowles & Moncada, 1992). The potency of the endothelium regulatory mechanisms in the porcine ophthalmic artery suggest that these mechanisms mediated by NO may play an important physiologic role in the regulation of blood flow to the eye.

Venturini et al (1991) found NOS is present in whole bovine retina homogenates and in rod outer segments. They concluded that NOS activity which was measured spectrophotometrically is dependent on Ca^{2+} and NADPH. The activity of NOS could be inhibited by L-NMMA but not D-NMMA and activity was restored with exogenous L-arginine. Nitric oxide synthase (NOS) has been immunohistochemically localized in whole bovine retina homogenate, in isolated outer segments of rod photoreceptors, in the autonomic nerve fibers of the choroid, and in the retinal pigment epithelium (Bredt et al, 1990).

Studies by Haefliger, et al (1992) using human ophthalmic arterial rings obtained 5-10 hours post-mortem and placed in a similar myograph system to that of Yao found NO formation in response to acetylcholine and bradykinin. The responses were significantly reduced by N^G-nitro-L-arginine (L-NNA). Furthermore, relaxations of the human ophthalmic artery in response to histamine were inhibited by L-NNA. The receptor involved in NO release evoked by histamine must be of the H_1 histaminergic subtype since H_2 histaminergic receptors were shown to induce direct, nitric oxide independent relaxation preventable by blockade with cimetidine. These myograph studies concluded that the human ophthalmic artery exhibits a basal release of nitric oxide and is in a state of constant vasodilation resulting from the production of nitric oxide. These in-vitro findings suggest that NO plays an important physiologic role in the regulation of ocular blood flow.

It seems feasible that the L-arginine:NO pathway in the eye may function in phototransduction by direct stimulation of the particulate isoform of guanylate cyclase or serve a function in the regulation of blood flow (Horio & Murad, 1991). Nitric oxide is an endogenous activator of soluble guanylyl cyclase and participates in signal transduction during vasodilation and neurotransmission

Veriac et al (1993) investigated the role of NO and oxygen free radicals in the rabbit retina

under high intraocular pressure (100 mmHg). They related hypoxic changes to the retina with electroretinogram (ERG) extinction. They report that hypoxic changes, as determined by ERG, were prevented by pre-treatment of intravitreal administration of sodium nitroprusside, a nitric oxide donor. Hypoxic changes were also prevented by intravenous pre-treatment with superoxide dismutase and catalase, both oxygen free scavengers. Furthermore, if nitro-L-arginine was administered intravitrealy the anti-hypoxic protective effects were lost. They concluded that NO maintains retina perfusion at high intraocular pressure by vasodilation and that ischemia at high intraocular pressure impeded the effects of NO through generation of oxygen free radicals such as the oxide peroxynitrite ($ONOO^-$).

Joyner et al (1993), using the technique of light-dye in-vivo microscopy, investigated the role of the endothelium in mediating the acetylcholine induced vasodilation of microvessels of the choroid and retina from the human eye grafted into the hamster cheek pouch. L-NAME reduced the acetylcholine response in retinal microvessels but not choroidal microvessels.

This project examines mechanisms which govern the regulation of ocular blood flow. We will investigate the mechanism by which the retina maintains its autoregulatory capacity. The mechanism(s) operant in the regulation of retinal and uveal blood flow appear to be radically different. 1) Is the vasoactive metabolite nitric oxide involved in maintaining the autoregulatory capacity of the retinal vasculature ? 2) Is nitric oxide involved in establishing the low basal vascular tone of the uveal vasculature ? 3) When uveal blood flow decreases (due to a decreased perfusion pressure gradient), is retinal blood flow affected differently when nitric oxide synthase is blocked ? We will investigate the vascular regulatory interrelationship between the retina and uveal circulations.

The findings of this project could provide greater understanding of the pathogenic mechanisms involved in normo-tension and high-tension glaucoma (Luscher, 1991; Gasser & Flammer, 1991). Failure of regulatory vascular reactivity is an important component of many retinal vascular diseases that occur very early in the evolution of these diseases (Yoshida et al, 1983). Endothelial dysfunction of ocular vessels may represent a new mechanism in the pathogenesis of

ocular complications associated with a disturbance of regional blood flow. Among these complications are diabetic retinopathy (Robison & Laver, 1993), hypertensive vascular disease (Luscher & Vanhoutte, 1990), and ocular vasospasms (Luscher, 1991). Conducting such investigations on the regulatory capacity of the retinal vasculature could demonstrate the important physiological role for endothelium dependent vasoactive substances in the regulation of the ophthalmic circulation, and lead to direct clinical application in ophthalmology.

We examined the potential mechanisms at play governing the autoregulatory capacities of the retina and choroid by altering perfusion pressure to the eye in the presence of intravenously administered nitric oxide synthase inhibitor (L-NAME) or its inactive enantiomer (D-NAME). We measured volumetric blood flow to the retina and uvea by the radiolabelled microsphere method in piglets.

MATERIALS AND METHODS

Selection of Animal Model:

In order to eventually apply the current theories and findings of this study to the regulation of ocular blood flow in humans, it is imperative that preliminary studies be conducted utilizing an animal eye-model that shares neurological, structural, and vascular similarities to the human eye (Molnar et al, 1985). The porcine eye has neuroanatomic and vascular similarities to the human eye. And is in many respects more like that of humans than the rabbit, cat, dog, sheep, horse, goat, and cattle (Prince et al, 1960).

The porcine retina is holangiotic (entirely vascularized) as is the human retina (Wolff, 1976). Furthermore, the porcine retina reveals an area sufficiently devoid of blood vessels to suggest macular qualities, a characteristic found only in man, cat, and some other primates (Prince et al 1960; Wolff, 1976). In addition, the porcine retina is well endowed with cones due to its diurnal evolution (Prince et al, 1960).

The choroidal tapetum (a reflective tissue layer) is seen in most mammals, but it is absent in humans, pigs, and rabbits (Prince et al, 1960; Wolff, 1976). The choroid is found only in the vertebrate eye (Wolff, 1976). The pig's choroidal vessels range in size from capillaries to 70μm in diameter; the human choroidal vessels are of a similar diameter (Prince et al, 1960; Ernest, 1989b). Bruch's membrane in the human is well developed, measuring 2-4μm in thickness. The pig's Bruch's membrane is also well developed and more apparent than in many other animals (Prince et al, 1960; Wolff, 1976).

In contrast, the eye of many other domestic animals differs significantly from that of humans. The rabbit has a merangiotic retina (partly vascularized), lacks a macula, and is almost exclusively composed of rods (Prince et al, 1960). The cat has a holangiotic retina with a macula and a peripheral cone to rod ratio of 25:1 but possesses a tapetum 60-80 μm thick (Prince et al, 1960). The dog and sheep both possess a fibrous tapetum, and a retina predominantly composed of rods (Prince et al, 1960; Wolff, 1976).

Surgical Preparation:

All experiments were performed on 1-2 week old (3-4 kg) domestic piglets (Thomas D. Morris, Inc. Reisterstown, MD) of either gender. Animals were anesthetized with an intra-peritoneal injection of sodium pentobarbital (30 mg/kg). Usually a cephalic or antecubital vein was accessed with a 22 gauge microcatheter to maintain a surgical plane of anesthesia until other vascular access was obtained. Anesthesia was maintained during surgery by constant infusion (approximately 16 mg/kg/hr) for the duration of the experimental procedure. Animals were intubated (Mallinckrodt Type ET-3.0mm ID, Glen Falls, NY), to maintain an open airway and placed on a positive pressure respirator pump (Harvard Apparatus Dual Phase model 613, Millis, MA). Ventilatory rate (18-25 breaths/min.) and tidal volume (50 ml/stroke) were controlled to maintain end-expired carbon dioxide (CO_2) between 5-6%. End expired CO_2 was continuously monitored with a calibrated Sensormedics CO_2 analyzer (Medical Gas Analyzer LB-2, Anaheim, CA).

Body temperature was monitored by rectal temperature and maintained constant (39^0 C) with the use of a K-pad (American Hamilton K-20, Cincinnati, OH) and a thermostatically controlled heating lamp (Thermistemp-74, Yellowspring, OH). Two arterial, and two venous heparinized catheters (Cordis 5-F Angiographic Catheter, Miami, FL) were introduced into the femoral vessels to measure blood pressure, make microsphere measurements, blood gas analysis, supplemental anesthesia, intravenous fluids and administration of D-NAME or L-NAME (both from Sigma Chemical Co., St. Louis, MO). Arterial blood pressure was measured from a catheter advanced into the abdominal aorta from the left femoral artery. All vascular pressures were referenced to the hydrostatic plane at the level of the heart. Pressure transducers (Gould Statham P23ID & P23Db series, Oxnard, CA) were calibrated with a mercury manometer (Spectramed X-caliber, Oxnard, CA). Continuous measurements of arterial pressure (mean and pulsatile), heart rate, and intraocular pressure (IOP) were recorded on a polygraph (Gould 8-Channel RS3800, Cleveland, OH). Supplemental O_2 was administered as needed to keep arterial PO_2 between 80-100 mmHg. Anaerobic arterial blood samples were collected for determination of PO_2, PCO_2, pH,

(Instrumentation Laboratory pH/Blood Gas Analyzer 1306, Lexington, MA) and oxygen content, and arterial hemoglobin content (Radiometer OSM3-Hemoximeter, Cleveland, OH). The blood samples were well agitated prior to blood gas analysis.

A heat cautery (Geiger Instruments, Geiger, PA) was utilized to perform a left lateral thoracotomy for the intra-atrial injection of radiolabelled microspheres. A Weitlander retractor (Roboz Surgical Instruments, Rockville, MD) was utilized to expose the heart and access the left atria at the level of the fourth intercostal space. The upper lung lobe was displaced dorsally and any atelectasis was overcome by reinflating the lungs with positive pressure ventilation at the completion of the catheterization procedure. The catheter was introduced and secured into the left atria and catheter position was verified at necropsy. After completion of the lateral thoracotomy the animal was placed in a prone position without head elevation for the remainder of the experimental procedure.

The eyes were held open by a pair of micro dissecting retractors (Roboz Surgical Instruments, Rockville, MD) and each ocular globe stabilized for the cannulation procedure by suturing the conjunctiva. The animals were paralyzed by systemic injection of pancuronium bromide (1 mg/kg/IV; Elkins-Sinn, Inc. Cherry Hill, NJ) to prevent eye movement caused by contraction of the extra ocular muscles. Animals were heparinized at the completion of the cannulation procedure (0.5ml/kg/IV; 1000 units/ml heparin sodium; Elkins-Sinn, Inc. Cherry Hill, NJ). Manipulation and monitoring of intraocular pressure (IOP) was accomplished by cannulation of the anterior chamber of the eye. The approach of anterior chamber cannulation for altering intraocular pressure is widely used, and is considered by many to be the method of choice for inducing acute changes in intraocular pressure in experimental animals (Barany, 1964; Ffytche et al, 1974; Sossi & Anderson, 1983; Novack & Stefansson, 1990; Coleman et al, 1991). Two 23 gauge needles were inserted thru the cornea near the limbus and into the anterior chamber where the needles were immobilized **(Figure 3).** The intraocular pressure was regulated by hydrostatic pressure. One needle was connected via tygon tubing to a variable height, fluid-filled reservoir.

Figure 3: Apparatus for monitoring and manipulating intraocular pressure (IOP). Two 23 gauge needles were inserted near the limbus into the anterior chamber of each eye. One needle was connected via tubing to a movable reservoir containing mock aqueous humor. The IOP was regulated hydrostatically by altering the height of the reservoir. The second needle was connected via tubing to a pressure transducer for the continous monitoring of IOP. Intraocular pressure measured at the anterior chamber was verified at the posterior pole of the eye by inserting a 23 gauge needle directly into the vitreous chamber at the completion of the experimental protocol. A stopcock arrangement allowed alternating measurements of anterior and vitreous chamber pressures by a single transducer without changing needle position.

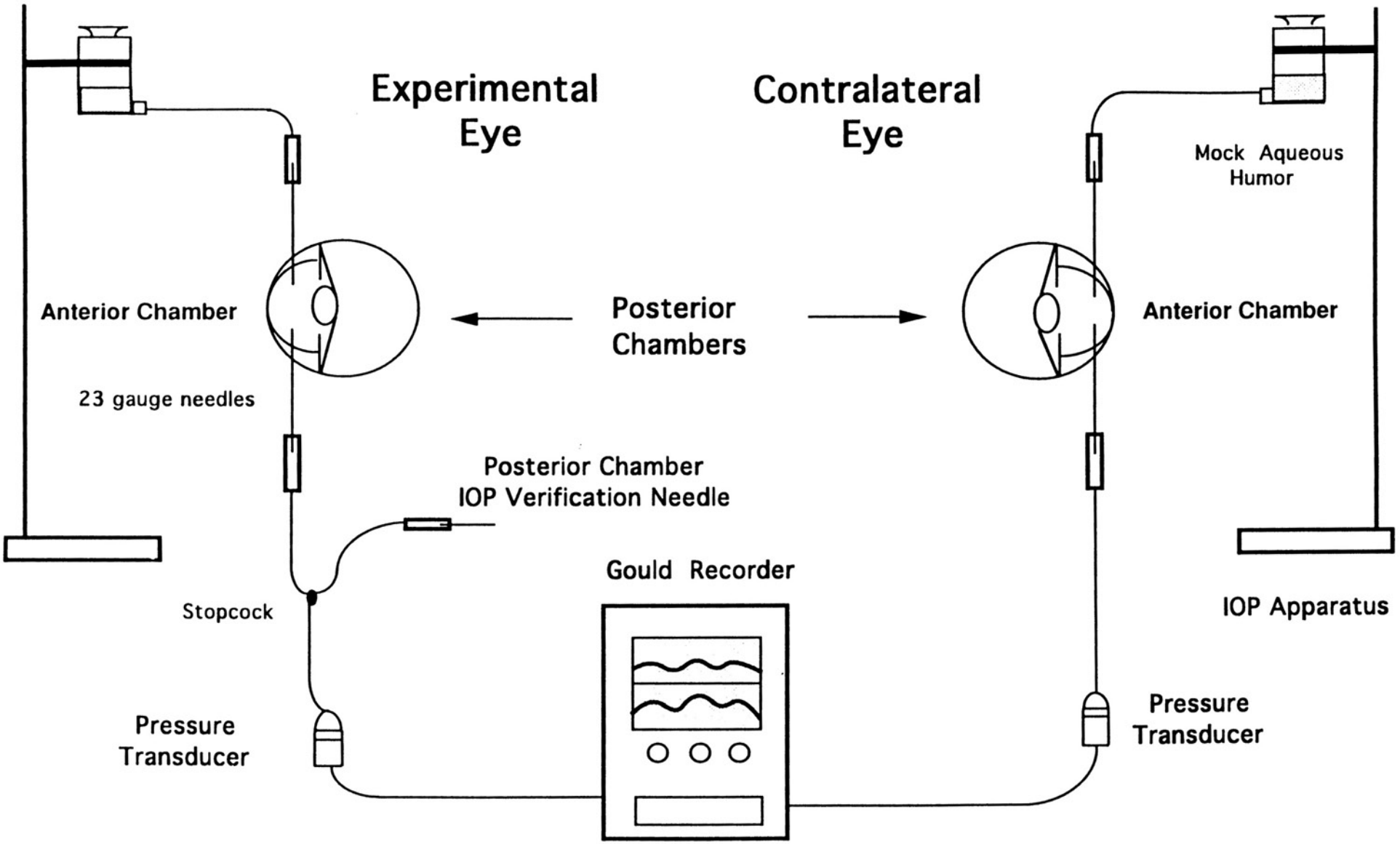
Experimental Eye
Contralateral Eye
Mock Aqueous Humor
Anterior Chamber
Posterior Chambers
Anterior Chamber
23 gauge needles
Posterior Chamber IOP Verification Needle
Gould Recorder
Stopcock
IOP Apparatus
Pressure Transducer
Pressure Transducer

Altering the height of the reservoir governed the hydrostatic pressure in the anterior chamber of the eye. The infused fluid was "mock" aqueous humor prepared to the same osmolarity (287 mOsm/kg; Na^+ 127 mEq/L) and composition as natural aqueous humor. The composition of aqueous humor has been well characterized and the preparation of "mock" aqueous humor for intraocular infusions has been described (Barany, 1964) (see Appendix). The mock aqueous humor was stored covered at 4^0C, and warmed to $37^0 \pm 5^0$C prior to use. Fresh batches of the aqueous humor were prepared as needed. A second 23 gauge needle was inserted thru the cornea at the limbus and immobilized in the anterior chamber of each eye. The needles were connected via tygon tubing to a transducer for the continuous monitoring of intraocular pressure. Ocular perfusion pressure (OPP) was defined as the difference in mean arterial blood pressure determined from the abdominal aorta minus the mean pressure measured at the anterior chamber of the eye (MAP-IOP). Verification that the recorded anterior chamber pressure reflected the pressure transmitted to the posterior pole of the eye was accomplished at the completion of the experimental protocol. An additional 23 gauge needle was inserted through the sclera into the vitreous chamber. A stopcock arrangement allowed the pressures of the anterior chamber and vitreous chamber of the eye to be measured interchangeably by a single transducer without changing needle position. Tests to verify the proper functioning of the intraocular apparatus and proper balance of pressure transducers were conducted at the completion of the surgical protocol (**Figure 4**). The ocular perfusion pressure was controlled by varying intraocular pressure hydrostatically, without controlling the prevailing blood pressure. Seventy-five minutes were allowed for stabilization of the animals prior to data collection to minimize the effects from cannulation and surgical manipulations (see temporal control studies).

At the completion of the surgical protocol the animals were euthanized by anesthetic overdose (90 mg/kg) or saturated KCL to effect. The eyes were enucleated and the kidneys were removed and placed in 10% buffered formalin. The eyes were dissected while fresh. The retina, choroid, and anterior uvea (iris, ciliary body, ciliary process) were isolated from each eye and dried for 12 hours at 105.0^0C in pre-weighed glass vials. The choroid was separated from the anterior

Figure 4: Characteristic pulsatile and mean intraocular pressure (IOP) tracing form the right eye. Shown are 2-3 mmHg pulsatile oscillations which coincide with the cardiac cycle. Mean baseline IOP is 14 mmHg. Arrow shows a hydrostatically induced acute elevation in IOP caused by raising the height of the reservoir containing mock aqueous humor. The responsiveness of the system to changes in the height of the reservoir was verified at the completion of each experiment. The sinusoidal IOP tracings demonstrate the response of sequentially lowering and then raising the reservoir of the IOP-apparatus. Note the short time-constant for the response.

Time scale for IOP tracing:

A. Pulsatile IOP = 4 seconds; mean IOP = 5 seconds; chart speed 5 mm/second

B. 11 seconds; chart speed 5 mm/second

C. 2 seconds; chart speed 25 mm/second

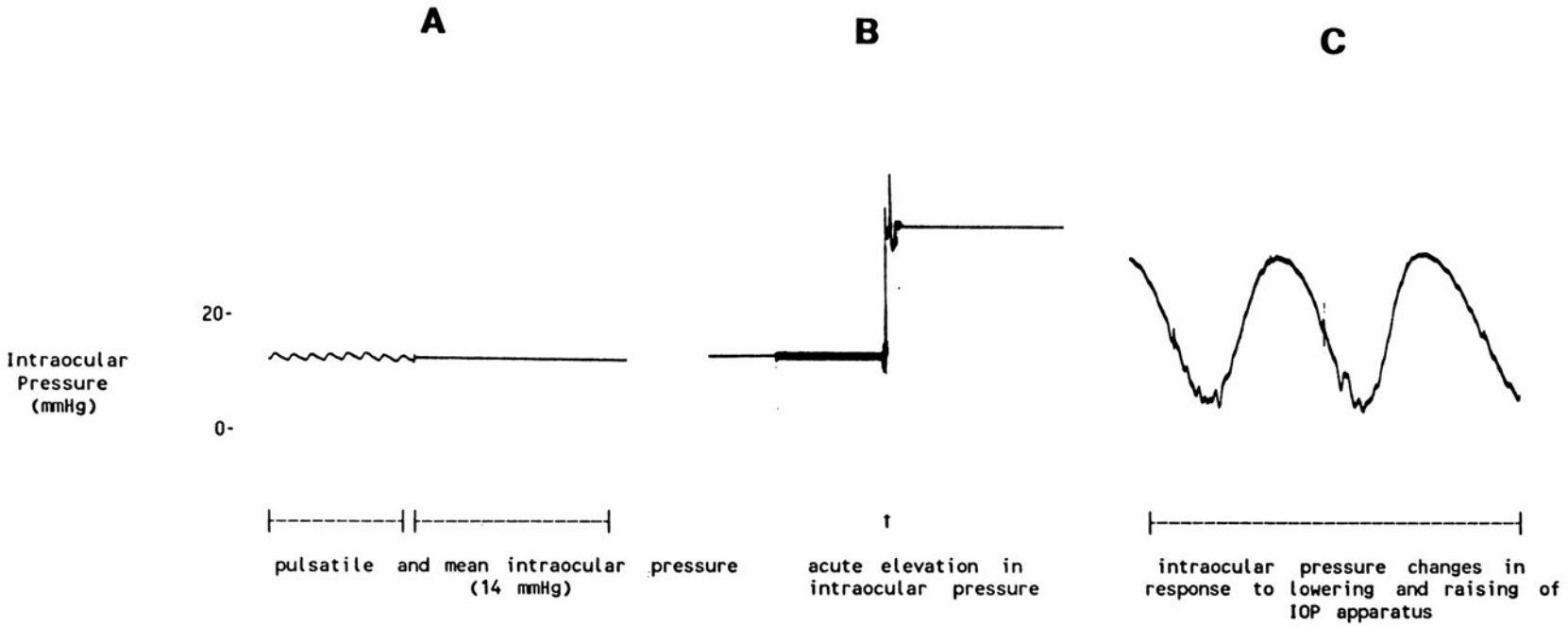
A
B
C
Intraocular Pressure (mmHg)
20-
0-
pulsatile and mean intraocular pressure (14 mmHg)
acute elevation in intraocular pressure
intraocular pressure changes in response to lowering and raising of IOP apparatus

uvea at the ora serrata. The dry weights of the eye tissues were utilized for blood flow determinations. All ocular blood flow measurements are expressed as: milliliters/minute/100 grams of dry tissue weight. Wet tissue weights were used for kidney flow. All tissues were placed into gamma tubes for subsequent gamma-radiation counting by least-squares analysis of the gamma spectra.

The use and handling of the animals in this study conformed to the guideline and regulations established by the United States Department of Health and Human Services as stipulated in the Guide for the Care and Use of Laboratory Animals. All animals were treated according to the guidelines set forth by the Uniformed Services University of the Health Sciences. The investigator of this study has taken every precaution to insure the humane use of these animals in accordance with the following: The "U.S. Government Principles for the Utilization and Care of Vertebrate Animals Used in Testing, Research, and Training", USUHS Instruction 3204 "The Use of Animals in USUHS Programs," Public Health Service "Policy on Humane Care and Use of Laboratory Animals," the 1990 "Report of the AVMA Panel on Euthanasia", and the ARVO Resolution on the use of Animals in Research.

Temporal Control Studies

We have observed variable ocular blood flows for a period of time following surgical manipulation. Therefore, we conducted a temporal control study to establish the optimum post-surgical period in which to perform ocular blood flow determinations. Regional ocular blood flow determinations were made in six piglets (average 10 ± 3 days old; average 3.5 ± 0.22 kg) for the retina, choroid, and anterior uvea from each eye at six pre-determined time intervals. The temporal control group of piglets were matched by age and weight to the experimental group of animals (average 9 ± 3 days old; average 3.5 ± 0.12 kg). Three temporal control experiments were conducted at the commencement of the study. Three additional animals were utilized as temporal controls at a later time. The duration of the temporal control studies spanned a period of six

months and included a total of six piglets. Baseline intraocular pressure (left 12 ± 1 mmHg; right 10 ± 1 mmHg) measurements were recorded immediately following cannulation of the anterior chamber. Time zero was designated as the completion of the cannulation procedure to the anterior eye chambers. The first blood flow measurement was obtained at an average time of 6 minutes after completing the surgical protocol. Sequential blood flow determinations were obtained at an average time of: 24, 44, 64, 84, and 106 minutes (± 1 min for all time points) post completion of the surgical protocol. Blood flow determination in one piglet at the 6 minute time point was not possible due to difficulties with the microsphere blood reference withdrawal pump. The mean (± SEM) blood flows for the left, right and combined retinal, choroidal and anterior uveal tissues at the various time points were determined. Blood gases were determined prior to all blood flow measurements. Based on evaluation of this data it was determined that 60 to 85 minutes stabilization post surgical manipulation and anterior chamber cannulation was sufficient prior to making blood flow determinations in the experimental animals. This stabilization period was favored since it allowed a reasonable time course for the completion of the experimental protocol.

Studies With The Vehicle Control D-NAME And With The Nitric Oxide Synthase Inhibitor L-NAME

A total of 12 piglets were utilized. The animals in each group (n=6) were matched by age and weight (L-NAME 10 ± 3 days, 3.4 ± 0.21 kg; D-NAME 9 ± 4 days, 3.6 ± 0.11 kg). Constant infusions (Sage Instruments, Syringe Pump-351, Cambridge, MA) of D-NAME or L-NAME were accomplished via a catheter introduced into the right femoral vein. Either L-NAME or D-NAME (30 mg/kg/hr) were infused starting 45 minutes post-completion of the surgical protocol and for a minimum of thirty minutes prior to the first blood flow determination. On this time schedule, the first blood flow determination was obtained at 75 minutes post-completion of surgery, which based on our temporal control data demonstrated stability of ocular blood flow.

Baseline intraocular pressure, control ocular perfusion pressures, and baseline blood flow measurements for the retina, choroid, and anterior uvea were determined for both eyes in each

group. The perfusion pressure of ONE eye was incrementally reduced as follows : 60 mmHg, 50 mmHg, 40 mmHg, 30 mmHg, 20 mmHg. Blood gas analyses were conducted immediately preceding each microsphere injection. The intraocular pressure of the contralateral eye was monitored in the same described fashion but, the intraocular pressure was maintained near baseline (12 ± 2 mmHg) for the duration of the experiment. The eye which was subjected to experimentally induced changes in perfusion pressure was randomly assigned in each animal. A minimum of ten minutes was allowed for stabilization of intraocular pressure after each induced change in ocular perfusion pressure gradient (Barany, 1964).

Hemodynamic Parameters:

Baseline hemodynamic parameters of blood pressure, heart rate, and Hct were recorded. Baseline mean arterial blood pressure was 92 ± 4 mmHg, mean systolic and mean diastolic blood pressures were 119 ± 5 mmHg and 75 ± 4 mmHg, respectively. Mean heart rate was 197 ± 13 beats/minute, and no change in heart rate occurred after administration of D-NAME or L-NAME (**Table I**). Mean arterial pressure did not change following D-NAME infusion (**Figure 5**). After thirty minutes of L-NAME infusion there were significant increases (31 mmHg, 36%) in mean arterial blood pressure (from 86 ± 5 to 117 ± 2 mmHg) in all animals tested. Diastolic pressure increased by 51 % (from 68 ± 4 to 103 ± 2) , while systolic pressure increased 24 % (from 112 ± 5 to 139 ± 4 mmHg). Administration of L-NAME significantly elevated total peripheral resistance and reduced cardiac output. Cardiac outputs were calculated in milliliters/minute and also normalized to the weight of the animals. The mean cardiac output with D-NAME was 553 ± 25 ml/min (150 ± 6 ml/min/kg). The mean cardiac output with L-NAME was 384 ± 20 ml/min (118 ± 8 ml/min/kg), a 31% reduction from the D-NAME treated animals. When normalized to animal weight the reduction in cardiac output with L-NAME was 21%.

Table I: Hemodynamic parameters for the D-NAME, L-NAME and L-Arginine treated animals. Shown are the average heart rates, mean and pulsatile blood pressures, cardiac outputs in ml/min and normalized to animal weight (ml/min/Kg). No change in mean heart rate was observed following drug treatments. Significant increases in blood pressure were observed following L-NAME. L-NAME significantly reduced cardiac output by 31% from the D-NAME treated animals, and cardiac output showed a 21% reduction when normalized to animal weight.

Table I. HEMODYNAMIC PARAMETERS FOR D- & L-NAME AND L-ARGININE TREATED ANIMALS

	Baseline	D-NAME	L-NAME	L-ARG
Average Heart rate, beats/min	197 ± 13	200 ± 21	193 ± 20	180 ± 41
Mean arterial blood pressure, mmHg	92 ± 4	86 ± 5	117 ± 2*	97 ± 8
Systolic blood pressure, mmHg	119 ± 5	112 ± 5	139 ± 4*	107 ± 10
Diastolic blood pressure, mmHg	75 ± 4	68 ± 4	103 ± 2*	82 ± 5
Cardiac output, L/min	N/A	553 ± 25	384 ± 20†	527 ± 54
Cardiac output, L/min/Kg	N/A	150 ± 6	118 ± 8 †	146 ± 17

Values are means ± SEM.
* Significantly different from baseline control $p<0.05$.
† Significantly different from D-NAME $p<0.05$.

Figure 5: Effects of systemic D-NAME infusion (30 mg/kg/hr) on blood pressure. Baseline MAP pre D-NAME was 107 mmHg and pulsatile BP of 135/90. Thirty minutes post D-NAME infusion MAP remained essentially unaffected with a MAP of 105 mmHg and pulsatile BP of 135/90. Mean HR was 197 ± 13 beats/minute, no change in HR was observed after administration of D-NAME or L-NAME.

Bottom Trace: Effects of systemic L-NAME infusion (30 mg/Kg/hr) on blood pressure. Baseline MAP pre L-NAME was 100 mmHg and pulsatile BP of 125/85. After thirty minutes post L-NAME infusion MAP was elevated in all animals tested. MAP increased by 35 mmHg (35%) to 135 mmHg and pulsatile BP of 160/120. Diastolic pressure increased by 41%, while systolic pressure increased 28%.

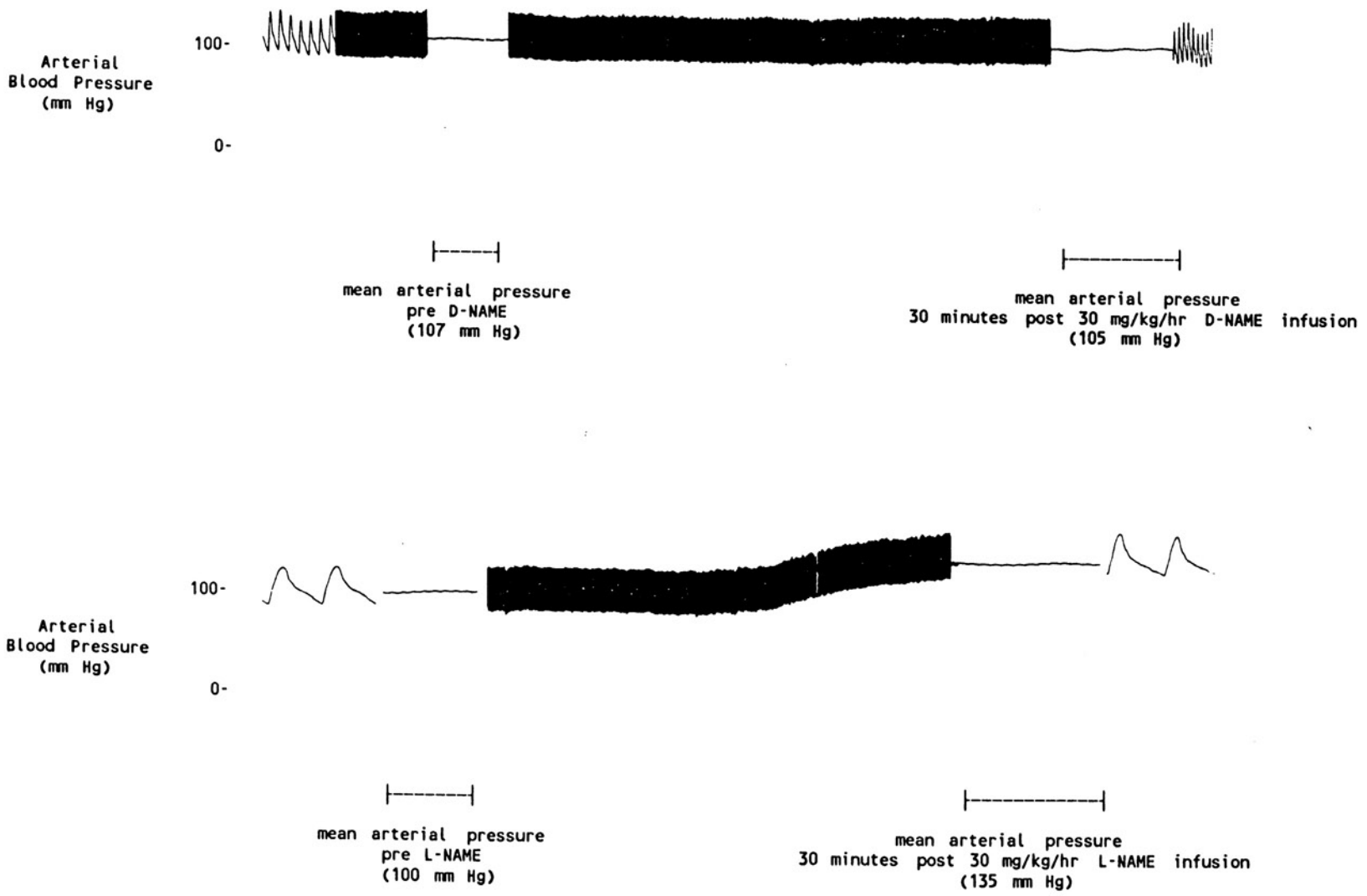
Arterial
Blood Pressure
(mm Hg)
100-
0-
mean arterial pressure
pre D-NAME
(107 mm Hg)
mean arterial pressure
30 minutes post 30 mg/kg/hr D-NAME infusion
(105 mm Hg)
Arterial
Blood Pressure
(mm Hg)
100-
0-
mean arterial pressure
pre L-NAME
(100 mm Hg)
mean arterial pressure
30 minutes post 30 mg/kg/hr L-NAME infusion
(135 mm Hg)

MAP and IOP Matched Animals:

To assure that decreased ocular blood flow to the uvea resulted from nitric oxide blockade by L-NAME and not as a result of increased sympathetic tone to the uveal circulation elicited as a protective response from overperfusion under acute elevations in mean arterial pressure, we matched and compared blood flow for specific cases from the D-NAME and L-NAME treated animals which had similar mean intraocular pressures and a similar mean arterial pressure range. From a total of 12 animals, two to four animals per group were matched at each of the following mean ocular perfusion pressures (± 2 mmHg): 60, 50, 39, 31, and 21 mmHg. These ocular perfusion pressures were grouped with the following range of mean arterial blood pressure: 105-112, 110-115, 115-120, 110-120, 105-112 mmHg, respectively. Blood flow to the retina, choroid, and anterior uvea in the pressure matched categories was compared between the D-NAME and L-NAME treated animals.

Reversal of NOS Blockade With Exogenous L-Arginine

L-arginine (Sigma Chemical Co., St. Louis, MO) was administered to five piglets to antagonize the nitric oxide blockade induced with L-NAME. An L-NAME infusion was administered as previously described and was maintained throughout the experimental protocol. Mean and pulsatile blood pressures were recorded for baseline conditions, following L-NAME infusion, and following L-arginine administration (**Figure 6**). Two isotopes were used to make blood flow determinations. The first blood flow determination was taken after a minimum of thirty minutes of L-NAME infusion. The ocular perfusion pressure of ONE eye (randomly selected) was maintained at the baseline perfusion pressure (99 ± 4 mmHg), while the contralateral eye had its OPP decreased from baseline to a perfusion pressure of 26 ± 2 mmHg. A minimum of ten minutes were allowed for stabilization of intraocular pressures prior to any blood flow determinations. Blood gases were analyzed prior to all microsphere injections.

Figure 6: Mean and pulsatile blood pressure tracing for baseline conditions, following L-NAME infusion, and following L-arginine bolus administration. Baseline MAP of 85 mmHg was elevated to 117 mmHg following 30 minutes of L-NAME infusion (30 mg/kg/hr). Tracing shows a dose-related marked transient hypotensive effect following intracardiac bolus administration of L-arginine (180 mg/kg approximately 6 times the dose of L-NAME). In this animal, the dose of L-arginine antagonized 28% of the elevation in MAP induced by L-NAME infusion.

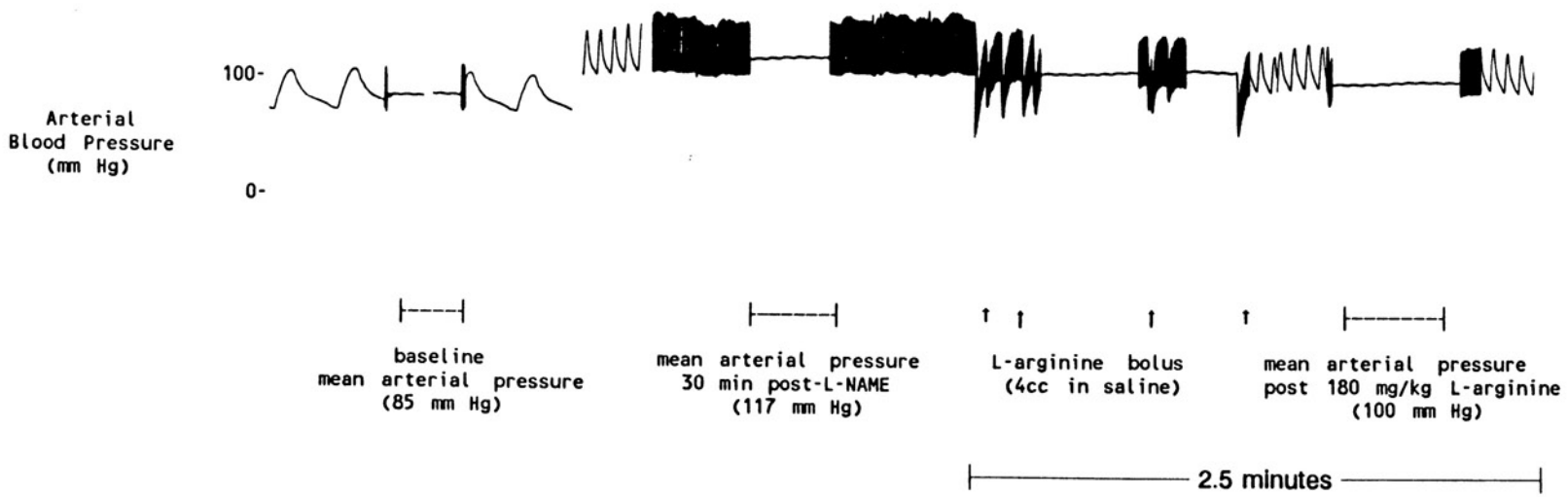
Arterial
Blood Pressure
(mm Hg)
100-
0-
baseline
mean arterial pressure
(85 mm Hg)
mean arterial pressure
30 min post-L-NAME
(117 mm Hg)
L-arginine bolus
(4cc in saline)
mean arterial pressure
post 180 mg/kg L-arginine
(100 mm Hg)
2.5 minutes

The second blood flow measurement was taken at 10 minutes following administration of L-arginine. An exogenous bolus (4 mls) of L-arginine (180 mg/kg; approximately 6x the dose of L-NAME) was dissolved in saline (pH =11) and administered via catheter directly into the left atria. This dose of L-arginine antagonized 13.4 ± 7 % of the elevation in mean arterial blood pressure induced by L-NAME infusion. Because L-arginine caused a sudden drop in mean arterial pressure, the perfusion pressure of the eye with an experimentally altered pressure was adjusted prior to and after L-arginine administration in order to maintain a relatively constant perfusion pressure of 28 ± 3 mmHg.

MICROSPHERES: Historical Development:

Injecting particles to measure circulatory parameters was pioneered by Pohlman in 1909 using small starch granules to map the flow pattern in the fetal pig heart. Subsequent experiments on the study of the circulation in various vascular beds used modifications of different type particles injected into the intravascular compartment. Prinzmetal et al (1947) performed coronary perfusions with glass microspheres to study the collateral circulation of the heart. Radioactive ^{24}Na glass microspheres were developed in 1958 using neutron bombardment. During 1961-63 ceramic microspheres with various radionuclides were developed. Both the glass and ceramic microspheres had the disadvantage of high densities which promoted rapid settling within the blood stream. Macroaggregates of albumin labelled with ^{121}I were developed in 1964. The macroaggregates of albumin had the distinct advantage that they did not experience rapid sedimentation in the blood because they were lower in density, but they suffered from a wide variability in size.

Use of dextran and "carbonized" plastic radiolabelled microspheres to study the distribution of blood flow, cardiac output, and organ blood flow was pioneered by Rudolph and Heymann in 1967. These microspheres had tremendous practical and theoretical advantages over those previously described. They had a specific density (1.25-1.30 g/ml) comparable to that of whole blood (1.05-1.098 g/ml), had a uniform size distribution, and the nuclide was incorporated into the plastic which minimized leaching of the radioactivity.

Current Manufacturing Specifications Of Microspheres:

Polystyrene radiolabelled microspheres (density: 1.3-1.4 g/ml) are distributed by New England Nuclear Corporation (NEN) in sterile injection vials. We purchase multiple 10ml vials of 15±1μm diameter microspheres suspended in 0.9% NaCl and 0.01% Tween 80. A 0.05% solution of the detergent polyoxyethylene 80 sorbitan monooleate (Tween 80) is added by our laboratory to prevent aggregation of microspheres. The region of interest (ROI) energy range over which gamma emissions were counted and integrated, the half-life, and the principal gamma emission energies of the isotopes are shown on **Table II**. Selection of the various isotopes was determined based on half-life and on the easily distinguishable differences between their gamma energy spectral distribution characteristics.

Table II: Physical characteristics of the isotopes. Shown are the energy ranges over which gamma emissions were counted and integrated (ROI), the half-life, and the principal gamma emission energies (keV) of each isotope.

Table II.

Physical characteristics of 15±1 μm diameter radiolabelled microspheres

Radionuclide	Region of Interest (ROI) Windows	Half-Life (days)	Principal γ Energy (keV)
^{153}Gadolinum	64-100	241.5	97 103
^{114m}Indium	150-250	49.5	190-192 (also 558 and 725)
^{113}Tin	348-452	115.1	392-393
^{85}Strontium	464-560	64.8	514
^{95}Niobium	660-812	35.1	765-766
^{46}Scandium	880-1300	83.8	889 1120

Sources: NEN-TRAC microsphere technical data sheet; Linden, 1983; Lide, 1993.

QUANTITATION OF MICROSPHERES:

Counting Equipment:

A 512 multichannel pulse height sodium iodide (NaI) crystal gamma counter detector (Tracor Analytic 2250, Elk Grove Village, IL) with a total energy range of 0-2048 KeV was utilized to analyze the gamma emission spectra of the isotopes. Region of interest (ROI) windows were established for each of the isotopes. The energy window for each isotope were empirically adjusted using standards of pure isotope. This method of adjustment optimized counts by compensating for spectral distribution shifts due to electronic fluctuations from high voltage or gain instability. The ROI windows were not contiguous but were specifically selected to include the major spectral energy peak(s) of each isotope. Spectral regions which comprised low count rates for a given isotope were not included in the ROI window, thus minimizing the counts of other isotopes in that ROI window.

With the exception of Indium (^{114m}In) the remaining five isotopes have few measurable counts above their principal energy peak(s). Below the principal energy peak of each isotope substantial counts can be detected due to Compton interactions of gamma emissions. Compton interactions (also referred to as incoherent scattering or Compton Scattering) is due to photon-electron interactions (Compton, 1961). The incident photon with linear momentum collides with a weakly bound electron, initially at rest. The photon can transmit energy and linear momentum to an individual electron in an elastic collision with the electron. The photon after the collision scatters off at an angle and has less energy than before the collision. Compton scattering is due to the decrease in energy (lower KeV) of the scattered photon in imparting recoil energy to the electron (Compton, 1961). Compton interactions of gamma emissions is the predominant interaction which occurs for the range of photon energies (KeV) used in this study. Comptom interactions of emissions from the higher energy isotopes contribute to "crossover" counts in the lower energy isotopes which must be accounted for in order to determine the counts which belong exclusively

to the isotope of interest. Each isotope used has a characteristic gamma-radiation emission with an easily distinguishable energy peak. Since more than one isotope was present in any given piece of tissue, it was necessary to adjust for Compton interactions of higher energy emitting isotopes in the characteristic energy peak of the lower energy emitting isotopes. For instance, scandium (^{46}Sc) has few measurable counts above its principal energy peaks (889, 1120 KeV). However, Compton interactions below (to the left of) the principal energy peaks of scandium produce "crossover" factors in all lower gamma energies ROI windows.

A characteristic example of the total gamma counts from each isotope standard detected at the various ROI windows is represented in **Table III**. Average ambient background gamma counts for each isotope were determined from blank tubes at the time of analysis. The average background count for each isotope is subtracted from the total counts to yield "corrected counts."

The blood sample tubes were rinsed with deionized water to promote red blood cell hemolysis and prevent suspension of microspheres. This provides a settled microsphere configuration which is considered to provide the optimal counting efficiency (Rudolph & Heymann, 1967). The counting vials were never filled over 3 cm high so as to avoid counting distortions due to different counting geometries. Differences in the microsphere configuration among samples during analysis can lead to count distortions arising from reduced counting efficiency. The settled microsphere configuration matched the configuration of the dessicated ocular tissue best.

The shape of the gamma spectrum for any pure sample of isotope is constant (Rudolph & Heymann, 1967). Therefore the counts of any isotope in a mixture can be determined knowing what proportion of each isotope appears in each ROI energy window. When a particular isotope was not utilized (e.g., during the L-arginine experiments, where only two microspheres were used) the factors of the missing isotopes were not included in the matrix notation.

Table III: Characteristic example of the total gamma counts from each isotope standard detected at the various Region of Interest (ROI) windows. Average ambient background gamma counts for each isotope were determined from blank tubes at the time of analysis. The average background count for each isotope is subtracted from the total counts to yield "corrected counts".

Table III.

ISOTOPE Region Of Interest (ROI) WINDOWS

	Gd	In	Sn	Sr	Nb	Sc
Standards						
Gd	3086508	134268	542	495	217	526
In	109274	357765	29166	33386	31816	25257
Sn	134734	69269	559367	1458	726	296
Sr	135535	99966	32428	434538	463	1349
Nb	33955	30136	28393	19392	103466	3419
Sc	87291	77170	91343	86215	87359	379842
Average Background	210.2	112.2	87	266.8	44.4	82.2

Simultaneous Equation Method

Decomposition and analytic quantitation of the gamma spectra for the six isotopes was performed by the technique of Schosser et al (1979). Since a tissue specimen from the eye contains a mixture of six known isotopes (i), and since there are six nonoverlapping Region of Interest (ROI) windows, one for each isotope, i = w. Let C_{iw} represent the counts of the i^{th} isotope in the w^{th} region of interest window. Therefore the cross-over factor (F) of the i^{th} isotope in the w^{th} region of interest window is shown in **Table IV** and denoted by:

$$F_{i,w} = C_{iw}/C_{ii} \qquad (1)$$

The cross-over factor for any particular isotope is expressed as a fraction of the "corrected counts" measured in the principal energy window of the isotope of interest. Thus, the cross-over factor for the isotope of interest in its own ROI window is unity. For instance, to determine the cross-over factor of tin (Sn) in the niobium (Nb) ROI window the following calculation is performed from the data in **Table III**: (28393-87)/(103466-44.4) = 0.273695 which yields the fraction of tin (Sn) counts in the Niobium (Nb) window.

Let C_w represent the counts observed from a mixture of isotopes in the w^{th} window. Therefore the contribution of each isotope to the w^{th} window is denoted by:

$$C_w = F_{1,w}X_1 + F_{2,w}X_2 + F_{3,w}X_3 + F_{4,w}X_4 + F_{5,w}X_5 + F_{6,w}X_6 \qquad (2)$$

Where: F = the cross-over factor for each isotope in a defined ROI window

X = the unknown quantity of counts from a particular isotope

Table IV: The cross-over factor for any particular isotope is expressed as a fraction of the "corrected counts" measured in the principal energy window of the isotope of interest. The cross-over factor for the isotope of interest in its own Region of Interest (ROI) window is unity.

Table IV.

CROSS-OVER FACTOR SOURCE MATRIX

	Gd	In	Sn	Sr	Nb	Sc
Gd	1	0.304943	0.240530	0.311613	0.326283	0.229304
In	0.04346	1	0.123653	0.229934	0.290304	0.202911
Sn	0.000147	0.081305	1	0.0744719	0.273695	0.240299
Sr	7.394e-05	0.092601	0.002129	1	0.184924	0.226322
Nb	5.592e-05	0.088833	0.001218	0.000963	1	0.229920
Sc	0.000143	0.070388	0.000382	0.002917	0.032264	1

The count in each ROI window is the linear sum of the counts of each isotope in that ROI window (Linden, 1983). The unknown quantity of X_i of the i^{th} isotope present in the mixture has an expected contribution to the integral counts in the w^{th} region of interest (ROI) window of:

$$F_{i,w}X_i \qquad (3)$$

where $X=[X_1,X_2,X_3,X_4,X_5,X_6]$ is the sum of unknown isotope quantity.

The quantitation of the energy spectra from a complex isotope mixture is accomplished by formulating N simultaneous linear equations for N isotopes having N Regions of Interest (ROI) windows (Linden, 1983). We utilized six isotopes to generate six linear equations with six unknowns. We solved the unknown amounts of each isotope in the mixture by expressing the linear equations in matrix notation. The source matrix is the cross-over factor matrix shown in **Table IV** and is generically represented below as M.

$$M = \begin{vmatrix} F_{1,1} & F_{1,2} & F_{1,3} & F_{1,4} & F_{1,5} & F_{1,6} \\ F_{2,1} & F_{2,2} & F_{2,3} & F_{2,4} & F_{2,5} & F_{2,6} \\ F_{3,1} & F_{3,2} & F_{3,3} & F_{3,4} & F_{3,5} & F_{3,6} \\ F_{4,1} & F_{4,2} & F_{4,3} & F_{4,4} & F_{4,5} & F_{4,6} \\ F_{5,1} & F_{5,2} & F_{5,3} & F_{5,4} & F_{5,5} & F_{5,6} \\ F_{6,1} & F_{6,2} & F_{6,3} & F_{6,4} & F_{6,5} & F_{6,6} \end{vmatrix}$$

To solve the simultaneous equations and determine the amount of the individual isotope in the mixture, the cross-over factor source matrix undergoes Gauss-Jordan matrix inversion $(M)^{-1}$ with full row and column pivoting (transformation) of the matrix $(M^t)^{-1}$. The solution of X is obtained as denoted below:

$$C = M^t X \qquad (4)$$

$$X = (M^t)^{-1} C$$

Principles and Assumptions of the Microsphere Technique

The radiolabelled microsphere technique has been shown by numerous investigators (Rudolph & Heymann, 1967 and Wagner et al, 1969) to be a reliable method for measuring regional blood flow to many tissues in a wide variety of species. Experiments using 10μm and 15μm diameter radiolabelled microspheres to study regional ocular blood flow in rabbits, cats and pigs have determined that 15μm diameter spheres yield accurate determinations of blood flow to the various regions of the uvea and retina (Alm & Bill, 1972a, 1973b). The precision of blood flow determination in the retina when using 10μm sized spheres is high. However, the 10μm diameter spheres have a tendency (50%) to pass through the capillary meshwork of the anterior uvea, specifically the ciliary processes thereby causing underestimates of blood flow (Bill, 1983). Feline studies (Alm & Bill, 1972a) have determined that 5% or less of 15μm diameter spheres injected into the left ventricle were found in the lungs, indicating that at least 95% of the spheres are trapped in the capillary beds of the systemic circulation. This high degree of entrapment using 15μm diameter microspheres has been found in many other species.

The assumptions which must be fulfilled for the accurate determination of blood flow utilizing radioactive microsphere technique are the following:

1) The microspheres are uniformly mixed in arterial blood and have the same rheology as red blood cells. Ideally microspheres should be injected into the left atria so that they mix thoroughly with the blood as they pass into the left ventricle and are ejected into the systemic circulation via the aorta. Having a homogeneous distribution within the blood, their entrapment within the capillaries is proportional to the blood flow. The microspheres are rigid and too large to pass through the capillaries of the perfused tissue and are entrapped in the capillary bed. Therefore, by comparing the radioactivity in tissue samples to that of an arterial blood sample withdrawn at a known flow rate, the blood flow to tissue samples can be calculated.

2) Microspheres themselves do not alter blood flow or general hemodynamic parameters.

3) Essentially all microspheres are removed from the circulation (entrapment) in their first pass through the microcirculation.

4) Microspheres provide an instantaneous determination of regional blood flow or cardiac output under steady-state conditions. During a bolus injection the concentration of microspheres in arterial blood is not constant. To ensure that the number of microspheres or counts is directly proportional to blood flow of the perfused tissue, all measurements must be made under identical steady-state conditions.

5) To have an accuracy of blood flow determination within ± 10% of mean flow estimate at the 95% confidence level, at least 384 microspheres must be trapped in the tissues and present in the reference withdrawal sample (Heymann et al, 1977).

Determination of Blood Flow and Cardiac Output

Regional ocular blood flow was determined using 15±1μm diameter radiolabelled microspheres (New England Nuclear Corporation, Wilmington, DE) using the surrogate organ reference withdrawal technique (Heymann et al, 1977; Buckberg et al, 1971). To eliminate the necessity of measuring blood flow to a reference organ or tissue Buckberg et al (1971) have described the technique of a surrogate organ reference withdrawal. We utilized this technique as

the calculation standard to determine organ blood flow and cardiac output. A syringe pump (Harvard Apparatus Infusion/Withdrawal Pump, Millis, MA) withdrew a reference arterial blood sample beginning 15 seconds preceding the injection until 2 minutes post injection, at a rate of 1.03 milliliters/minute from a catheter placed into the right femoral artery. Ocular blood flow is expressed as milliliters/minute/100 gram dry weight. This method of measuring blood flow has been shown to be accurate provided at least 384 spheres were collected in the tissues and reference withdrawal sample (Buckberg et al, 1971). We injected between 2.5-2.8x10^6 microspheres per isotope into the left atria suspended in 0.9% NaCl and 0.01% Tween 80. We established that the injected number of spheres does not alter general hemodynamics and yields an adequate density of spheres (384/tissue) in the retina by which to perform the blood flow calculations (Buckberg et al, 1971 & Nose, 1985).

Radiolabelled microspheres were sonicated for at least 30 minutes prior to injection, vortexed before withdrawal into a 3cc injection syringe, and injected via a catheter into the left atrium. Injection of the microspheres into the left atria insures an adequate mixing of the microspheres with the blood before ejection into the systemic circulation (Buckberg et al, 1971). Homogeneous distribution of the microspheres in the vasculature was confirmed by evaluating total blood flow to the kidneys. To optimize injection efficiency, the injection syringe was flushed twice with heparinized saline and these flushes were injected into the left atria. Intra-atrial microsphere injections were made over a 30 second interval. The sequence of microsphere isotope injections was randomized. The following six gamma-emitting radionuclides: ^{153}Gd, ^{114}In,^{113}Sn, ^{85}Sr, ^{95}Nb, ^{46}Sc with a specific activity of 7-15 mCi/g, were utilized to determine regional blood flow to the eyes at each of six perfusion pressures.

Organ blood flow was determined by the following formula and expressed as milliliters/minute/100 grams dry tissue weight:

$$\text{ocular blood flow} = \frac{(\text{counts in ocular tissue}) \times (\text{reference withdrawal rate}) \times (100)}{(\text{dry tissue weight}) \times (\text{counts in reference withdrawal})} \quad (5)$$

The ratio of flow to counts in the blood reference withdrawal sample (Q_r / C_r) is theoretically the same as the ratio of total cardiac output ($C.O._t$) to total counts injected (C_t). This enables cardiac output to any tissue to be calculated if blood flow to tissue and its radioactivity are known. The cardiac output (C.O.) can be determined by the following formula:

$$C.O. = \frac{(\text{counts injected}) \times (\text{withdrawal rate})}{(\text{counts in reference withdrawal})} \quad (6)$$

Counts injected refers to total counts available as determined from the source vial minus residual counts in injection syringe and cardiac catheter. Counts in reference withdrawal refers to total counts minus average ambient background counts.

Determination of Vascular Resistance

Vascular resistance (mmHg/ml·min 100gm dry weight) was calculated by dividing the ocular perfusion pressure at the time of microsphere injection by regional flow. Vascular resistances for the D-NAME and L-NAME treated animals for the retina, choroid, and anterior uvea were determined.

Quantitation Of Autoregulation

Quantitation of blood flow autoregulation was assessed by the method of Norris et al (1979)

and Granger & Norris (1980). The perfusion pressure-flow data for D-NAME and L-NAME treated animals were normalized to control ocular perfusion pressure (OPP_c) and control retinal blood flow (Q_c) for each group. The pressure-flow relationship is expressed as the ratio of the control pressure-flow point for each group. Since the relationship between retinal blood flow (Q) and ocular perfusion pressure (OPP) was non-linear, we utilized polynomial regression analysis (Marquart-Levenberg algorithm based on least-squares) to generate a best-fit line for the normalized perfusion pressure-flow data points (GB-Stat Version 4.0, Dynamic Microsystems, Inc. Silver Spring, MD). The complexity of the polynomial regression equation was selected based on the more accurate fit for the data (Bevington, 1969). Higher order polynomial regressions were tested, but did not show a significant improvement in the fit and therefore were rejected.

To establish statistically significant variations between the D-NAME and L-NAME polynomial regressions an F-statistic was utilized to compare the two resultant polynomial equations. The F-statistic was calculated as described by Granger & Norris (1980) and Motulsky & Ransnas (1987). The error sum of squares for each second degree polynomial regression, and the error sum of squares from a second degree polynomial regression on the combined data pool were calculated as follows:

$$F = \frac{(ESS_{D+L} - ESS_D - ESS_L)/(df_{D+L} - df_i)}{(ESS_D + ESS_L)/ df_i} \qquad (7)$$

Where ESS is the error sum of squares for the D-NAME or L-NAME regressions, and df is the degrees of freedom for the combined (df_{D+L} = 69) and individual regressions (df_i = 33).

The value for the F statistic was interpolated from the table for critical values of the F-distribution for an alpha of 0.05 and the appropriate degrees of freedom. Two regressions on the

whole can be nonsignificantly different from each other, yet demonstrate significant differences in blood flow at specified ocular perfusion pressures. We established 95% confidence limits along each polynomial regression. We compared the overlap of the 95% confidence limits along the regression lines. Overlap of the 95% confidence limits at specific regions along the regressions demonstrate that the two regressions are not significantly different at these specified values. Regions where the 95% confidence limits are non-overlapping demonstrate significant differences in ocular blood flows at the specific ocular perfusion pressures.

Determination of Compensatory Power in Blood Flow Regulation

The degree of compensation in the autoregulatory capacity of the retinal vasculature was determined for the mean pressure-flow (OPP, Q) relationships at six experimentally determined values along the pressure-flow curve utilizing the closed loop gain formula for the flow regulator (Norris et al, 1979; Ueeda et al, 1992; Borgdorff et al, 1988; Granger & Norris, 1980; Griffith & Edwards, 1990). In addition, the compensatory power in blood flow regulation was assessed by defining the polynomial equation in arbitrary 0.10 increments in OPP/OPP_c applied to the closed loop gain formula:

$$G_c = 1-[(\Delta Q/Q/(\Delta P/P)] \qquad (8)$$

where $(\Delta Q/Q/\Delta P/P)$ is the slope of the normalized perfusion pressure-flow curve at the given points (OPP,Q). Where P and Q are specific ocular perfusion pressure and ocular blood flow points, respectively and $\Delta P = P_{initial} - P$, and $\Delta Q = Q_{initial} - Q$. When G_c is greater than unity ($G_c > 1$) it denotes overcompensation of blood flow. When G_c is equal to unity ($G_c = 1$) the slope of the normalized perfusion pressure-flow curve is zero. This occurs when flow is independent of perfusion pressure and is indicative of perfect autoregulatory capacity. When G_c equals zero (G_c

= 0) blood flow changes proportionally with perfusion pressure which is characteristic of a pressure passive, nonautoregulating vascular bed. When G_c is a fractional component of unity (e.g., G_c = 0.3) it denotes that flow regulation in a given vascular bed is able to compensate for 30% of the applied perturbation. A positive G_c is indicative of autoregulation. A negative G_c is indicative that the change in flow is proportionally greater than the applied change in pressure. This would occur at ocular perfusion pressures below the lower limit of the autoregulatory plateau.

Statistical Analysis

For the temporal control studies a two-factor repeated measures ANOVA was performed to determine whether or not there were significant differences in retinal, choroidal, and anterior uveal blood flow values of the left eye versus the right eye over the various time points. A two-tailed unpaired T-test was performed to compare flows at 6 minutes and at the 84 minutes time point (±1 minutes).

One way repeated measures ANOVA with Bonferroni multiple comparisons were conducted within each experimental group to compare blood flows at each ocular perfusion pressure to baseline control blood flow values. A two-factor repeated measures ANOVA with Bonferroni multiple comparisons were conducted between the D-NAME and L-NAME treated groups to determine significant differences in blood flow measurements at each ocular perfusion pressure. Retinal blood flows in the D-NAME and L-NAME groups were analyzed using polynomial regression and protected T-tests. Linear regression analysis was utilized to characterize the relationship of choroidal and anterior uveal blood flows at the various ocular perfusion pressures. The 95% confidence limits along the linear regression for mean blood flow values in the L-NAME and D-NAME treated animals were utilized to compare to compare uveal blood flow after L-arginine administration. A paired two-tailed T-test comparing left versus right total kidney flow in the D-NAME and L-NAME treated animals was used to verify homogeneity of microsphere distribution. Differences between data were considered to be significant when $p < 0.05$.

RESULTS

Temporal Control Studies:

We have obtained consistent baseline blood flow values for the retina, choroid, and anterior uvea (**Table V.** & **Figure 7**). Consistent eye blood flow measurements were obtained for all temporal control animals. Bilateral baseline intraocular pressures (left 12 ± 1 mmHg; right 10 ± 1 mmHg) and ocular perfusion pressures (left 70 ± 8 mmHg; right 67 ± 8 mmHg) for our temporal control studies did not differ significantly from each other. Statistical analysis for combined ocular flows showed that retinal ($F = 1.28$,$p > 0.2$), choroidal ($F = 0.23$, $p > 0.8$) and anterior uveal ($F = 0.23$, $p = 0.9$) blood flows did not vary significantly at time points greater than 6 ± 1 minutes and were stable by 24 ± 1 minutes post-surgery. Results of a two-factor repeated measures ANOVA which compared the left versus the right ocular blood flows showed no significant unilateral difference in ocular blood flows at any of the time points (> 6 ± 1 minutes). A two-tailed unpaired T-test comparing ocular blood flow at 6 ± 1 minutes and at 84 ± 1 minutes showed no significant difference ($p > 0.05$) in retinal, choroidal, and anterior uveal blood flows at the two time points. Blood gas analysis at the various time points were stable and are shown in **Table VI**.

D-NAME and L-NAME Treated Animals:

Baseline intraocular pressures between D-NAME (left 13 ± 1 mmHg; right 12 ± 1 mmHg) and L-NAME (left 11 ± 1 mmHg; right 12 ± 1 mmHg) treated animals, as well as left and right eye IOP within each group did not vary significantly. Comparison of baseline ocular perfusion pressures between the two groups revealed statistically significant differences (D-NAME: left 82 ± 4 mmHg, right 83 ± 3 mmHg ; L-NAME: left 106 ± 3 mmHg, right 106 ± 2 mmHg). We changed the perfusion gradient to the eye by increasing IOP, rather than controlling mean arterial pressure. Ocular blood flow values for D-NAME and L-NAME treated groups at six ocular perfusion pressures were determined (**Table VII** & **Figure 8**).

Table V: Ocular blood flow measurements (ml/min/100 gm dry tissue) for the retina, choroid and anterior uvea at various time points post-completion of surgical protocol. Time zero was designated as the completion of the anterior eye chamber cannulation. Repeated measures ANOVA comparing blood flows after time point of 6 minutes revealed no differences in blood flow over time. No differences in blood flow were obtained between left and right eyes. A two-tailed unpaired T-test at 6 minutes compared to 84 minutes revealed a nonsignificant difference in blood flow.

Table V. OCULAR BLOOD FLOW (ml/min/100gm dry wt) VERSUS TIME POST-COMPLETION OF SURGICAL PROTOCOL

TIME ELAPSED Post-Surgery (minutes)	6 ± 1	24 ± 1	44 ± 1	64 ± 1	84 ± 1	106 ± 1
RETINA						
Left	157 ± 41	179 ± 24	186 ± 11	208 ± 15	230 ± 28	237 ± 19
Right	174 ± 39	182 ± 30	221 ± 24	210 ± 26	216 ± 27	224 ± 27
Left + Right	165 ± 27	181 ± 18	203 ± 14	209 ± 14	223 ± 19	231 ± 16
CHOROID						
Left	15053 ± 5518	17428 ± 3082	18255 ± 2337	17281 ± 2229	17735 ± 2628	17640 ± 2929
Right	15690 ± 4698	18121 ± 4028	18417 ± 2548	18008 ± 2420	18127 ± 1730	17572 ± 1731
Left + Right	15372 ± 3418	17775 ± 2420	18336 ± 1649	17644 ± 1572	17931 ± 1501	17606 ± 1622
ANTERIOR UVEA						
Left	4064 ± 1053	5787 ± 924	5014 ± 800	5687 ± 461	5505 ± 666	5674 ± 626
Right	5949 ± 1478	5619 ± 626	5892 ± 520	6248 ± 781	5845 ± 886	5387 ± 533
Left + Right	5006 ± 911	5703 ± 533	5453 ± 474	5967 ± 441	5675 ± 531	5530 ± 394

All values are represented as means ±SEM. n=6

Figure 7: Ocular blood flow determinations for the retina, choroid, and anterior uvea from each eye (left and right) were determined in six piglets at six pre-determined time intervals. Shown are mean (± SEM) blood flows for each eye, dashed lines represent the combined mean ocular flow. Time zero was designated as the completion of the cannulation procedure to the anterior eye chambers. Sequential blood flow determinations were obtained at an average time (± 1) of 6, 24, 44, 64, 84, 106 minutes post completion of the surgical protocol. Blood flow stability was obtained by 24 minutes post-surgery. Prior to this time point there was a greater variability in blood flow values.

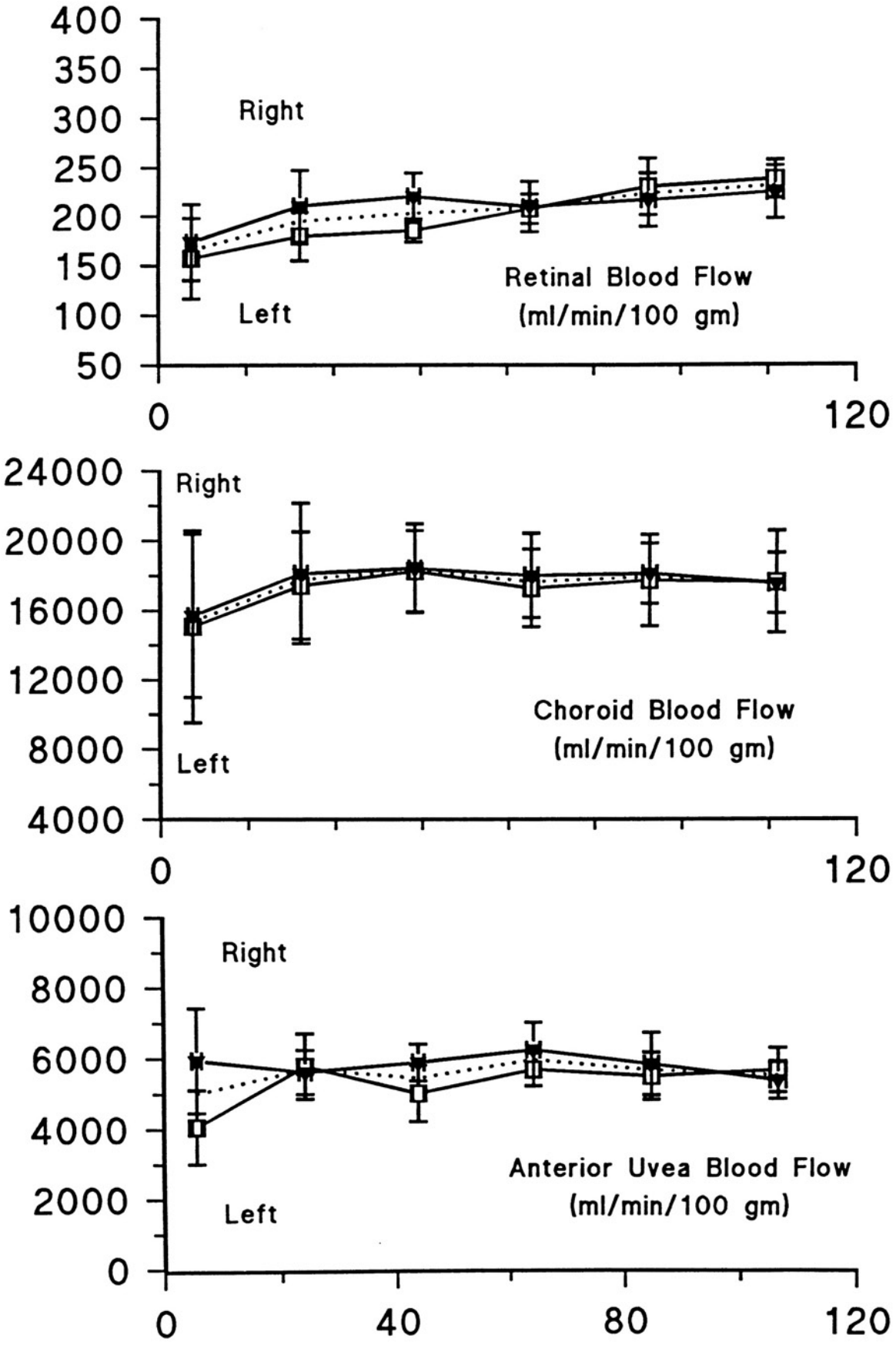
400
350
300
250
200
150
100
50
Right
Left
Retinal Blood Flow
(ml/min/100 gm)
0
120
24000
20000
16000
12000
8000
4000
Right
Left
Choroid Blood Flow
(ml/min/100 gm)
0
120
10000
8000
6000
4000
2000
0
Right
Left
Anterior Uvea Blood Flow
(ml/min/100 gm)
0
40
80
120
Elapsed Time Post Surgery (min)

Table VI: Arterial blood data taken for the temporal control studies (n=6). Blood gases were determined prior to each microsphere injection. Blood gas parameters of pH, PCO_2, and PO_2 were within physiological limits and stable for the duration of the experimental protocol.

Table VI. ARTERIAL BLOOD DATA FOR TEMPORAL CONTROL STUDIES

TIME ELAPSED Post-Surgery (in minutes)	PH	PCO_2	PO_2
6 ± 1	7.45 ± .01	38 ± 1	85 ± 6
24 ± 1	7.45 ± .01	38 ± 1	99 ± 13
44 ± 1	7.45 ± .02	39 ± 1	99 ± 15
64 ± 1	7.45 ± .02	39 ± 1	104 ± 18
84 ± 1	7.44 ± .02	39 ± 1	99 ± 19
106 ± 1	7.44 ± .02	38 ± 2	105 ± 22

Values are means ± SEM.

Choroidal Blood Flow:

The relationship between choroidal blood flow and ocular perfusion pressures was linear for both D-NAME ($r=0.80$) and L-NAME ($r=0.75$) treated animals (**Figure 8**). Choroidal autoregulation was not apparent. Bonferroni multiple comparisons revealed significant ($P<.01$) decreases in blood flow at all ocular perfusion pressures when compared to control for both D-NAME and L-NAME treated animals. Mean baseline choroidal blood flow with L-NAME showed a 47% decrease ($p<.001$) compared to D-NAME. Mean choroidal blood flows were decreased in the L-NAME treated animals at each ocular perfusion pressure when compared to D-NAME. Two-factor repeated measures ANOVA with Bonferroni multiple comparison tests of choroidal blood flow with D-NAME and L-NAME revealed significant blood flow reductions ($p<.01$) at ocular perfusion pressures of 50 and 60 mmHg.

Anterior Uvea Blood Flow:

The relationship between anterior uvea blood flow and ocular perfusion pressures was linear for both D-NAME ($r=0.74$) and L-NAME ($r=0.86$) treated animals (**Figure 8**). Repeated measures ANOVA with Bonferroni multiple comparisons revealed significant reductions in blood flow from control values at all ocular perfusion pressures tested ($p= < 0.01$). Mean baseline anterior uvea blood flow with L-NAME showed a 43% decrease ($p< 0.01$) compared to D-NAME, no significant reduction in blood flows between treatment groups were obtained at lower ocular perfusion pressures.

Table VII: Retinal, choroidal, and anterior uveal blood flow measurements at various perfusion pressures in the presence of D-NAME and L-NAME. Significant differences from baseline retinal blood flows were obtained with D-NAME at OPP of 20 mmHg. With L-NAME significant differences from baseline blood flows were obtained at OPP of 40, 30, and 20 mmHg. Baseline retinal blood flows for both groups were in close agreement. Significant reductions in choroidal blood flow with L-NAME were seen at control OPP, 60 mmHg, and at 50 mmHg. Significant blood flow reductions in the anterior uvea were obtained with L-NAME at baseline ocular perfusion pressure when compared to D-NAME.

Table VII. OCULAR BLOOD FLOW (ml/min/100gm dry wt) AT VARIOUS PERFUSION PRESSURES WITH D-NAME AND L-NAME

OCULAR PERFUSION PRESSURE (OPP) (mm Hg)	BASELINE CONTROL	OPP 60 mmHg	OPP 50 mmHg	OPP 40 mmHg	OPP 30 mmHg	OPP 20 mmHg
D-NAME						
RETINA	225 ± 24	229 ± 15	260 ± 23	227 ± 28	193 ± 22	124 ± 21*
CHOROID	13419 ± 1360	7364 ± 1535	6056 ± 1187	3149 ± 635	2551 ± 675	1766 ± 628
ANTERIOR UVEA	8198 ± 870	4181 ± 1360	3501 ± 762	1704 ± 476	2289 ± 909	1161 ± 458
L-NAME						
RETINA	233 ± 49	163 ± 24	163 ± 23	146 ± 26*	96 ± 15*	49 ± 13*
CHOROID	7112 ± 1803†	3163 ± 575†	2470 ± 589†	1438 ± 160	1070 ± 110	588 ± 171
ANTERIOR UVEA	4701 ± 744†	2426 ± 233	1975 ± 385	993 ± 172	666 ± 101	305 ± 99

All values are represented as means ± SEM.
D-NAME n=6 ; L-NAME n=6
* Significantly different from baseline control flows $p<0.05$.
† Significantly different from D-NAME flows $p<0.05$.

Figure 8: Shown are the mean (± SEM) blood flows (BF) at six ocular perfusion pressures (OPP) in the presence of (★) D-NAME or (O) L-NAME (n=6 in each group). For all figures the first measurement from the right in each group is the baseline control flow-pressure measurement. A one-way repeated measures ANOVA with Bonferroni multiple comparisons was conducted to compare BF at the various OPP to baseline control flow within each group. Two-factor repeated measures ANOVA with Bonferroni multiple comparisons was utilized to compare retinal, choroidal and anterior uveal blood flows between the D-NAME and L-NAME treated groups at a specific OPP. Mean baseline retinal BF did not differ significantly in the two groups. For D-NAME treated group significant retinal BF differences from baseline control were obtained at an OPP of 20mmHg (denoted by *). Flows at higher OPPs did not vary significant from D-NAME baseline control. The L-NAME group revealed significant reductions from L-NAME baseline retinal BF at an OPP of 40 mmHg and below (denoted by *). Significant differences in flow between D-NAME and L-NAME groups ($F = 4.39$, $p < 0.05$) were obtained at OPP of 60 mmHg and below (protected T-tests) (denoted by ▵). Mean baseline choroidal and anterior uveal BF with L-NAME showed a 47% and a 43% decrease in BF, respectively compared to baseline BF with D-NAME. For both groups significant BF differences from baseline controls were obtained at OPPs of 60 mmHg and below (denoted by ← *). Significant decreases in choroidal BF between D-NAME and L-NAME groups were obtained at OPP of 60 mmHg and 50 mmHg ($F = 4.38$; $p<0.05$)(denoted by ▵). No significant differences in choroidal BF between groups were obtained at OPP below 50 mmHg. Linear regression analysis (solid lines) on the raw data revealed an $r=0.80$ and $r=0.75$ for the D-NAME and L-NAME treated groups, respectively. Significant decreases in anterior uveal BF between groups were obtained only at baseline OPP (denoted by ▵). Linear regression analysis (solid lines) on the raw data revealed an $r=0.74$ and $r=0.86$ for the D-NAME and L-NAME treated groups, respectively.

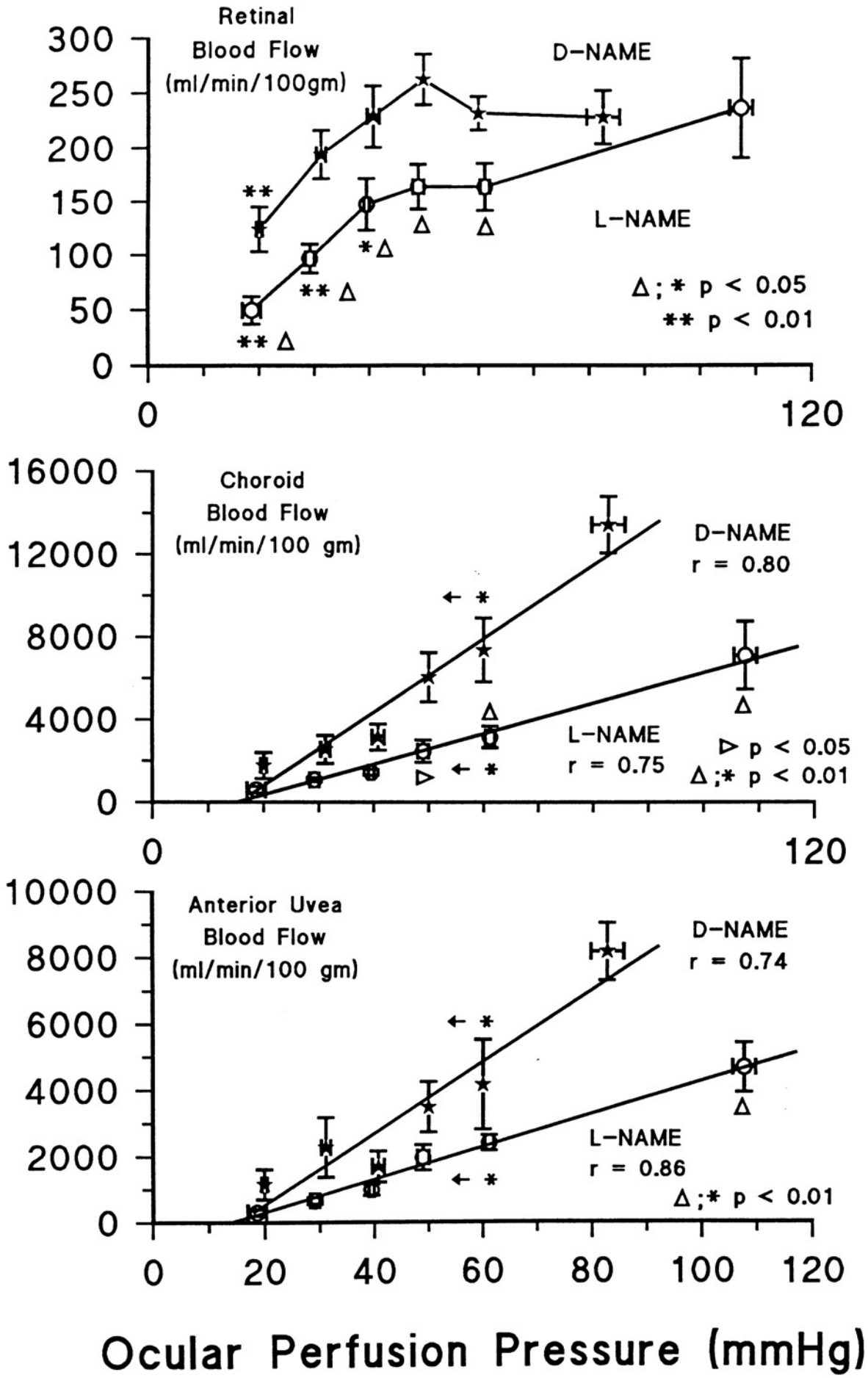
Retinal
Blood Flow
(ml/min/100gm)
300
250
200
150
100
50
0
D-NAME
L-NAME
Δ; * p < 0.05
** p < 0.01
0
120
Choroid
Blood Flow
(ml/min/100 gm)
16000
12000
8000
4000
0
D-NAME
r = 0.80
L-NAME
r = 0.75
▷ p < 0.05
Δ;* p < 0.01
0
120
Anterior Uvea
Blood Flow
(ml/min/100 gm)
10000
8000
6000
4000
2000
0
D-NAME
r = 0.74
L-NAME
r = 0.86
Δ;* p < 0.01
0
20
40
60
80
100
120
Ocular Perfusion Pressure (mmHg)

Retinal Blood Flow: A two-factor repeated measures ANOVA comparing retinal blood flows with D-NAME and L-NAME over the various ocular perfusion pressures revealed a significant treatment effect ($F = 4.39$, $p = 0.004$). These results are shown in **Table VII** and illustrated in **Figure 8**. Protected T-tests comparing retinal blood flow between D-NAME and L-NAME at the various ocular perfusion pressures revealed significant differences ($p < 0.05$) at OPP of 60 mmHg and below. A one-way repeated measures ANOVA with Bonferroni multiple comparisons within each group demonstrated that retinal blood flow in the D-NAME treated animals differed significantly from baseline flows only at an ocular perfusion pressures of 20 mmHg. While retinal blood flow in the L-NAME treated animals differed significantly from baseline flows at ocular perfusion pressures of 20, 30, and 40 mmHg.

Retinal Autoregulation:

The relationship between retinal blood flow and ocular perfusion pressure was non-linear (**Figure 9 bottom**). A second order polynomial regression for each group yielded the best-fit lines for the data, the correlation coefficient for each polynomial regression was $r=0.69$. An F-Statistic comparison between the two polynomial regressions demonstrated that, on the whole, the two regressions did not differ significantly. The F-statistic revealed an $ESS_L=2.15$, $ESS_D=1.32$, $ESS_{L+D}= 3.99$, and the value for $F= 0.14$. The interpolated value of the F-distribution ($F_{.05[36,33]}$) is approximately $F= 1.8$. The 95% confidence limits along each regression demonstrates that between the normalized ocular perfusion pressures from 0.26 to 0.65 there is no overlap of the 95% confidence limits for the polynomial regressions. Therefore, significantly different retinal blood flows exist between this specific range of ocular perfusion pressures. The autoregulatory gain values for retinal blood flows were positive with both D-NAME and L-NAME, indicative of some autoregulation in both groups (**Figure 9 top**). The autoregulatory gain (G_c) for retinal blood flow with D-NAME at OPP/OPP_c of 0.40 ($OPP= 30$ mmHg) is approximately 0.80, indicative of extensive autoregulatory

Figure 9:

Top: The autoregulatory gain (G_c) of the retinal circulation determined at the normalized perfusion pressure points. G_c is defined by applying the gain formula to the second order polynomial equations. For D-NAME: $Q/Q_c = -0.0793 + 3.3363\ (OPP/OPP_c) - 2.2738\ (OPP/OPP_c)^2$. For L-NAME: $Q/Q_c = -0.0667 + 2.4143\ (OPP/OPP_c) - 1.3637\ (OPP/OPP_c)^2$. Solid symbols (★ = D-NAME; ● = L-NAME) represent the mean flow-pressure relationships at five experimentally determined values. Open symbols (O) represent calculated values obtained by defining the polynomial equation in arbitrary 0.10 increments in OPP/OPP_c applied to the gain formula. The arrowed vertical lines represent statistically significant differences in autoregulatory gain as determined from non-overlapping 95% confidence limits for the polynomial regressions in the figure below.

Bottom: Retinal Blood flows (Q) and Ocular Perfusion Pressure (OPP) data normalized to control flow-pressure values (Q_c, OPP_c, respectively). Shown are mean (±SEM) retinal blood flow with (★) D-NAME and (O) L-NAME at six flow-pressure points. The raw data in each group (n=36) were fit by a least squares method (both groups r=0.69) to a second order polynomial equation ($Y=A+B(X)+C(X)^2$), represented by the solid curved lines. An F-statistic comparison of the two polynomial regressions revealed a non-significant difference between the two regressions on the whole. The 95% confidence limits along each regression are shown by the dotted lines. Only the lower 95% confidence band for the D-NAME and the upper 95% confidence band for the L-NAME treated groups are shown. Regions where non-overlapping 95% confidence limits occur are denoted between the arrowed vertical lines. Non-overlapping 95% confidence limits demonstrate significantly different retinal blood flows at the specific range of ocular perfusion pressures (OPP/OPP_c = 0.26 to 0.65).

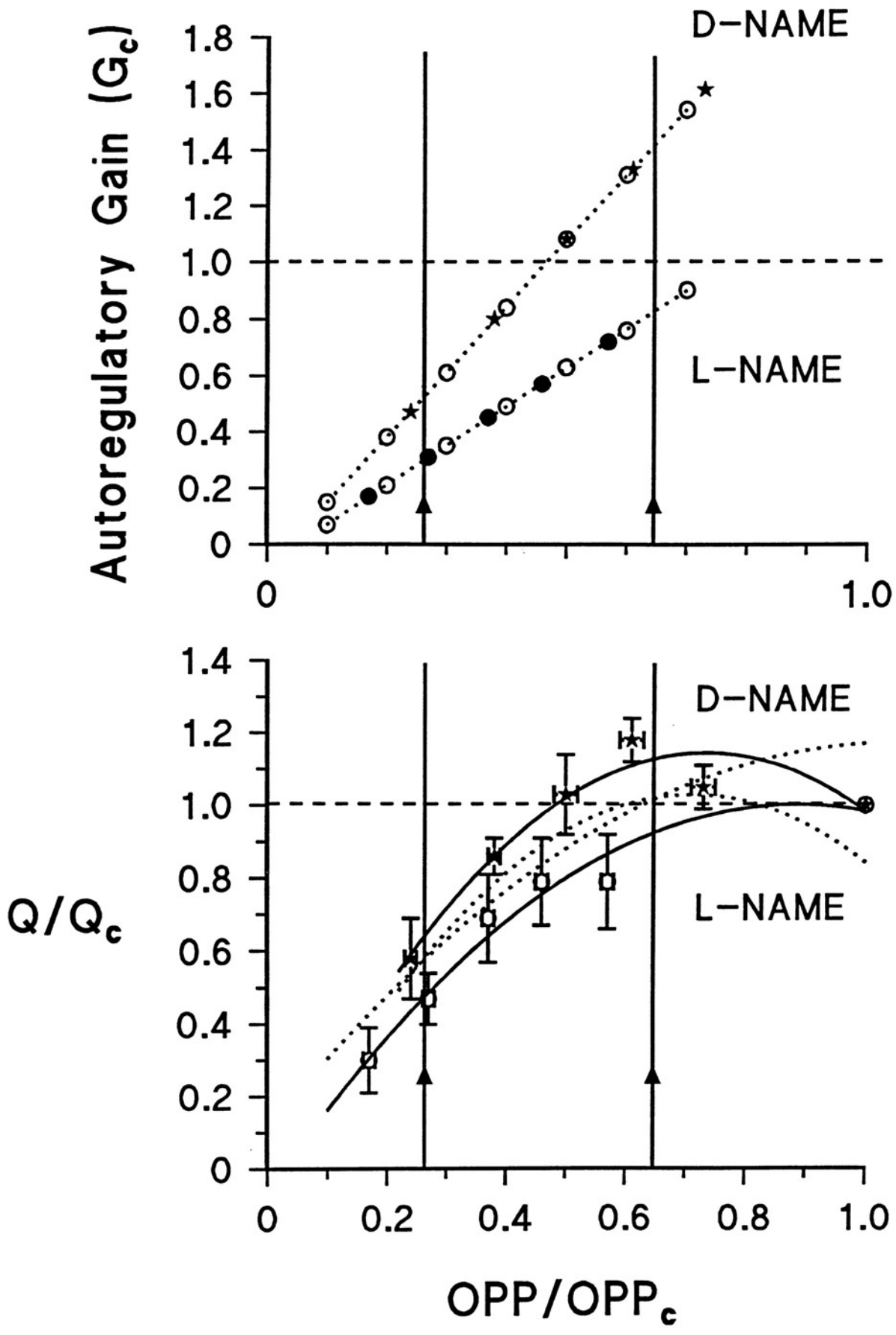
Autoregulatory Gain (G_c)
D-NAME
L-NAME
1.8
1.6
1.4
1.2
1.0
0.8
0.6
0.4
0.2
0
0
1.0
Q/Q_c
D-NAME
L-NAME
1.4
1.2
1.0
0.8
0.6
0.4
0.2
0
0
0.2
0.4
0.6
0.8
1.0
OPP/OPP_c

capacity. At an OPP of 40 mmHg G_c was 1.06 indicating complete autoregulation. By contrast, with L-NAME at OPP/OPP_c of 0.27 and 0.37 (OPP= 30 and 40 mmHg, respectively) the G_c is 0.31 and 0.47 indicating that the retinal vasculature was able to compensate for 31% and 47% of the applied disturbance and has lost approximately 69% and 53% of its autoregulatory capacity at these ocular perfusion pressures, respectively. A G_c greater than unity was obtained with D-NAME at OPP/OPP_c of 0.61, and 0.73 (OPP= 50 and 60 mmHg, respectively). At these ocular perfusion pressures with D-NAME the G_c was able to compensate fully to the applied disturbance and even demonstrates over compensation of blood flow regulation. No $G_c > 1$ was observed at any ocular perfusion pressure with L-NAME. At an ocular perfusion pressure of 20 mmHg the autoregulatory gain is approximately 0.47 with D-NAME and 0.17 with L-NAME indicating some autoregulatory capacity. Extrapolated values at lower OPP/OPP_c approach zero as would be predicted when near the lower limit of retinal autoregulatory capacity. Non-significant differences in G_c between the two groups, based on overlapping of 95% confidence limits, were observed at ocular perfusion pressures of 20 mmHg and 60 mmHg.

Values obtained for the autoregulatory gain (G_c) of the retinal circulation coincide nicely with those predicted by applying arbitrary 0.10 increments in OPP/OPP_c applied to the gain formula. Therefore, the second order polynomial regression provided an accurate prediction of the data.

Contralateral Eye Blood Flow :

Four animals were utilized for the D-NAME treated group and five animals were utilized for the L-NAME treated group. Intraocular pressure was maintained near baseline and continuously monitored. Retinal blood flows for the contralateral eye were stable for the duration of the experimental protocol. Within each group blood flows did not vary significantly at the measured time points. Blood flows with the L-NAME treated group were consistently lower, but not significantly different from the D-NAME treated group. These results are shown in **Table VIII** and **Figure 10**. Choroidal blood flow with L-NAME was reduced at all time points compared to D-NAME

Table VIII: Contralateral eye blood flow at the various time points in the presence of D-NAME and L-NAME

Table VIII. CONTRALATERAL EYE BLOOD FLOW (ml/min/100 gm dry wt) AT VARIOUS TIME POINTS WITH D-NAME AND L-NAME

TIME ELAPSED (in minutes)	BASELINE 96 ± 6	120 ± 6	142 ± 6	164 ± 7	187 ± 6	203 ± 7
D-NAME						
RETINA	247 ± 32	260 ± 37	276 ± 38	278 ± 36	265 ± 45	285 ± 46
CHOROID	15034 ± 1747	11686 ± 1721*	12488 ± 1855	10906 ± 1800*	9331 ± 1319*	9323 ±1542*
ANTERIOR UVEA	8563 ± 928	7115 ± 688	6695 ± 734	5204 ± 872*	3870 ± 441*	3243 ± 217*
L-NAME						
RETINA	200 ± 30	166 ± 22	178 ± 29	159 ± 25	167 ± 20	181 ± 19
CHOROID	6860 ± 1076	6048 ± 932	6145 ± 1202	5056 ± 1058	4994 ± 816	4690 ± 489*
ANTERIOR UVEA	3649 ± 534	3198 ± 426	3346 ± 476	2372 ± 105	2227 ± 200*	1917 ± 273*

All values are represented as means ± SEM.
D-NAME n=5 ; L-NAME n=6
* Significantly different from baseline control $p<0.05$.

Figure 10: Shown are the mean (± SEM) blood flows for the contralateral eye at six time points in the presence of (★) D-NAME (n=5) or (O) L-NAME (n=6). The intraocular pressure of the contralateral eye was maintained near baseline and was continously monitored. For all figures the first symbol from the left in each group are the baseline control flow-temporal measurements. Blood flow within each group were compared to baseline flow values using repeated measures ANOVA with Bonferroni multiple comparisons. Consistent blood flow values were obtained at time intervals in which significant differences in blood flow were obtained in the experimental eye.

Retina: Blood flows were stable for the duration of the experimental protocol in both groups. Retinal blood flow in the L-NAME treated group was consistently, but not significantly reduced (D-NAME group n=5). One way ANOVA with Bonferroni multiple comparisons was utilized to compare blood flows within each group over time.

Choroid: Blood flows were significantly reduced with L-NAME when compared to D-NAME (denoted by ▵). Consistent blood flow measurements were obtained with L-NAME from approximately 100 to 190 minutes, at longer time points significant reductions from L-NAME baseline blood flow were obtained (denoted by *). In the D-NAME treated group blood flow was consistent until at least 140 minutes post surgery. At later time points significant reductions in blood flows were obtained (denoted by * →).

Anterior uvea: Blood flow was significantly reduced with L-NAME when compared to D-NAME. Consistent blood flow measurements were obtained with L-NAME from approximately 100 to 160 minutes, at longer time points significant reductions from L-NAME baseline blood flow were obtained (denoted by *). In the D-NAME treated group blood flow was consistent until at least 140 minutes post surgery. At later time points significant reductions in blood flows were obtained (denoted by * →).

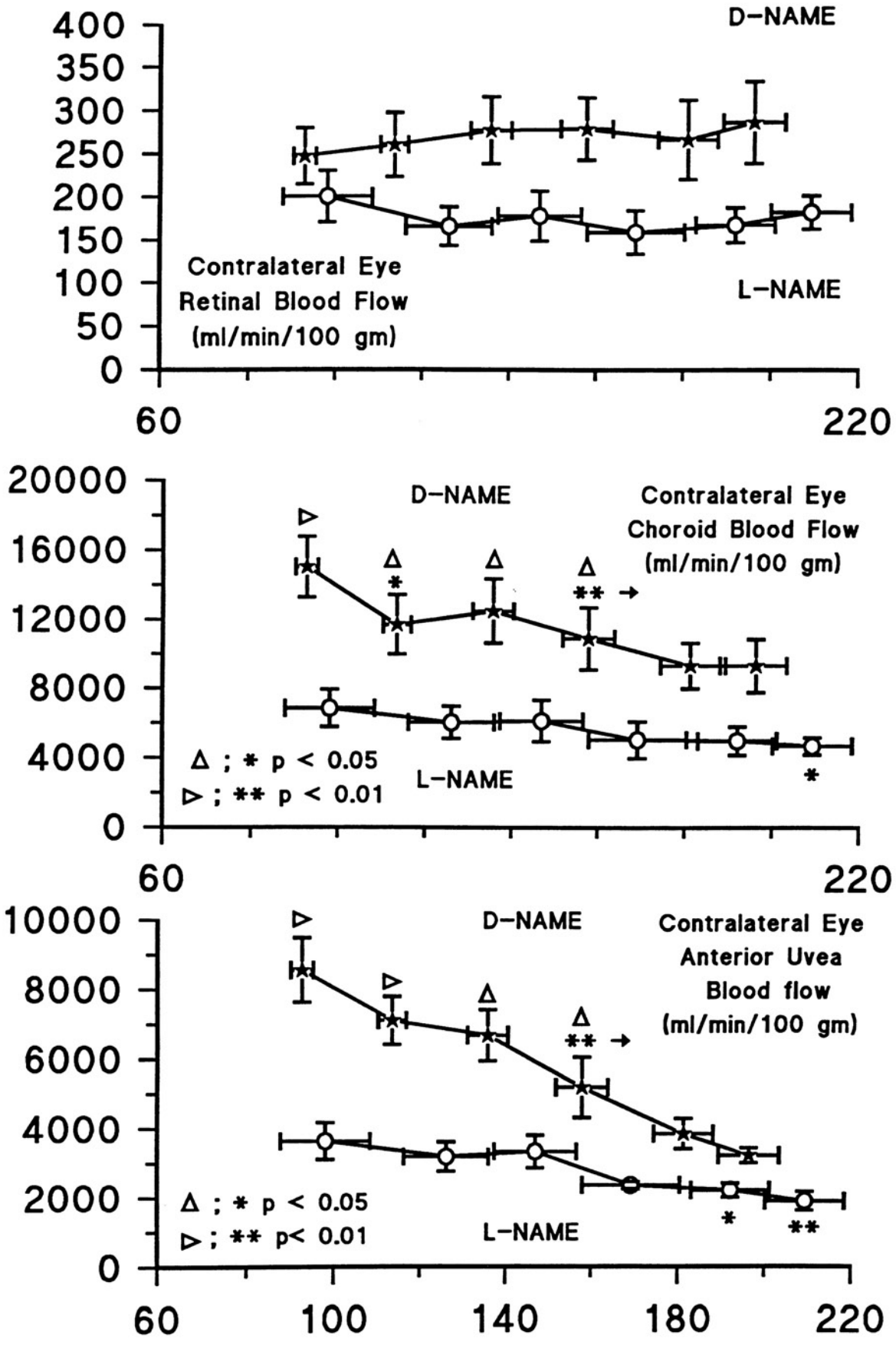
D-NAME
400
350
300
250
200
150
100
50
0
Contralateral Eye
Retinal Blood Flow
(ml/min/100 gm)
L-NAME
60
220
20000
16000
12000
8000
4000
0
D-NAME
Contralateral Eye
Choroid Blood Flow
(ml/min/100 gm)
Δ ; * p < 0.05
▷ ; ** p < 0.01
L-NAME
60
220
10000
8000
6000
4000
2000
0
D-NAME
Contralateral Eye
Anterior Uvea
Blood flow
(ml/min/100 gm)
Δ ; * p < 0.05
▷ ; ** p< 0.01
L-NAME
60
100
140
180
220
Elapsed Time Post Surgery (min)

choroidal blood flows. Consistent blood flows were obtained for the two treatment groups until at least 140 minutes post-surgery. At later time points significant reductions in blood flow were obtained. Mean arterial and OPP in the contralateral eye over time were stable. Slight elevations in MAP and OPP were observed starting at 140 minutes in the D-NAME treated group (**Figure 11**).

Blood Gas Analysis For D-NAME, L-NAME, and Contralateral Eye:

Blood gas parameters of pH, PCO_2, and PO_2 between the D-NAME and L-NAME treatment groups did not vary significantly and were within physiological limits as shown in **Table IX.** The PO_2 in the L-NAME treated animals was on the average consistently higher (10 mmHg) than with D-NAME, but physiologically and statistically not significant. On the average, hematocrit was 4% lower in the D-NAME treated animals but it is not significantly different from L-NAME.

Mean Arterial Pressure (MAP) and Intraocular Pressure (IOP) Matched Animals:

The D-NAME and L-NAME treated animals were matched by mean arterial and mean intraocular pressures. Based on the selection criteria, of matched IOP and MAP between groups, blood flow comparisons were conducted on a selected number of animals and not the full complement of animals. Comparisons of blood flow between treatment groups at each ocular perfusion pressure were conducted using one way ANOVA with Bonferroni multiple comparisons. With the exception of choroidal blood flow at an ocular perfusion pressure of 20 mmHg, ocular blood flows in the L-NAME treated animals were reduced at each OPP when compared to D-NAME flows. A statistically significant difference in retinal blood flow between groups was obtained at an OPP of 30 mmHg. A significant difference ($p<0.001$) in choroidal blood flow between treatment groups was obtained at an OPP of 60 mmHg. No significant differences in blood flow between groups were obtained for the anterior uvea. These results are shown in **Figure 12**.

Figure 11: Mean arterial pressure (MAP) and ocular perfusion pressure (OPP) in the contralateral eye over time for the D-NAME and L-NAME treated animals. Intraocular pressure (IOP) was maintained near baseline pressures (12 ± 2 mmHg) for the duration of the experimental protocol. Ocular perfusion pressure is defined as MAP-IOP.

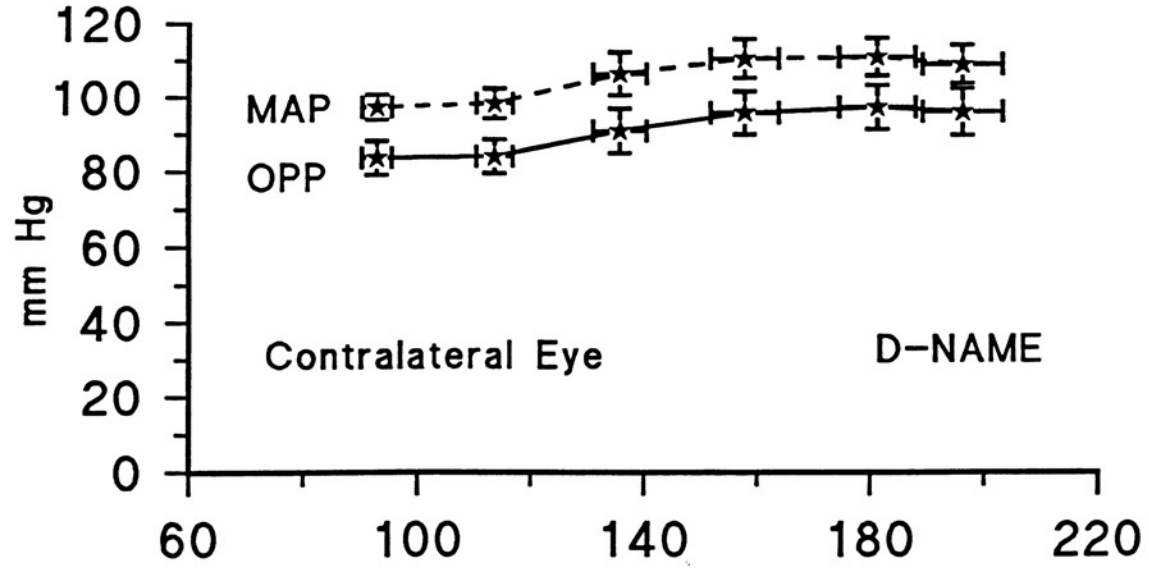

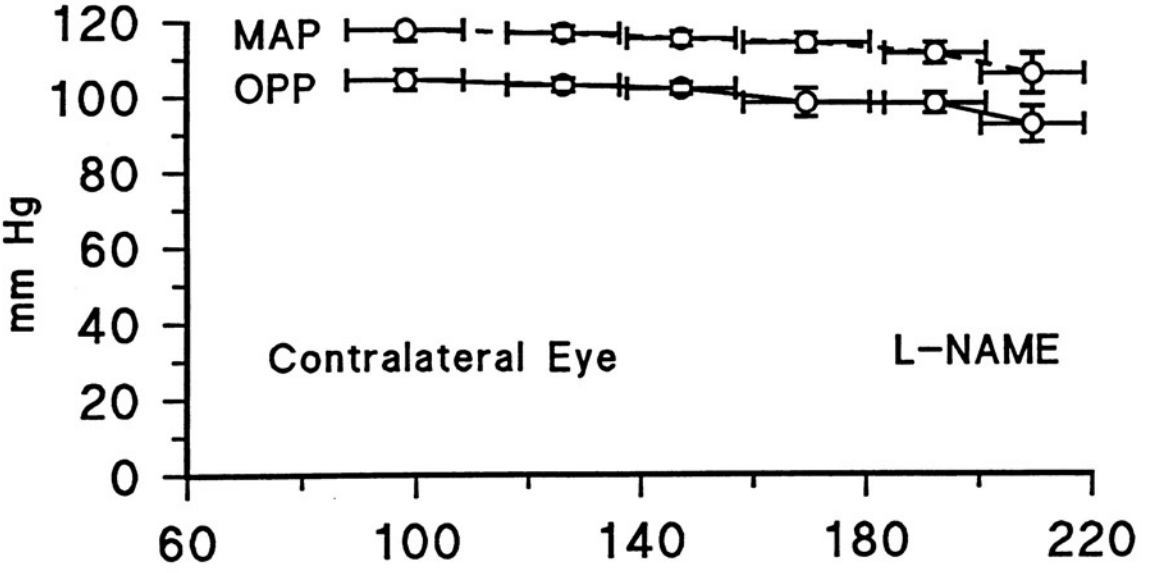

Elapsed Time Post Surgery (min)

Table IX: Anaerobic arterial blood gas analysis for the D-NAME and L-NAME treated groups at each OPP tested. Blood gas analysis of pH, PCO_2, PO_2, and Hct were conducted prior to each microsphere injection.

Table IX. ARTERIAL BLOOD DATA FOR D-NAME AND L-NAME TREATED ANIMALS

	pH		PCO_2, mmHg		PO_2, mmHg		Hct	
	D-NAME	L-NAME	D-NAME	L-NAME	D-NAME	L-NAME	D-NAME	L-NAME
CONTROL	7.47 ± .02	7.46 ± .02	37 ± 1	36 ± 1	89 ± 3	99 ± 13	37 ± 1	39 ± 1
OPP 60 mmHg	7.46 ± .01	7.46 ± .02	38 ± 1	36 ± 1	90 ± 4	102 ± 11	36 ± 1	41 ± 3
OPP 50 mmHg	7.45 ± .02	7.44 ± .01	36 ± 1	35 ± 1	90 ± 4	104 ± 14	35 ± 1	39 ± 2
OPP 40 mmHg	7.44 ± .01	7.43 ± .02	37 ± 1	34 ± 2	89 ± 4	98 ± 08	35 ± 1	38 ± 2
OPP 30 mmHg	7.43 ± .01	7.39 ± .02	37 ± 1	36 ± 1	89 ± 4	97 ± 11	34 ± 1	39 ± 3
OPP 20 mmHg	7.44 ± .02	7.39 ± .02*	38 ± 1	36 ± 1	87 ± 2	102 ± 10	33 ± 1	38 ± 3

Values are means ± SEM.
* Significantly different from D-NAME $p<0.05$.

Figure 12: Ocular blood flow of L-NAME (open bars) and D-NAME (hatched bars) treated animals. Graph demonstrates blood flow from several animals which were matched in a narrow range of similar mean arterial pressures at various ocular perfusion pressures. Only matched animals are included and the graph does not represent the full complement of animals. Ocular blood flow was consistently lower at the various ocular perfusion pressures in the presence of L-NAME. Significantly different blood flows between groups are denoted by the asterisk. Retinal blood flow was significantly different ($p<0.05$) at an OPP of 30 mmHg, choroidal blood flow was significantly different at an OPP of 60 mmHg. No difference in blood flow was obtained for the anterior uvea.

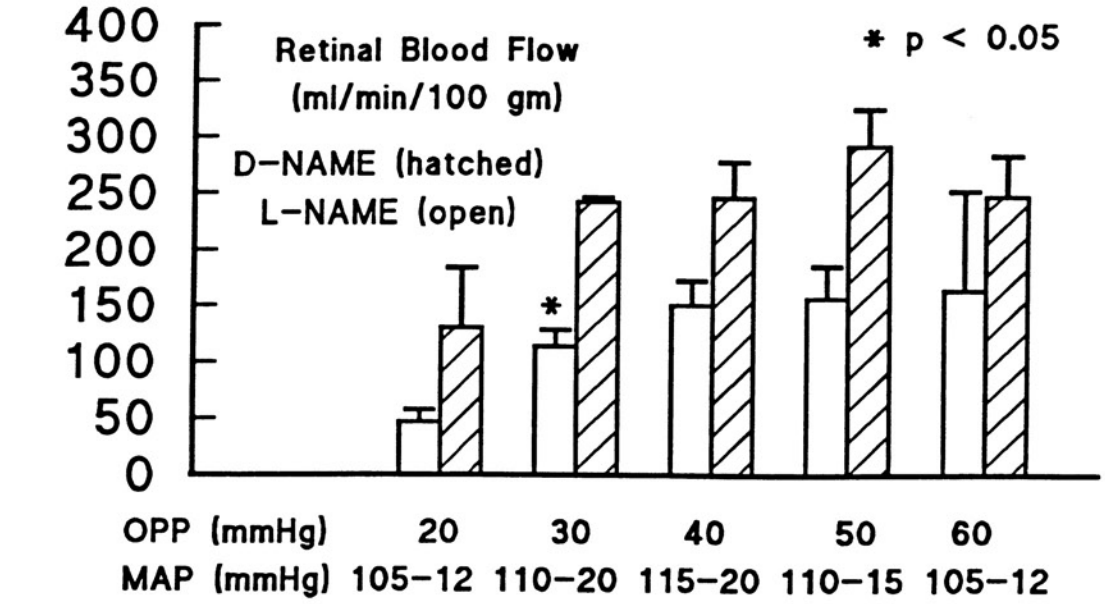
400
350
300
250
200
150
100
50
0
Retinal Blood Flow
(ml/min/100 gm)
D-NAME (hatched)
L-NAME (open)
* p < 0.05
*
OPP (mmHg) 20 30 40 50 60
MAP (mmHg) 105-12 110-20 115-20 110-15 105-12

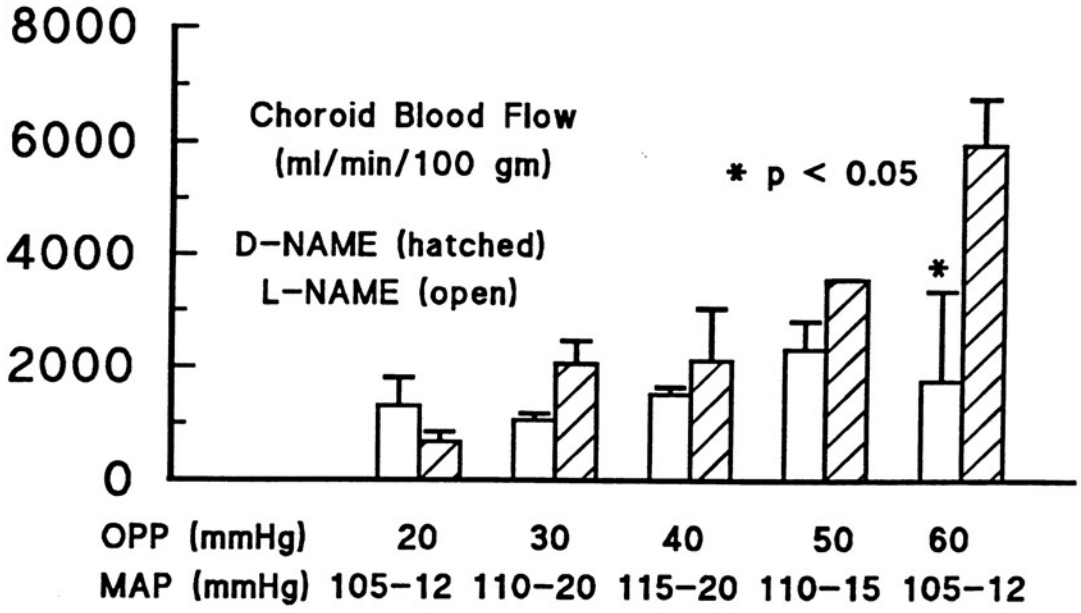
8000
6000
4000
2000
0
Choroid Blood Flow
(ml/min/100 gm)
D-NAME (hatched)
L-NAME (open)
* p < 0.05
*
OPP (mmHg) 20 30 40 50 60
MAP (mmHg) 105-12 110-20 115-20 110-15 105-12

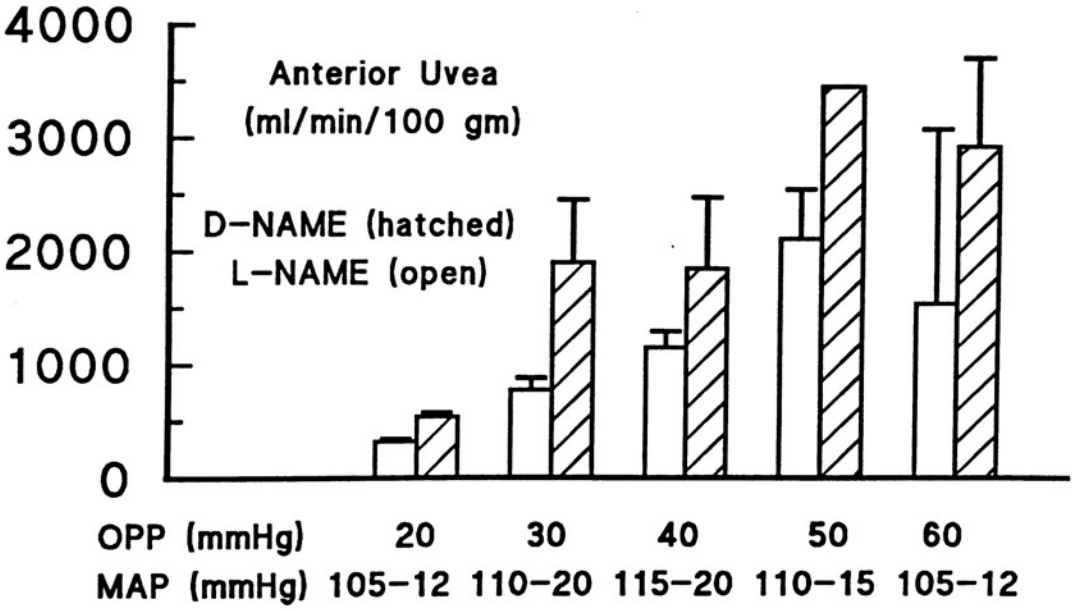
4000
3000
2000
1000
0
Anterior Uvea
(ml/min/100 gm)
D-NAME (hatched)
L-NAME (open)
OPP (mmHg) 20 30 40 50 60
MAP (mmHg) 105-12 110-20 115-20 110-15 105-12

Vascular Resistances:

Retinal vascular resistances were calculated for the D-NAME and L-NAME treated group (**Figure 13**), using repeated measures ANOVA with Bonferroni multiple comparisons. The D-NAME treated group revealed no significant change in retinal vascular resistance from control at OPP of 30 to 60 mmHg. L-NAME treated group revealed significant increases in vascular resistances from control at OPP of 30 and 40 mmHg. Significant differences ($p < 0.01$) in vascular resistance were obtained between D-NAME and L-NAME at OPP of 30 and 40 mmHg.

Choroidal vascular resistances in the D-NAME treated group were significantly greater ($p < 0.01$) than control at OPP of 30, 40 mmHg. The L-NAME treated group revealed significant increases in vascular resistance from control at 30, 40, and 50 mmHg. Significant differences in vascular resistance between groups were obtained at OPP of 30, 40, and 50 mmHg.

Anterior Uvea vascular resistance did not change significantly at the tested ocular perfusion pressures with D-NAME. Significant increase ($p < 0.01$) in vascular resistance from L-NAME control were obtained at an OPP of 30 and 40 mmHg. Vascular resistances between groups were not significantly different at the tested OPP.

Reversal with L-Arginine:

Baseline intraocular pressure (13 ± 2 mmHg) and baseline ocular perfusion pressure (84 ± 9 mmHg) were determined. Blood flow measurements were taken during L-NAME infusion and compared to blood flows obtained after L-arginine bolus administration ($n=5$, at high OPP; and $n=4$, at low OPP) (**Figure 14**). Retinal blood flows obtained at ocular perfusion pressures of 99 ± 4 mmHg during L-NAME infusion showed an increase of 6.4% following L-arginine administration. At a OPP of 28 ± 3 mmHg retinal blood flow was increased by 17% following L-arginine administration. Antagonism of NOS blockade by exogenous L-arginine was not apparent. Ocular perfusion pressure decreased significantly ($p=.035$) to 84 ± 9 mmHg following L-arginine administration. The L-arginine bolus antagonized on the average 13.4 ± 7 % of the elevation in mean arterial pressure

Figure 13: Shown are the mean (± SEM) vascular resistances (mmHg/ml·min/100gm dry) for the experimental eye at five ocular perfusion pressures in the presence of (★) D-NAME (n=6) or (O) L-NAME (n=6). For all figures first symbol from the right in each group is the baseline vascular resistance. Resistances within each group were compared to baseline values using repeated measures ANOVA with Bonferroni multiple comparisons. Significant increases in vascular resistances from baseline values within each treatment group are denoted by the asterisk.

Retina: Significant differences in vascular resistance from baseline (denoted by *) and between treatment groups (denoted by ▵) were obtained at ocular perfusion pressures of 30 and 40 mmHg.
Choroid: Significant differences in vascular resistance from baseline (denoted by *) and between treatment (denoted by ▵) groups were obtained at ocular perfusion pressures of 30, 40, 50 mmHg.
Anterior uvea: No apparent change in vascular resistance form baseline values were obtained for the D-NAME treated group. Significant differences in resistance from L-NAME baseline are denoted by the asterisk.

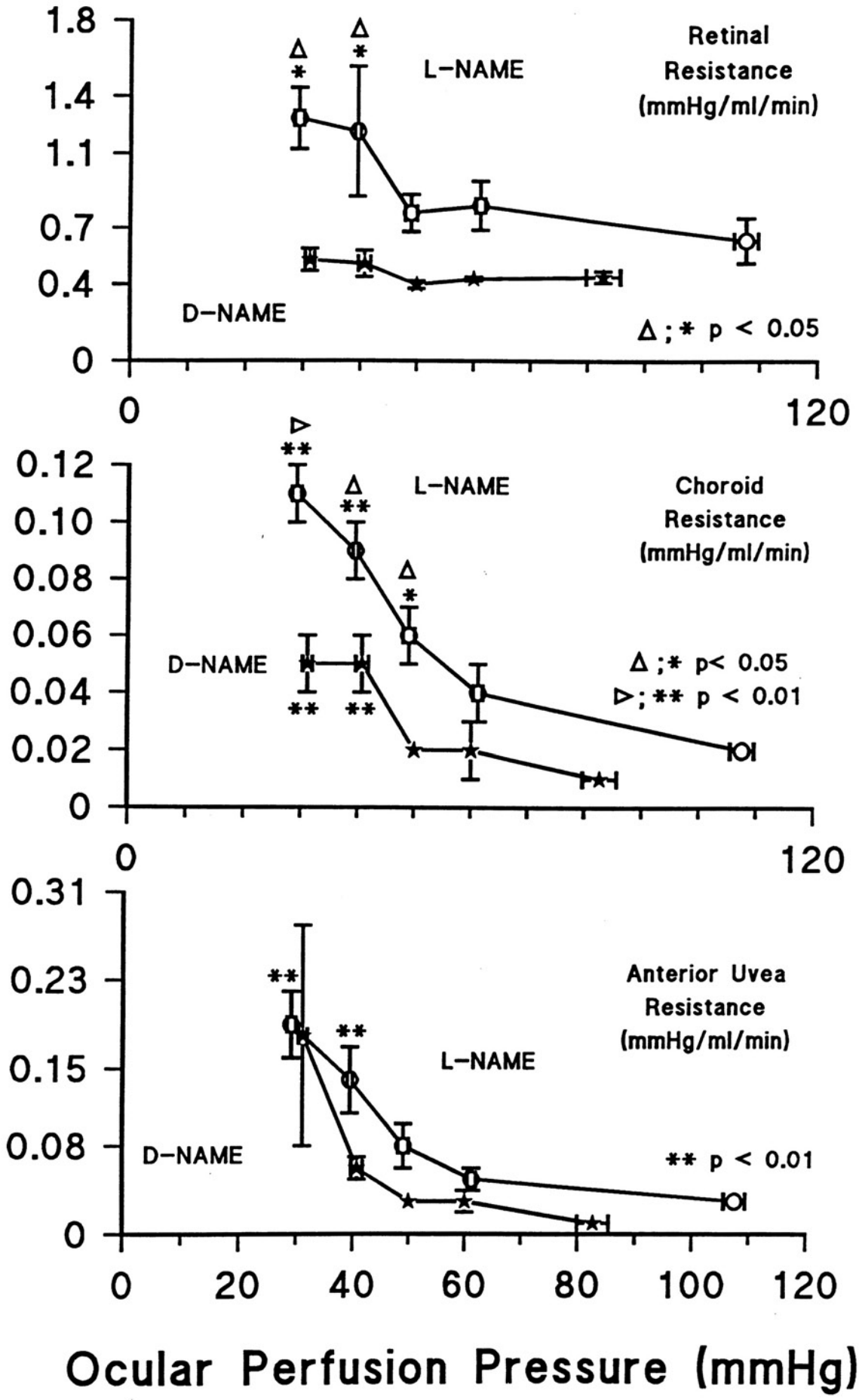
1.8
1.4
1.1
0.7
0.4
0
Retinal
Resistance
(mmHg/ml/min)
L-NAME
D-NAME
Δ ;* p < 0.05
0
120
0.12
0.10
0.08
0.06
0.04
0.02
0
Choroid
Resistance
(mmHg/ml/min)
L-NAME
D-NAME
Δ ;* p< 0.05
▷; ** p < 0.01
0
120
0.31
0.23
0.15
0.08
0
Anterior Uvea
Resistance
(mmHg/ml/min)
L-NAME
D-NAME
** p < 0.01
0
20
40
60
80
100
120
Ocular Perfusion Pressure (mmHg)

Figure 14: Reversal of NOS blockade with exogenous L-arginine administration (n=5). Represented by solid lines are the blood flow values for the retina, choroid, and anterior uvea from the D-NAME and L-NAME treated animals (n=12). Dashed lines represent 95% confidence limits. Symbols represent mean (± SEM) blood flow after 30 minutes of (O) L-NAME infusion (30 mg/kg/hr) and after 10 minutes of 180 mg/kg intra-atrial bolus administration of (●) L-arginine, in addition to the constant L-NAME infusion. One randomly selected eye was maintained at baseline OPP while the contralateral eye had its OPP lowered to 28 ± 3 mmHg on the same animal. The mean and SEM values of uveal blood flows following L-arginine administration at the high OPP were above the 95% confidence limits for the mean blood flow values obtained for L-NAME treated animals. This increase in blood flow was not statistically significant (two tail T-test) when compared to baseline L-NAME blood flow. Antagonism of NOS blockade in the retina by exogenous L-arginine was not apparent.

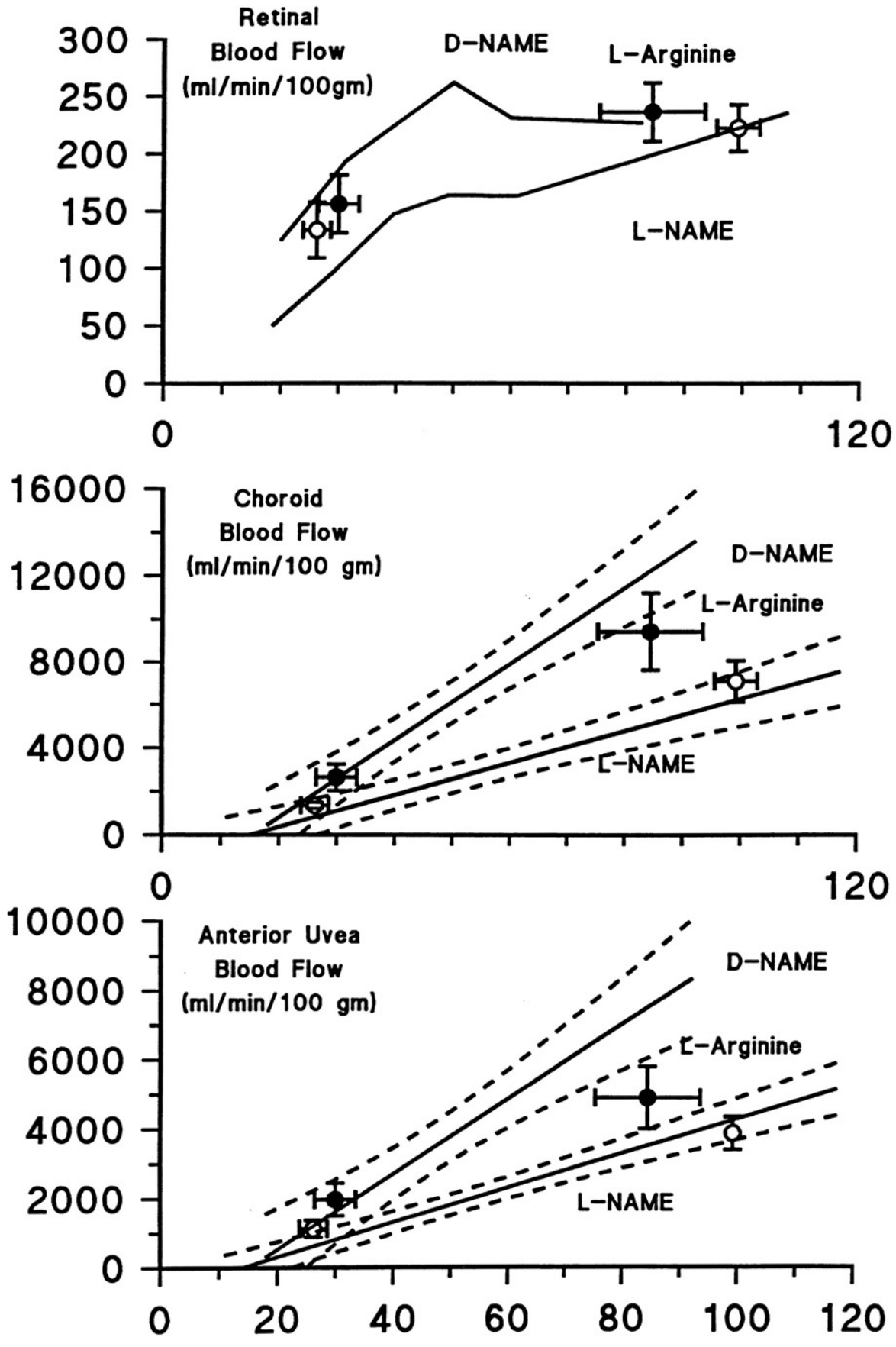
Retinal
Blood Flow
(ml/min/100gm)
D-NAME
L-Arginine
L-NAME
300
250
200
150
100
50
0
0
120
Choroid
Blood Flow
(ml/min/100 gm)
D-NAME
L-Arginine
L-NAME
16000
12000
8000
4000
0
0
120
Anterior Uvea
Blood Flow
(ml/min/100 gm)
D-NAME
L-Arginine
L-NAME
10000
8000
6000
4000
2000
0
0
20
40
60
80
100
120
Ocular Perfusion Pressure (mmHg)

Choroidal induced with L-NAME infusion (from 112 ± 3 mmHg to 97 ± 8 mmHg).blood flow at an ocular perfusion pressure of 84 ± 9 mmHg showed a 32.6% increase following L-arginine bolus administration when compared to L-NAME. Anterior uveal blood flow increased by 26.5% following L-arginine administration when compared to L-NAME. The mean and standard error of the mean values of choroidal and anterior uveal blood flows following L-arginine administration at the high OPP were above the 95% confidence limit for the mean blood flow values obtained for L-NAME treated animals. At a OPP of 28 ± 3 mmHg choroid and anterior uveal blood flows following L-arginine were within the 95% confidence limit for the D-NAME treated groups. Blood gas analysis comparison between pre-L-arginine and post L-arginine conditions are shown in **Table X**. No significant differences were obtained.

Kidney Flows:

A two-tailed paired T-test comparing bilateral total kidney blood flow for the D-NAME and L-NAME treated animals revealed non statistically significant differences ($p = 0.10$). The right and left kidneys received mean blood flows of 678 ± 31 and 700 ± 32 ml/min/100 gm wet tissue weight, respectively.

Table X: Comparison of hematocrit (Hct) and blood gas analyses preceeding L-arginine administration and after 180 mg/kg bolus administration of l-arginine. No significant differences between pH, PCO_2, PO_2, and Hct were observed.

Table X. ARTERIAL BLOOD DATA FOR L-ARGININE TREATED ANIMALS

	pH	PCO_2, mmHg	PO_2, mmHg	Hct
PRE L-ARGININE	7.44 ± .02	37 ± 1	95 ± 3	37 ± 2
POST L-ARGININE	7.41 ± .01	35 ± 1	92 ± 4	40 ± 3

Values are means ± SEM.

DISCUSSION

It has been demonstrated that nitric oxide plays a significant role in the regulation of ocular blood flow in neonate piglets. To our knowledge this is the first in-vivo study to demonstrate the role of nitric oxide in the ocular microcirculation using radiolabelled microspheres with simultaneous measurement of blood flow to the retina, choroid, and anterior uvea. We have demonstrated that enantiomeric specific blockade of NOS by L-NAME compromises the autoregulatory capacity of the retinal vasculature, and that NO is a mediator in establishing the resting basal tone of the uveal circulation.

The mechanism operative in the modulation of blood flow to the retina and uveal circulations are very different. Linear pressure-flow relationships to the uveal circulation in response to reductions in perfusion pressure gradients by increasing IOP have been previously reported (Alm & Bill, 1973b; Ernest, 1989a,b). In this study we altered ocular perfusion pressure by manipulating IOP hydrostatically without controlling the prevailing MAP. We felt that decreasing ocular perfusion pressure by elevating IOP rather than lowering MAP has more pertinent clinical relevance, for instance in acute closed-angle glaucoma (Grunwald et al, 1988; Alder et al, 1989 & 1990). Furthermore, altering IOP rather than MAP to control ocular perfusion pressure assured hemodynamic stability for the microsphere technique. Hemodynamic stability is an essential requirement when measuring blood flow with the microsphere technique.

However, some authors (Kiel & Shepherd, 1992) suggest that this method of changing ocular perfusion pressure suppresses the capacity of the choroidal circulation to autoregulate and that the efficacy of the autoregulation is dependent on IOP. In pentobarbital anesthetized albino rabbits using a laser Doppler flowmeter the authors demonstrated evidence of choroidal autoregulation when arterial pressure was controlled to change the ocular perfusion gradient and when the IOP was less than 25 mmHg. As the authors suggest it is feasible that increasing IOP may not be the appropriate stimulus for eliciting choroidal or anterior uvea blood flow autoregulation. In our study we failed to observe any apparent capacity of the choroid or anterior

uvea circulations to autoregulate blood flow. We obtained a strong linear correlation between blood flow and ocular perfusion pressure. Our findings are consistent with the findings of Alm & Bill (1973b) and Friedman (1970) who manipulated IOP to alter OPP and measured blood flow changes using radiolabelled microspheres.

Elevating IOP raises ocular venous pressure. Bill (1963) showed that intraorbitally the pressure in the vortex veins (which drain the choroid) is equal to IOP over a broad range of intraocular pressures. Employing the use of IOP elevations (or venous pressure elevation) to study blood flow autoregulation provides insight which helps to elucidate between the metabolic and myogenic mechanism responsible for autoregulation in the various vascular beds (Granger & Shepherd, 1973; Johnson, 1964). According to the myogenic theory altering transmural pressure gradient by raising the venous pressure (ie, IOP in our case) decreases the perfusion pressure gradient and increases the transmural pressure gradient (Kiel & Shepherd, 1992). This evokes a myogenic vasoconstriction according to the law of LaPlace, which along with a fall in perfusion pressure gradient will cause a reduction in blood flow. According to the metabolic theory, decreased blood flow caused by a decreased perfusion pressure gradient results in accumulation of vasoactive metabolites which causes blood flow to remain at baseline values. The use of elevation in intraocular pressure is a useful method to determine which mechanism, myogenic or metabolic, predominates in the particular vascular beds of the ocular circulation. Only the metabolic mechanism of blood flow regulation would maintain baseline blood flow values during elevations in IOP.

These findings are consistent with a strong myogenic component to the uveal circulation for the maintenance of blood flow. These findings are in agreement with Kiel & Shepherd (1992) who used a myogenic mathematical model of the choroid and were able to simulate the results from experimental observations.

This study has established that the high basal blood flow to the choroid and to the anterior uvea is mediated by nitric oxide. We were able to reduce basal choroidal and anterior uvea blood

flow by 47% and 43%, respectively, by enantiomeric specific blockade of NOS with L-NAME. The influence of NO in the maintenance of uveal blood flow was more apparent at the high ocular perfusion pressures than at the lower OPP. This suggests that there is a constant basal release of NO in the choroidal and anterior uveal circulations.

The choroidal vasculature which receives more blood flow per gram of tissue than perhaps any other tissue in the body, is exposed to high shear stress. Since the arterio-venous oxygen difference of the choroid is approximately 3%, the high blood flow to the choroid is not due to tissue metabolic demands. Therefore, we postulate that the basal release of NO in the uveal circulation is a result of shear stress. Physical stimuli such as shear stress, and pulsatile stretching of the vessel wall can stimulate the release of NO and may be physiologically the most important mechanism of NO release from the vascular endothelium (Busse et al, 1993). It has been documented that shear stress-induced release of NO is a major factor regulating vascular tone. The basal release of NO has been reported to represent a large portion (20-40%) of the total NO releasing capacity of endothelial cells. It is feasible that the basal release of NO is mediated by a Ca^{2+} dependent and Ca^{2+} independent NOS and that the two pathways contribute synergistically to the basal release of NO. However, utilizing analogues of L-arginine, one is not able to differentiate between the pathways. In cultured bovine endothelial cells it has been found that an increase in shear stress is associated with an increase in Ca^{2+} and consequently an increase in NO formation. In some instances, shear stress induced vasodilation can be mediated by a flow-sensitive potassium channel which results in the production of NO (Busee et al, 1993). In addition, shear stress-dependent release of NO may be mediated by agonists that stimulate the endothelium in an autocrine manner. In cultured endothelial cells flow has been shown to induce the release of ATP, substance P, and acetylcholine.

At high intraocular pressures the perfusion pressure gradient is reduced, resulting in decreased blood flow and thus, attenuating the fluid shear stress dependent release of NO and minimizing the vasodilator contribution of NO to the choroidal and anterior uvea vasculatures. We

obtained convergence of the linear regressions representing uveal blood flow for each treatment group at the low ocular perfusion pressures. Given the current experimental design it is not possible to isolate the factors which may contribute to the observed convergence of uveal blood flow in the two treatment groups at the low ocular perfusion pressures. These results indirectly support the notion that the predominant effect of NO on the uveal circulation is at baseline and higher ocular perfusion pressures, where shear stress would be greater and act as the mediator of NO release.

An alternative explanation could be obtained from investigating blood flow patterns of the contralateral eye. Analysis of blood flow to the contralateral eye, which had the IOP maintained near baseline (12 ± 2 mmHg) for the duration of the experimental protocol, provides evidence for stability of ocular blood flow over time. Significant differences in blood flow to the experimental eye were obtained at time points at which the contralateral eye demonstrated stability of flow. It is apparent that convergence of uveal blood flow, but not retinal blood flow, occurred in the contralateral eye.

In an attempt to explain this observation we analyzed MAP and OPP changes over time. Since IOP was held constant near baseline IOP, the MAP and OPP parallel each other. There was less than a 10 mmHg reduction in OPP and MAP in the L-NAME treated group for the duration of the experiment. In the D-NAME treated group slight elevation in MAP and OPP were evident at approximately 140 minutes post completion of the surgical protocol. Clearly, these minor fluctuations cannot account for the magnitude in the reduction of uveal blood flow seen over time. However, the observed reduction in uveal blood flow to the contralateral eye correlate closely with changes in cardiac output (L-NAME $r=0.81$; D-NAME $r=0.69$). In contrast, ocular blood flow to the eye which had the perfusion pressure gradient experimentally manipulated showed no correlation between ocular blood flow and cardiac output (L-NAME $r=0.37$; D-NAME $r=0.29$). We postulate that because the uveal circulation is pressure passive, the reduction of uveal blood flow in the contralateral eye is predominantly due to reductions in cardiac output overtime.

The observed reduction of blood flow over time in the contralateral eye could also be consistent with an effect of D-NAME on blood flow. It has been reported that alkyl esters of L-arginine such as L-NAME and possibly D-NAME are muscarinic receptor antagonists (Buxton et al, 1993). Although competitive blockade of NOS by L-NAME is enantiomerically specific, it is possible that there is an allosteric binding site for these arginine analogues on the muscarinic receptor which is not sensitive to enantiomeric alterations due to structural homology. It is feasible that a cumulative effect of D-NAME caused the observed reduction in uveal blood flow by muscarinic antagonism. This hypothesis is consistent with an average elevation of 11 mmHg in MAP seen after 140 minutes of D-NAME infusion.

It must be stressed that although this suggests that D-NAME may not be a true "inactive enantiomer", presently homologous enantiomers are the best vehicle controls available in part due to the lack of D-transport mechanisms. This does not signify that the dramatic reductions seen in uveal blood flow following L-NAME are mediated by antagonizing muscarinic receptors rather than competitive blockade of the NOS enzyme. Although some degree of blood flow reduction could be attributed to muscarinic antagonism. One is able to differentiate between these two effects because NOS blockade by L-NAME is sensitive to reversibility with exogenous L-arginine, while muscarinic receptor antagonism is not (Buxton et al, 1993).

Currently, enantiomeric analogues of L-arginine provide the best method by which to investigate the physiological role of NO in-vivo. The L-analogues prevent the production of NO and affect any process dependent on NO production. The use of these analogues to conduct in-vivo studies present some unavoidable drawbacks. The D- or L- analogues are likely to adversely affect processes which involve L-arginine, not exclusively NOS enzyme and NO production. Arginine is involved in amino acid metabolism to form glutamic acid, which is used in the CNS for formation of GABA. Arginine is involved in polyamine biosynthesis and these analogues could be incorporated or substituted into proteins. Arginine is a key member in the ornithine-urea cycle, which is the principal catabolic pathway, and has been found in human aqueous humor (133μmole/L) although

its function is currently unknown (Altman & Dittmer, 1974). Furthermore, these analogues have limited selectivity making it impossible to differentiate the effects of the calmodulin-dependent and calmodulin-independent effects of the NOS enzyme.

Pharmacological effects on ocular blood flow merit some discussion. Pharmacological effects could also contribute to the observed reduction in blood flow over time in both treatment groups. Pentobarbital has been shown to have some vagolytic effects. The effects of sodium pentobarbital and chloralose/urethane anesthesia on ocular blood flow has been investigated (Alm & Bill, 1973b). Retina blood flows were slightly reduced per given perfusion pressure in 67% of monkeys anesthetized with sodium pentobarbital anesthesia when compared to same dose of chloralose/urethane anesthesia. The autoregulatory capacity of the retinal circulation under sodium pentobarbital anesthesia was not significantly affected in comparison to chloralose/urethane anesthesia. Monkeys receiving the barbiturate anesthetic sodium pentobarbital demonstrated autoregulation of retinal blood flow during increased IOP, showing a 1% mean increase in retinal blood flow when perfusion was reduced. The response with chloralose anesthesia showed a mean retinal blood flow increase of 5% for the same changes in perfusion pressure. Therefore blood flow changes to the retina was not significantly affected by the choice of anesthetic agent, although a barbiturate anesthetic could have a tendency to attenuate the autoregulatory response of the retinal circulation.

The non-depolarizing neuromuscular blocking agent pancuronium bromide (1 mg/kg/IV) was utilized to cause paralysis of the extraocular muscles and to eliminate chest wall resistance and ineffective spontaneous ventilations. Although this drug does not cross the blood-retinal or blood-brain barrier because of a quaternary nitrogen which makes it poorly soluble in lipid (Katzung, 1989), it has been shown to have vagolytic action and enhance the release or blocked reuptake of norepinephrine.

The possibility that blood flow reductions over time could be a result of extensive blood withdrawal required for microsphere technique or the result of excessive arteriolar and capillary

plugging due to multiple serial injections of microspheres was considered. We concluded that both these options are highly unlikely. The temporal control studies as well as the retinal blood flow of the contralateral eye demonstrate consistent blood flow estimations and provide evidence against any artifactual blood flow estimate due to an exclusive isotope. Alm & Bill (1972a, 1973b) have conducted studies investigating the effect of different dosages of injected spheres and concluded using two extreme dosages of microspheres that the calculated eye blood flows for the retina and choroid were not affected. The iris was apparently more susceptible to capillary plugging at the high dose than the remaining ocular circulation, as well as other regions of the cerebral circulation. Showing a substantial reduction (53%) in mean blood flow at the high dose. Their "high dose" was substantially greater than the total number of spheres which we injected.

This study has demonstrated that enantiomeric specific blockade of NOS by L-NAME significantly compromises the autoregulatory capacity of the retinal circulation. The influence of NO in establishing a basal tone to the retinal microcirculation is less clearly defined, but its role appears to be less significant than in the modulation of retinal autoregulation. In each eye retinal baseline blood flow values in the D-NAME and L-NAME treated groups did not differ significantly. However, consistently lower retinal blood flows were obtained with L-NAME regardless of whether the ocular OPP gradient was decreased or maintained near baseline. In-vitro studies in large ophthalmic vessels have shown a role for NO in maintaining basal vascular tone (Yao et al, 1991; Haefliger et al, 1992). Our findings, although inconclusive with regards to a basal role of NO in the retinal microcirculation, are not in opposition to the previously reported findings. Our findings do suggest that the retinal microcirculation is perhaps less dependent on NO for basal tone than the larger caliber vessels supplying the retinal circulation.

Nitric oxide appears to exert its predominant effect on retinal autoregulation at ocular perfusion pressures of 30, 40, and 50 mmHg. The influence of NO in maintaining retinal blood flow at the lower OPP of 20 mmHg appears to be decreased in comparison to the higher ocular perfusion pressures. The apparent decreased contribution of NO in maintaining retinal blood flow

at this lower OPP could stem from several possible mechanisms. At an OPP of 20mm Hg we are near the lower limit of retinal autoregulation indicated by a G_c which approaches zero. It is possible that the effect of NO per se (isolated from tissue metabolic changes) are negligible at this OPP. At the low OPP both the retinal and choroidal circulations are extensively compromised. The retina has one of the highest oxygen requirements of any tissue in the body as well as high requirements for glucose and other metabolites. It is highly dependent on the choroidal circulation to meet these nutritional requirements. At the low OPP the retina is susceptible to hypoxia and ischemia. It has been well documented that hypoxic tissue generates oxygen free radicals (Veriac et al, 1993). It is possible that ischemia can impede the effects of NO through oxygen-derived free radical generation caused by hypoxia at high intraocular pressures. Hypoxia could trigger the release of a vasoconstrictor agent or expedite the inactivation of NO by reactions with oxygen free radicals. Alternatively, hypoxia could inhibit NOS activity primarily through the depletion of oxygen. The NOS enzyme requires molecular oxygen as a substrate. The activity of the NOS enzyme under hypoxic conditions has been investigated and has led to contradictory findings.

Rengasamy and Johns (1991) characterized the modulation of NOS activity by measuring L-[^{3}H] citrulline formation in bovine cerebellum homogenates during high and low oxygen tensions. Hypoxia markedly inhibited NOS activity primarily through the depletion of oxygen. Not all studies, however, have shown that hypoxia decreases NOS activity. Pohl and Busse (1989) reported that hypoxia stimulated NOS activity in the rabbit femoral artery and aorta. It is postulated that the enhanced synthesis of NO is due to an increase in cellular Ca^{2+} at a low PO_2 (20-50 mmHg). The effect of hypoxia on NOS activity is currently an area of debate, however during hypoxia the effective concentration of NO and therefore its effects would likely be attenuated due to rapid inactivation by oxygen free radicals.

Other feasible mechanisms by which the role of NO in the retinal circulation could be influenced is by interaction of other vasoactive metabolites which may constitute a significant contribution to the maintenance of retinal blood flow during metabolic alterations. Gidday & Park

(1993), investigated ocular blood flow using videomicroscopy in newborn piglets and concluded that endogenous adenosine does not contribute to the maintenance of basal tone, but plays an important role in the metabolic regulation of retinal blood flow mediated via A-2 receptors. Adenosine would be a good mediator because its production is linked to ATP production and thus would serve to increase retinal blood flow under conditions of reduced oxygen supply. Several studies have documented calcium-dependent retinal adenosine release, and increases in intracellular Ca^{2+} have been reported during hypoxia (Gidday & Park, 1993). Therefore contributing effects by other vasodilator agents such as adenosine or prostacyclin in the maintenance of ocular blood flow at low ocular perfusion pressures may mask the vasodilator effects brought about by NO.

The effects of acute changes in intraocular pressure on regional eye blood flow have been determined using 15μm radiolabelled microspheres in monkeys and cats (Alm & Bill, 1972a & 1973b). The spontaneous pressure of one eye was monitored (mean IOP 10mmHg; OPP = 82mmHg) and the contralateral eye was stabilized for a minimum of 20 minutes at a mean intraocular pressure of 30mmHg (PP = 62mmHg). The eyes with increased IOP showed a 30% reduction in blood flow to the choroid and a 30-34% reduction in the prelaminar portion of the optic nerve head when compared to the control eye. Blood flow in the retina, the iris and ciliary processes and muscles did not show a statistically significant reduction in blood flows, suggesting that these structures have sufficient autoregulatory capacities within the pressure range investigated. In a similar study (Alm & Bill, 1972a) using cats, moderate reductions in perfusion pressures resulted in either no change or an increase in blood flow to the retina. It is speculated that the increase in retinal blood flow during reductions in perfusion pressures is a compensation for a significant reduction in choroidal blood flow. Therefore, it appears that under certain circumstances the retinal vasculature may over-autoregulate in response to decreases in perfusion pressures.

The magnitude of the "over-compensatory" response in the retinal circulation to changes in IOP appears to be species dependent. It appears that the primate retina is less dependent on oxygen diffusion from the choroid than is the retina from cats. It is important to point out that there

are some distinct differences between the vascular anatomy of the cat eye and that of the pig which resembles more the human retina. We observed some evidence of over-compensation of retinal blood flow with D-NAME at an OPP of 50 mmHg, a perfusion pressure similar to that at which Bill and Alm described the observed phenomenon. In our studies, at an OPP of 50 mmHg, the choroidal circulation decreased by approximately 55% from baseline value. Our autoregulatory gain calculation for retinal blood flow with D-NAME at this OPP is above unity which is indicative of an overregulatory phenomenon. Interestingly, no such response was observed when nitric oxide was blocked with L-NAME. This observation suggests that nitric oxide may play a role in reactive hyperemic mechanisms in the retinal circulation.

A marked transient, dose-related hypotensive effect following intracardiac bolus administration of L-arginine (180 mg/kg) was observed. This systemic cardiovascular effect has been attributed to endogenous acetylcholine induced NO release (Cernadas et al, 1990). We selected to perform intracardiac injections of L-arginine in order to optimize the effective concentration of L-arginine reaching the brain and ocular circulation and to minimize ligand binding and interference by other plasma amino acid competitors.

Choroidal and anterior uveal blood flows showed a tendency to increase following L-arginine administration. However, the increases in blood flows at two perfusion pressures were not significantly different when compared to L-NAME control blood flows. Following L-arginine administration blood flows (mean ± SEM) were above the 95% confidence interval for the linear regression established for blood flow values in the prior series of L-NAME treated animals. Nitric oxide is synthesized stereospecifically from L-arginine. Therefore we postulate that the increase in ocular blood flow seen following L-arginine administration is due to the reversibility of the NOS blockade by L-NAME and that the increase in flow is thereby mediated via the NO:L-arginine pathway. At our high dose of L-arginine and in the absence of a D-arginine control we cannot exclude the possibility that the vasodilator effects of L-arginine may be endothelium independent, not stereospecific, and unrelated to NO (Calver et al, 1990). Therefore it is difficult to exclude other

elicited mechanisms which could have contributed to the increase in ocular blood flow. For instance, it has been shown that arginine can release histamine from isolated perfused skin in cats (Eldridge & Paton, 1954). L-arginine effects are widespread and have been shown to release growth hormone, insulin, glucagon, and prolactin (Cernadas et al, 1990).

In the absence of a D-arginine control the antagonism of NOS blockade by exogenous L-arginine administration remains inconclusive. L-arginine was administered as a bolus rather than by constant infusion. This may account for the lack of significant increase in blood flow compared to L-NAME control blood flow values. A constant infusion was attempted but invariably it caused an acute and profound hypotensive response which led to demise of the animal. The limited effectiveness of L-arginine to show complete reversal of retinal blood flow could stem from limitations in crossing of the blood-retinal barrier. L-arginine is a cationic amino acid which is transported across the blood-retinal barrier (BRB) and blood-brain barrier (BBB) via two main transport systems; 1) the L-system for neutral amino acids and 2) the cationic amino acid system (y+) (Bradbury, 1992). The L-system is present in isolated microvessels from the brain and retina. The BRB consists of two morphologically distinct sites: the retinal capillary endothelium and the retinal pigmented epithelium. The considerations to assess the permeability of L-arginine across the RBB are: The lipid solubility of the drug, its degree of protein binding and its affinity to naturally occurring transport systems which in part is dependent on side-chain hydrophobicity. The affinity of L-NAME or the lipophilic properties of L-NAME are much higher than L-arginine and therefore it is feasible that full reversibility of the L-NAME effect was not possible. Some transported amino acids can be extensively metabolized in the endothelial cells and this could have modified the extent of transport. The anesthetic agent sodium pentobarbital appears to reduce the permeability of the BBB and possibly the BRB, whether this is the result of a direct effect upon the vasculature or due to alterations in metabolism is still unclear.

Although precautions were taken to insure accurate ocular blood flow determination via the microsphere technique, methodological factors cannot be ruled out. Errors in blood flow

determinations could have resulted from: 1) non-representative arterial withdrawal samples 2) insufficient number of microspheres in the ocular tissues 3) inhomogeneous distribution of the microspheres into the ocular circulation and 4) variability in weight measurements. We attempted to minimize errors stemming from these specific sources in the following manner. The withdrawal pump was routinely calibrated and each withdrawal sample was closely scrutinized during the withdrawal procedure. The number of microspheres injected were calculated to optimized the number of spheres reaching the ocular circulation, without altering general hemodynamics. We optimized and monitored the homogeneity of microsphere distribution by conducting intraatrial microsphere injections and comparing blood flow to each kidney. We obtained equal blood flow estimates to the kidneys and eyes which provided evidence for homogeneity of microsphere distribution in the systemic circulation. We minimized variability in our weight measurements by utilizing dry rather than wet tissue weight to make blood flow determinations.

In conclusion, this study presented strong evidence which demonstrates that nitric oxide plays an important physiological role in the regulation of retinal, choroidal, and anterior uvea blood flow to the microcirculation. To our knowledge, these findings are the first in-vivo studies to demonstrate the role of nitric oxide in modulating the autoregulatory capacity of the retinal circulation. This study provides evidence that nitric oxide plays a role in regulating the basal tone of the uveal circulation. This is the first study to investigate the interrelationship of the uveal and retinal circulations under conditions of nitric oxide blockade, with altered perfusion pressure to the ocular circulation. These findings provide a new pathogenic mechanism for many ocular vascular diseases. These studies are of great interest both from a basic science perspective and for direct clinical application in ophthalmology.

Bibliography

1. Adelstein, R.S.; Conti, M.A. Phosphorylation of platelet myosin increases actin-activated myosin ATPase activity. Nature Lond.; 1975; 256: 597-598.

2. Alder, V.A.; and Cringle, S.J. Intraretinal and Preretinal PO2 response to acutely raised intraocular pressure in cats. American Journal of Physiology; 1989; 256: H1627-H1634.

3. Alder, V.A.; Ben-Nun, J.; and Cringle, S.J. PO2 profiles and oxygen consumption in cat retina with an occluded retinal circulation. Investigative Ophthalmology & Visual Science; 1990; 31(No.6): 1029-1034.

4. Alm, A.; and Bill, A. The oxygen supply to the retina, II. Effects of high intraocular pressure and of increased arterial carbon dioxide tension on uveal and retinal blood flow in cats: A study with radioactively labelled microspheres including flow determination in brain and some other tissues. Acta Physiol. Scand.; 1972a; 84: 306-319.

5. Alm, A.; and Bill, A. The oxygen supply to the retina I. Effect of changes in intraocular and arterial blood pressures, and in arterial PO2 and PCO2 on the oxygen tension in the vitreous body of the cat. Acta Physiol. Scand.; 1972b; 84: 261-274.

6. Alm, A.; and Bill, A. The effect of stimulation of the cervical sympathetic chain on retinal oxygen tension and on uveal, retinal and cerebral blood flow in cats. Acta physiol. Scand.; 1973a; 88: 84-94.

7. Alm, A.; and Bill, A. Ocular and optic nerve blood flow at normal and increased intraocular pressures in monkeys (Macaca irus): A study with radioactively labelled microspheres including flow determinations in brain and some other tissues. Exp. Eye Res.; 1973b; 15: 15-29.

8. Altman, P.L.; and Dittmer, D.S., eds. Biology Data Book. Second Ed. Vol. III. Bethesda, MD: Federation of American Societies for Experimental Biology; 1974.

9. Auker, C.R.; Parver, L.M.; Doyle, T.; and Carpenter, D.O. Choroidal blood flow I. Ocular tissue temperature as a measure of flow. Arch Ophthalmol; Aug. 1982;100: 1323-1326.

10. Barany, E. H. Simultaneous measurement of changing intraocular pressure and outflow facility in the vervet monkey by constant pressure infusion. Invest. Ophthalmology; 1964; (pp 135-143).

11. Bayliss, W.M. On the local reactions of the arterial wall to changes in internal pressure. Journal Physiology (London). 1902; 28: 220.

12. Berk, B.C.; Alexander, W.R. Vasoactive effects of growth factors. Biochemical Pharmacology; 1989; 38(2): 219-225.

13. Berne, R. Metabolic regulation of blood flow. Circulation Research; 1964; 15: 261-267.

14. Bevington, P.R. Data reduction and error anaysis for the physical sciences. St. Louis: McGraw Hill Inc.; 1969 P.237.

15. Bill, A. Blood circulation and fluid dynamics in the eye. Physiol. Rev.; 1975; 55: 383.

16. Bill, A. The uveal venous pressure. Arch Ophthalmol; 1963; 69: 780.

17. Bill, A.; and Sperber, G.O. Control of retinal and choroidal blood flow. Eye; 1990; 4: 319-325.

18. Bill, A. Handbook of Physiology. The Cardiovascular System IV, Chapter 22: Circulation in the Eye. Bethesda, Maryland: American Physiological Society; 1983.

19. Bok, D. Processing and transport of retinoids by the retinal pigment epithelium. Eye; 1990; 4: 326-332.

20. Borgdorff P; Sipkema P; Westerhof N. Pump perfusion abolishes autoregulation possibly via prostaglandin release. Am. J. Physiol. (Heart Circ. Physiol.); 1988; 255(24): H280-H287.

21. Bradbury M.W.B. Physiology and Pharmacology of the Blood-Brain Barrier. New York: Springer-Verlag; 1992.

22. Bredt D.S.; Ferris C.D.; Snyder S.H. Nitric oxide synthase regulatory sites. Phosphorylation by cyclic AMP-dependent protein kinase, protein kinase C, and calcium/calmodulin protein kinase; identification of flavin and calmodulin binding sites. J Biol Chem; 1992; 267(16): 10976-81.

23. Bredt D.S.; Hwang P.M.; Snyder S.H. Localization of nitric oxide synthase indicating a neural role for nitric oxide. Nature; 1990; 347: 768-70.

24. Bredt D.S.; Snyder S.H. Nitric oxide mediates glutamate-linked enhancement of cGMP levels in the cerebellum. Proc Natl Acad Sci; 1989; 86(22): 9030-3.

25. Buckberg, G.D.; Luck, J.C.; Payne, B.D.; Hoffman, J.I.E.; Archie, J.P.; and Fixler, D.E. Some sources of error in measuring regional blood flow with radioactive microspheres. Journal of Applied Physiology; Oct. 1971; 31(no.4): 598-604.

26. Bush P.A.; Aronson W.J.; Raifer, J.; Ignarro L.J. The L-arginine-nitric oxide-cyclic GMP pathway mediates inhibitory Nonadrenergic-Noncholinergic Neurotransmission in the corpus cavernosum of the human and rabbit. Circulation Suppl; 1993; 87(5): V-30.

27. Busse, R.; Mulsch, A.; Fleming, I.; Hecker, M. Mechanisms of nitric oxide release from the vascular endothelium. Circulation. 1993; 87:5; V-18.

28. Buxton, I.L.O; Cheek, D.J.; Eckman, D.; Westfall, D.P.; Sanders, K.M.; Keef, K.D. N-Nitro L-arginine methyl ester and other alkyl esters of arginine are muscarinic receptor antagonists. Circulation Research; 1993; 72: 387-395.

29. Calver, A.; Collier, J.; Vallance, T. L-arginine-induced hypotension. The Lancet. 1990; 336: 1016-1017.

30. Cernadas, M.R.; Gallego, M.J.; Lopez-Farre, J. L-arginine-induced hypotension. The Lancet. 1990; 336: 1017.

31. Chemtob, S.; Beharry, K.; Rex, J.; Chatterjee, T.; Varma, D.; Aranda, J.V. Ibuprofen enhances retinal and choroidal blood flow autoregulation in newborn piglets. Invest Ophthalmol Vis Sci;1991; 32: 1799-1807.

32. Coleman, A.L.; Quigley, H.A.; Vitale, S.; Dunkelberger, G. Displacement of the optic nerve head by acute changes in intraocular pressure in monkey eyes. Ophthalmology; 1991; 98: 35-40.

33. Compton, A.H. The scattering of x-rays as particles. Amer J Phys; 1961; 29: 817-820.

34. Cunha-Vaz, J.G; Shakib, M.; and Aston, N. Studies on the permeability of the blood-retinal barrier. Br. J. Ophthalmology; 1966; 50: 441.

35. Dawson, V.L.; Dawson, T.M.; London, E.D.; Bredt, D.S.; and Snyder, S.H. Nitric oxide mediates glutamate neurotoxicity in primary cortical cultures. Proc Natl Acad Sci; 1991; 88: 6368-6271.

36. Deutsch, T.A.; Read, J.S.; Ernest, T.J.; and Goldstick, T.K. Effects of oxygen and carbon dioxide on the retinal vasculature in humans. Arch. Ophthalmol.; 1983; 101:1278-1280.

37. Duling, B.R. Oxygen sensitivity of vascular smooth muscle II: in vivo studies. Am. J. Physiol.; 1974; 42: 227.

38. Eldridge, E.; Paton, W.D.M. Release of histamine from cat's isolated perfused skin by amino-acids. Journal of Physiology; 1954; 124: 27-28P.

39. Ernest, T.J. Retina Vol. I Editor Stephen J. Ryan. Chapter 7: Macrocirculation and microcirculation of the retina. New York: C.V. Mosby; 1989a. p. 65-66.

40. Ernest, T.J. Retina Vol. I. Editor Stephen J. Ryan. Chapter 8: Choroidal circulation p.67-68. New York: C.V. Mosby; 1989b.

41. Fantone, J.C.; Ward, P.A. Oxygen-derived radicals and their metabolites: relationship to tissue injury. Kalamazoo, MI: Upjohn Co.; 1985.

42. Faraci, F.M. Role of nitric oxide in regulation of basilar artery tone in vivo. Am J Physiol; 1990; 259: H1216-21.

43. Faraci, F.M.; Breese, K.R. Nitric oxide mediates vasodilation in response to activation of N-methyl-D-aspartate receptors in brain. Circulation Research; 1993; 72: 476-480.

44. Faraci, F.M.; Heistad, D.D. Regulation of cerebral blood vessels by humoral and endothelium-dependent mechanisms. Update on humoral regulation of vascular tone. Hypertension; 1991; 17(6pt 2): 917-22.

45. Ffytche, T.J.; Bulpitt C.J.; Kohner, E.M.; Archer, D.; and Dollery, C. Effect of changes in intraocular pressure on the retinal microcirculation. Brit. J. Ophthalmol.; 1974; 58: 514-522.

46. Folkow, B. Description of the myogenic hypothesis. Circulation research; 1964; 15: 279-85.

47. Forstermann, U; Harald, H.H.; Schmidt, W.; Pollock, J.S.; Sheng, H.; Mitchell, J.A.; Warner, T.D.; Nakane, M.; Murad, F. Isoforms of nitric oxide synthase. Characterization and purification from different cell types. Biochem Pharmacol; 1991; 42: 1849-1857.

48. Friedman, E. Choroidal blood flow: Pressure-flow relationships. Arch. Ophthalmol. 1970; 83:95.

49. Furchgott, R.F.; and Zawadzki, J.V. The obligatory role of endothelial cells in the relaxation of arterial smooth muscle by acetylcholine. Nature; 1980; 288: 373-376.

50. Garthwaite, J. Glutamate, nitric oxide and cell-cell signaling in the nervous system. TINS; 1991; 14: 60-67.

51. Gaskell, W.H. On the Changes of the blood-stream in skeletal muscles through stimulation of their nerves. J. Anat. & Physiol. 1877; 11: 360-402.

52. Gasser P.; Flammer J. Blood-cell velocity in the nail fold capillaires of patients with normal-tension and high tension glaucoma. Am J. Ophthalmol.; 1991; 111: 585.

53. Gidday, J.M.; and Park, T.S. Microcirculatory responses to adenosine in the newborn pig retina. Pediatric Research; 1993; 33(6): 620-627.

54. Granger, H.J.; and Norris, C.P. Intrinsic regulation of intestinal oxygenation in the anesthetized dog. Am J Physiol (Heart Circ. Physiol 7); 1980; 238: H836-H843.

55. Granger, H.J.; and Shepherd, A.P. Intrinsic microvascular control of tissue oxygen delivery. Microvasc. Res. 1973; 5:49.

56. Griffith, T.M.; Edwards, D.H. Myogenic autoregulation of flow may be inversely related to endothelium-derived relaxing factor activity. Am J Physiol; 1990; 258(27): H1171-80.

57. Grunwald, J.E.; Riva, C.E.; and Kozart, D.M. Retinal circulation during a spontaneous rise of intraocular pressure. British Journal of Ophthalmology; 1988; 72: 754-758.

58. Haefliger, I.O.; Flammer, J.; Luscher, T.F. Nitric oxide and endothelin-1 are important regulators of human ophthalmic artery. Invest Ophthalmol Vis SCi; 1992; 33: 7(2340-3).

59. Hartshorne, D.J.; Kawamura, T. Regulation of contraction-relaxation in smooth muscle. News in Physiological Science (NIPS); 1992; 7: 59-64.

60. Hayreh, S.S. Segmental nature of the choroidal vasculature. Br. J. Ophthalmol.; 1975; 59: 631-648.

61. Heymann, M.A.; Payne, B.D.; Hoffman, J.I.E.; and Rudolph, A.M. Blood flow measurements with radionuclide-labelled particles. Progress in Cardiovascular Diseases; July/Aug. 1977; 20(no.1): 55-79.

62. Hope, B.T.; Michael, G.J.; Kniggs, K.M.; and Vincent, S.R. Neuronal NADPH diaphorase is a nitric oxide synthase. Proc Natl Acad Sci; 1991; 88: 2811-2814.

63. Horio, Y.; Murad, F. Solubilization of guanylyl cyclase from bovine rod outer segments and effects of lowering Ca2+ and nitro compounds. J Biol Chem; 1991; 266(6): 3411-5.

64. Iadecola, C. Does nitric oxide mediate the increases in cerebral blood flow elicited by hypercapnia? Proc Natl Acad Sci; 1992; 89(9): 3913-6.

65. Ignarro, L.J.; Buga, G.M.; Byrns, R.E.; Wood, K.S.; Chaudhuri, G. Endothelium-derived relaxing factor and nitric oxide possess identical pharmacologic properties as relaxants of bovine arterial and venous smooth muscle. J Pharmacol Exp Ther; 1988a; 246(1): 218-26.

66. Ignarro, L.J.; Byrns, R.E.; Buga, G.M.; Wood, K.S.; Chaudhuri, G. Pharmacological evidence that endothelium-derived relaxing factor is nitric oxide: use of pyrogallol and superoxide dismutase to study endothelium-dependent and nitric oxide-elicited vascular smooth muscle relaxation. J Pharmacol Exp Ther; 1988b; 244(1): 181-9.

67. Ignarro, L.J.; Lippton, H.; Edwards, J.C.; Baricos, W.H.; Hyman, A.L.; Kadovitz, P.J.; Gruetter, C.A. Mechanism of vascular smooth muscle relaxation by organic nitrates, nitrites, nitroprusside and nitric oxide: evidence for the involvement of S-nitrosothiols as active intermediates. J Pharmacol Exp Ther; 1981; 218: 739-749.

68. Johnson, P.C. Autoregulation of blood flow. Circulation Research; 1964; 15: 1-290.

69. Joyner, W.L.; Tang, T.; Connelly, B.A.; Kimbrough, B. Does the endothelium play a significant role in the acetylcholine-induced dilation of the human choroid and retina in microvessels grafted into the hamster cheek pouch. ARVO abstract; 1993.

70. Katzung, B.G. Basic and Clinical Pharmacology. Appleton & Lange. East Norwalk, CN. 4th Ed. 1989; Cht. 26 pp 323.

71. Kiel, J.W.; Shepherd, A.P. Autoregulation of choroidal blood flow in the rabbit. Invest Ophthalmol Vis Sci; 1992; 33: 2399-2410.

72. Knowles, R.G.; Moncada, S. Nitric oxide as a signal in blood vessels. Trends in Biological Sciences (TIBS); 1992; 17: 399-402.

73. Knowles, R.G.; Palacios, M.; Palmer, R.M.; Moncada S. Formation of nitric oxide from L-arginine in the central nervous system: a transduction mechanism for stimulation of the soluble guanylate cyclase. Proc Natl Acad Sci; 1989; 86(13): 5159-62.

74. Lancaster, J.R. Nitric oxide in cells. American Scientist; 1992; 80(3): 248-259.

75. Leber, T. Circulations und ernahrungsverhaltnisse des auges in: Handbuch des gesamten augenheilkunde. Leipzig, East Germany: Springer Verlag; 1983. pp 1-89.

76. Lemmingson, W. Uber das Vorkommen von Vasomotor im RetinalKreislauf. Graefes Arch. Clin. Exp.; 1968; 176: 368.

77. Leone, A.M.; Richard, P.M.J.; Knowles, R.G.; Francis, P.L.; Ashton, D.S.; Moncada, S. Constitutive and inducible nitric oxide synthases incorporate molecular oxygen into both nitric oxide and citrulline. J. Biol. Chem.; 1991; 266: 23790-23795.

78. Lide, D.R. Handbook of chemistry and physics. Boca Raton, FL: Editor-in-Chief 73rd Ed. Chemical rubber Publishing Co.; 1993.

79. Lincoln, T.M.; Cornwell, T.L.; Taylor, A.E. cGMP-dependent protein kinase mediates the reduction of Ca2+ by cAMP in vascular smooth muscle cells. Am. J. Physiol. (Cell Physiol 27); 1990; 258: C399-C407.

80. Linden, R.J. Techniques in the life sciences. Ireland: Elsevier; 1983. Vol.P3/I.

81. Luscher, T.F. Endothelin, key to coronary vasospasms? Circulation; 1991; 23: 701.

82. Luscher, T.F.; and Vanhoutte, P.M. The endothelium: Modulator of cardiovascular function. Boca Raton, FL: CRC Press; 1990. pp 1-228.

83. Majid, D.S.; Navar, L.G. Suppression of blood flow autoregulation plateau during nitric oxide blockade in canine kidney. Am J Physiol; 1992; 262: F40-6.

84. Marshall, J.J.; Wei, E.P.; Kontos, H.A. Independent blockade of cerebral vasodilation from acetylcholine and nitric oxide. Am J Physiol; 1988; 255: H847-54.

85. Martin, W.; and Gillespi, J.S. In Novel Peripheral Transmitters. pp 65-79: Pergamon Press; 1990.

86. Mayer, B.; John, M.; Heinzel, B.; Werner, E.R.; Wachter, H.; Schultz, G.; Bohme, E. Brain nitric oxide synthase is a biopterin-and flavin-containing multifunctional oxido-reductase. FEBS lett.; 1991; 288(1-2): 187-191.

87. Molnar, I.; Poitry, S.; Tsacopoulos, M.; Gilodi, N.; and Leuenberger, P.M. Effect of laser photocoagulation on oxygenation of the retina in miniature pigs. Invest. Ophthalmol. Vis Sci; 1985; 26: 1410-1414.

88. Moore, K.L. The developing human: Clinically Oriented Embryology. 4th ed. Philadelphia, PA: W.B. Saunders Co.; 1988. Cht 19 pp 402-412.

89. Moses, R.A.; Hart, W.M. Adler's Physiology of the Eye: Clinical Application. St Louis, MO: The C.V. Mosby Co.; 1987. Cht 6 pp 183-203.

90. Motulsky, H.J.; Ransnas, L.A. Fitting curves to data using nonlinear regression: a practical and nonmathematical review. FASEB J.; 1987; 1: 365-374.

91. Munakata, M.; Masaki, Y.; Sakuma, I.; Ukita, H. Pharmacological differentiation of epithelium-derived relaxing factor from nitric oxide. J Appl Physiol; 1990; 69(2): 665-70.

92. Norris, C.P.; Barnes, G.E.; Smith, E.E.; Granger, H.J. Autoregulation of superior mesenteric flow in fasted and fed dogs. Am. J. Physiol.; 1979; 2: H174-H177.

93. Nose, Y.; Nakamura, T.; Nakamura, M. The microsphere method facilitates statistical assessment of regional blood flow. Bas Res. Cardiol. 1985: 80: 417-429.

94. Novack, R.L.; and Stefansson, E. Noninvasive Diagnostic Techniques in Ophthalmology, Chapter 25: Measurement of Retina and Optic Nerve Oxidative Metabolism in Vivo via Dual Wavelength Reflection Spectrophotometry of Cytochrome a,a3. New York: Springer-Verlag; 1990.

95. Palmer, R.M.; Ferrige, A.G.; Moncada, S. Nitric oxide release accounts for the biological activity of endothelium-derived relaxing factor. Nature; 1987; 327(6122): 524-6.

96. Parver, L.M.; Auker, C.; and Carpenter, D.O. Choroidal blood flow as a heat dissipating mechanism in the macula. American Journal of Ophthalmology; 1980; 89: 641-646.

97. Pelligrino, D.A.; Koening, H.; Sharp, A. Nitric oxide (NO) synthesis and cerebral vasodilatory responses in the rat. FASEB Journal; 1992; (abstract).

98. Pohl, U.; Busse, R. Hypoxia stimulates the release of endothelium-derived relaxant factor (EDRF). Am J. Physiol. 1989; 256:H1595-H1600.

99. Pohlman, A.G. The course of the blood through the heart of the fetal mammal, with a note on the reptilian and amphibian circulations. Anat Rec. 1909; 3:75-109.

100. Prince, J.H.; Diesem, C.D.; Eglitis, I.; and Ruskell, G.L. Anatomy and Histology of the Eye and Orbit in Domestic Animals. Sringfield, Illinois: Charles C. Thomas; 1960.

101. Prinzmetal, M.; Ornitz Jr., E.M.; Simkin, B. Arterio-venous anastomoses in liver, spleen and lungs. Am. J. Physiol. 1947; 152: 48-52.

102. Rapoport, R.M.; Draznin, M.B.; and Murad, F. Endothelium-dependent relaxation in rat aorta may be mediated through cyclic GMP dependent protein phosphorylation. Nature; 1983; 306: 174-176.

103. Rees, D.D.; Palmer, R.M.J.; Schulz, R.; Hodson, H.F.; Moncada S. Characterization of three inhibitors of endothelial nitric oxide synthase in vitro and in vivo. Br J Pharmacol; 1990; 101: 746-52.

104. Rengasamy, A.; Johns, R.A. Characterization of endothelium-derived relaxing factor/nitric oxide synthase from bovine cerebellum and mechanism of modulation by high and low oxygen tensions. J Pharmacol Exp Ther; 1991; 259(1): 310-6.

105. Robison, G.W.; Laver, N.R. Ocular lesions in animal model of human diabetes:Lessons from animal diabetes 4th Ed. Great Britain: Smith-Gordon; 1993. Cht 14. pp 145-16

106. Rosenblum, W.I. Endothelium-derived relaxing factor in brain blood vessels is not nitric oxide. Stroke; 1992; 23: 1527-1532.

107. Rudolph, A.M.; and Heymann, M.A. The Circulation of the Fetus in Utero. Circulation Research; Aug. 1967; 21: 163-184.

108. Said, S.I. Nitric oxide and vasoactive intestinal peptide: cotransmitters of smooth muscle relaxation. News in Physiological Science (NIPS); 1992; 7: 181-183.

109. Sandell, J.H. NADPH-diaphorase cells in the mammalian inner retina. Journal of comparative neurology; 1985; 238: 466-472.

110. Schosser, R.; Arfors, K.E.; Messmer, K. MIC-II-A program for the determination of cardiac output arterio-venous shunt and regional blood flow using the radioactive microsphere method. Computer Programs in Biomedicine; 1979; 9: 19-38.

111. Shibuki, K.; Okada, D. Endogenous nitric oxide release required for long-term synaptic depression in the cerebellum. Nature; 1991; 349: 326-328.

112. Shikano, K.; Long, C.J.; Ohlstein, E.H.; Berkowitz, B.A. Comparative pharmacology of endothelium-derived relaxing factor and nitric oxide. J Pharmacol Exp Ther; 1988; 247(3): 873-81.

113. Sossi, N.; and Anderson, D.R. Effect of elevated intraocular pressure on blood flow: Occurrence in cat optic nerve head studied with iodoantipyrine I-125. Arch. Ophthalmol.; 1983; 101: 98-101.

114. Stjernschantz, J.; Alm, A.; Bill, A. Effects of intracranial oculomotor nerve stimulation on ocular blood flow in rabbits: modification by indomethacin. Exp Eye Res; 1976; 23: 461-469.

115. Stuehr, D.J.; Kwon, N.S.; Nathan, C.F.; Griffith, O.W.; Feldman, P.L.; Wiseman, J. N-Hydroxy-L-arginine is an intermediate in the biosynthesis of nitric oxide from L-arginine. J.Biol. Chem.; 1991; 266:10: 6259-6263.

116. Toda, N.; Ayajiki, K.; Yoshida, K.; Kimura, H.; Okamura, T. Impairment by damage of the pterygopalatine ganglion of nitroxidergic vasodilator nerve function in canine cerebral and retinal arteries. Circulation Research 1993; 72:206-213.

117. Tornquist, P.; and Alm, A. Retinal and choroidal contribution to retinal metabolism in vivo. A study in pigs. Acta Physiol Scand; 1979; 106: 351-357.

118. Tornquist, P.; Alm, A.; and Bill, A. Permeability of ocular vessels and transport across the blood-retinal-barrier. Eye; 1990; 4: 303-309.

119. Ueeda, M.; Silvia, S.K.; Olsson, R.A. Nitric oxide modulates coronary autoregulation in the guine pig. Circulation Research; 1992; 70(1296-1303).

120. Vanhoutte, P.M. The endothelium and control of coronary arterial tone. Hosp Pract; 1988; 23(5): 77-90.

121. Venturini, C.M.; Knowles, R.G.; Palmer, R.M.; Moncada, S. Synthesis of nitric oxide in the bovine retina. Biochem Biophys Res Commun; 1991; 180(2): 920-925.

122. Veriac, S.; Tissie, G.; Bonne, C. Oxygen Free radicals adversely affect the regulation of vascular tone by nitric oxide in the rabbit retina under high intraocular pressure. Exp Eye Res; 1993; 56: 85-88.

123. Wagner, Jr., H.N.; Rhodes, B.A.; Sasaki, Y.; and Ryan, J.P. Studies of the circulation with radioactive microspheres. Investigative Radiology; 1969; 4(no.6): 374-386.

124. Winder, S.J.; and Walsh, M.P. Smooth muscle calponin. Inhibition of actomyosin Mg-ATPase and regulation by phosphorylation. J. Biol Chem. 1990; 265: 10148-10155.

125. Wolff, E. Anatomy of the Eye and Orbit. Philadelphia: W.B. Saunders Company; 1976.

126. Wong, S.K.F.; Garbers, D.L. Receptor guanylyl cyclases. J. Clin. Invest.; 1992; 90: 299-305.

127. Yao, K.; Tschudi, M.; Flammer, J.; Luscher, T.F. Endothelium-dependent regulation of vascular tone of the porcine ophthalmic artery. Invest Ophthalmol Vis Sci; 1991; 32: 1791-1798.

128. Yoshida, A.; Feke, G.T.; Morales-Stoppelo, J.; Collas, G.D.; Goger, D.G.; McMeel, J.W. Retinal blood flow alterations during progression of diabetic retinopathy. Arch. Ophthalmol.; 1983; 101: 225-227.

APPENDIX

Composition of Mock Aqueous Humor (to make two liters):

16.0 grams sodium chloride (NaCl)

0.70 grams potassium chloride (KCl)

0.34 grams calcium chloride (CaCl)

2.00 grams D-Glucose (Dextrose, anhydrous) ($C_6H_{12}O_6$)

120.0 milligrams magnesium chloride (MgCl)

138.0 milligrams sodium phosphate, dibasic (Na_2HPO_4)

27.40 milligrams sodium phosphate, monobasic (NaH_2PO_4)

Retinal Blood Supply

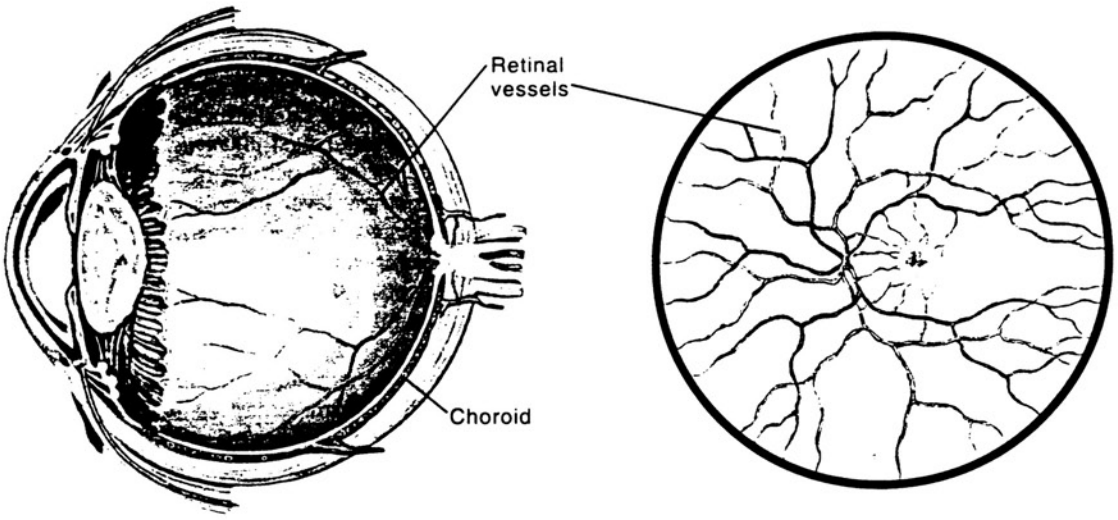

JOHN A. CRAIG M.D.
©CIBA-GEIGY

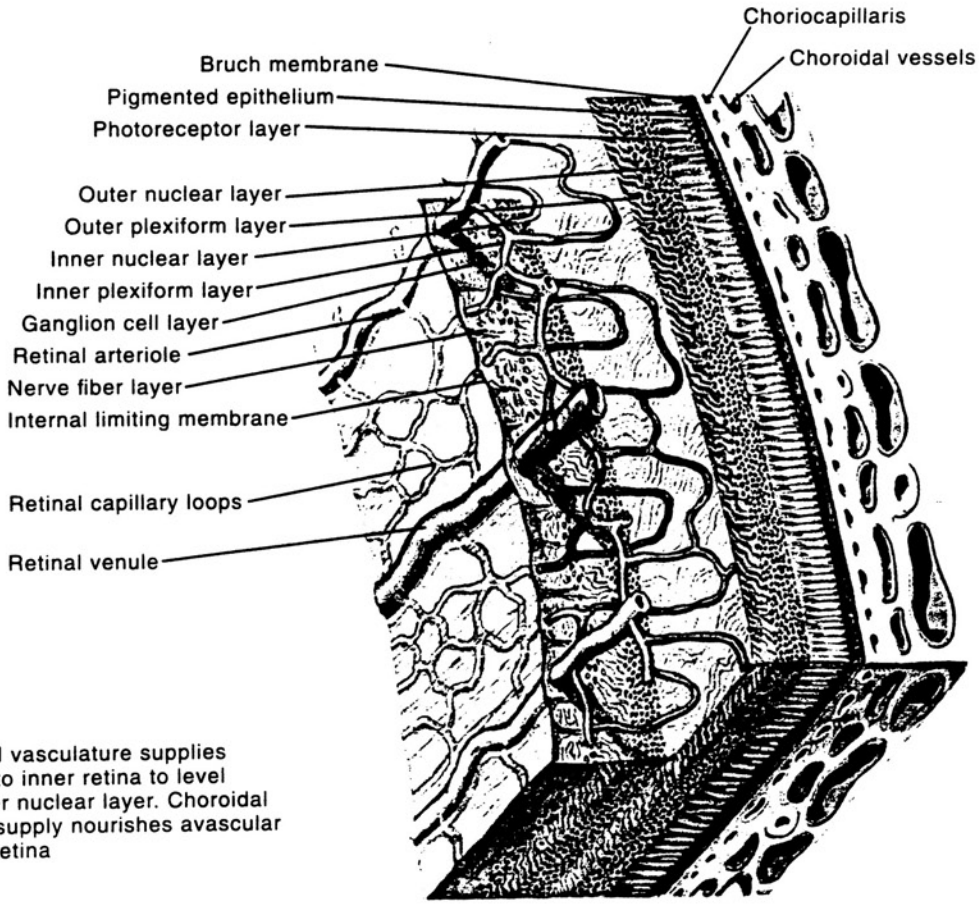

Retinal vasculature supplies blood to inner retina to level of inner nuclear layer. Choroidal blood supply nourishes avascular outer retina